



UNIVERSIDADE FEDERAL DE SANTA CATARINA
CENTRO TECNOLÓGICO
PROGRAMA DE PÓS-GRADUAÇÃO EM ENGENHARIA ELÉTRICA

Leonardo Bellincanta de Souza

**SINGLE-PHASE MODE OPERATION OF THREE-PHASE DAB
CONVERTER WITH TRIANGULAR AND SPS MODULATIONS**

Florianópolis
Dezembro de 2023

Leonardo Bellincanta de Souza

**SINGLE-PHASE MODE OPERATION OF THREE-PHASE DAB
CONVERTER WITH TRIANGULAR AND SPS MODULATIONS**

Dissertação submetida ao Programa de Pós-
Graduação em Engenharia Elétrica da Universidade
Federal de Santa Catarina para a obtenção do título
de Mestre em Engenharia Elétrica

Orientador: Prof. André Luís Kirsten, Dr.

Florianópolis
Dezembro de 2023

Catálogo na fonte pela Biblioteca Universitária da Universidade Federal de Santa Catarina.
Arquivo compilado às 21:41h do dia 04 de fevereiro de 2024.

Leonardo Bellincanta de Souza

SINGLE-PHASE MODE OPERATION OF THREE-PHASE DAB CONVERTER WITH TRIANGULAR AND SPS
MODULATIONS/ Leonardo Bellincanta de Souza. - Florianópolis, Dezembro de 2023-
94 p. : il. (algumas color.) ; 30 cm.

Orientador: Prof. André Luís Kirsten, Dr..

- Universidade Federal de Santa Catarina - UFSC

Departamento de Engenharia Elétrica e Eletrônica - EEL

Programa de Pós-Graduação em Engenharia Elétrica - PGEEL, Dezembro de 2023.

1. Comutação Suave. 2. Conversor DAB. 3. Eficiência Energética. 4. Modulação
Triangular. 5. *Single-Phase Mode*.

Leonardo Bellincanta de Souza

**SINGLE-PHASE MODE OPERATION OF THREE-PHASE DAB
CONVERTER WITH TRIANGULAR AND SPS MODULATIONS**

O presente trabalho em nível de mestrado foi avaliado e aprovado por banca examinadora composta pelos seguintes membros:

Prof. André Luís Kirsten, Dr.
Universidade Federal de Santa Catarina

Prof. Gierry Waltrich , Dr.
Universidade Federal de Santa Catarina

Prof. Walbermark Marques dos Santos , Dr.
Universidade Federal do Espírito Santo

Certificamos que esta é a **versão original e final** do trabalho de conclusão que foi julgado adequado para obtenção do título de Mestre em Engenharia Elétrica.

Prof. Telles Brunelli Lazzarin, Dr.
Coordenador do Programa de
Pós-Graduação em Engenharia Elétrica

Prof. André Luís Kirsten, Dr.
Orientador

Florianópolis
Dezembro 2023.

"I, a universe of atoms, an atom in the universe."
(FEYNMAN 1918 - 1988)

Acknowledgements

The years 2020, 2021, and 2022 were characterized by an unprecedented pandemic, akin to those experienced at the outset of the twentieth century. This scenario presented numerous challenges pertaining to physical, mental, and spiritual well-being.

In undertaking the endeavor of producing a Master's Thesis amidst these circumstances, the contribution of several key individuals was significantly evident. A myriad of intellectually stimulating and complex classes were offered by the esteemed faculty of the Power Electronics Institute (INEP).

In addition to the theoretical classes, I received specific guidance from Prof. Dr. Gierry Waltrich, who made invaluable recommendations concerning the Master's Programme. Additionally, Prof. Dr. André Kirsten's supervision was instrumental in the formulation of this Master's Thesis.

Beyond the faculty's guidance, I am indebted to the companionship provided by my colleagues Mateus Bueno, Cleiton Dal'Agnol, Brendon Kulak, and Valdecir Paris.

I extend my gratitude to the staff of the PPGEEL-UFSC, who provided assistance with numerous matters related to the Master of Science in Electrical Engineering procedures. My family, especially my mother Silvana and my father Josmar, have been a pillar of emotional support, for which I am deeply grateful. Lastly, my thanks extend to CNPQ and UNIEDU, whose monthly scholarships have facilitated the realization of this Master's Thesis.

Resumo

De acordo com o tipo de técnica de modulação aplicada ao conversor DAB, há um intervalo específico de comutação suave e, como consequência, níveis diferentes de perdas de condução, comutação e eficiência. Com a finalidade de se comparar intervalos de comutação suave e suas condições para as modulações *single phase-shift* e triangular, é realizada uma revisão de literatura em relação aos níveis de corrente do indutor de dispersão do transformador, princípios de operação, intervalo de e restrições de comutação suave. Nesta análise, com o objetivo de se obter uma melhora na eficiência para modos monofásicos dos conversores DAB trifásicos YY e YD, são avaliados os resultados mencionados acima para os modos monofásicos das modulações *single phase-shift* e triangular. São obtidos diagramas de condições de comutação suave destas duas técnicas de modulação e seus modos monofásicos correlacionados. Como a modulação triangular é conhecida por sua alta eficiência para aplicações de baixa potência, resultados de perdas de comutação, perdas de condução e eficiência são obtidos com o modelo de perdas do software PLECS. Então, com os resultados obtidos de eficiência e de perdas, ocorre a validação de resultados de simulação com estimativas calculadas de perdas e eficiência, evidenciando desta forma os resultados teóricos com os de simulação. Consequentemente, é concluído que os modos monofásicos dos conversores YY e $Y\Delta$, com modulação triangular, possuem menores níveis de perdas de comutação e condução, do que os modos monofásicos com modulação SPS, para aplicações em baixa potência.

Palavras-chave: Comutação Suave, Conversor DAB, Eficiência Energética, Modulação Triangular.

Resumo Expandido

Introdução

A indústria do transporte é responsável por 25% das emissões de gases do efeito estufa, sendo desta forma um contribuidor significativo para o aumento nas emissões. Depois de um século da dominação da indústria do óleo, especialistas acreditam que veículos elétricos, como os veículos puramente elétricos e veículos elétricos híbridos, podem revolucionar a demanda de energia no setor de transporte [1].

Os veículos elétricos tem se tornado mais populares devido a sua habilidade em emitir níveis baixos ou um nível zero de gases do efeito estufa e também devido a redução da dependência do petróleo. Há diferentes tipos de veículos elétricos, tais como: puramente elétricos (BEVs), veículos elétricos híbridos e do tipo plug-in (PHEVs) e veículos movidos a células de combustível e elétricos (FCEVs) [2].

Com a eletrificação dos sistemas de transporte, a demanda por carregadores onboard (OBCs) com elevados níveis de densidade de potência e eficiência energética tem crescido [3]. Considerando-se os níveis de potência, eles podem ser caracterizados em como de um ou dois estágios [4]. O foco desta dissertação de mestrado está em carregadores onboard (OBCs) de dois estágios, onde o primeiro estágio é responsável pela correção do fator de potência (PFC) e o segundo estágio estabiliza o barramento DC e controla a corrente da bateria para possibilitar os diversos modos de carga e descarga de acordo com requerimentos do sistema de bateria [5].

De acordo com [6], carregadores de baterias isolados frequentemente utilizam conversores como DAB, LLC ressonante e Full-Bridge com *Phase-Shift*. Devido a sua alta eficiência, isolamento galvânica e bidirecionalidade, o conversor DAB é o tipo de conversor mais utilizado, dentre as topologias deste tipo de circuito [7].

O conversor DAB regula a saída de tensão através da modulação dos semicondutores de potência, sendo que os semicondutores podem ser controlados através de três variáveis: defasagem angular (δ), configurações de razão cíclica (D_1 e D_2) e configurações de frequência de comutação (f_s) [8].

Para eliminar a potência reativa e a redução de perdas de condução, as técnicas de modulação EPS, DPS e TPS podem ser utilizadas [9]. Além de que, as modulações SPS, EPS e DPS podem ser considerados casos excepcionais da modulação TPS [10].

Em discussões de grupos de pesquisa, a utilização das modulações triangular e trapezoidal, de forma conjunta, provê uma operação eficiente do conversor DAB [11, 12].

Na modulação trapezoidal, duas formas de onda quadradas de tensão são aplicadas nos terminais do transformador e duas defasagens angulares são aplicadas internamente para cada braço das pontes completas do conversor [12].

Já o termo triangular se refere a forma de onda da corrente do indutor de dispersão do conversor DAB [12]. A região de comutação suave da modulação triangular possui uma faixa maior de comutação suave do que as configurações presentes nos conversores modulados com as modulações SPS e trapezoidal [13].

Os limites de comutação suave das modulações triangular e trapezoidal possuem a seguinte configuração: $P_{tri} < P < P_{trap}$, significando que a modulação triangular é adequada para aplicações de baixa potência [14]. Os conversores DAB3 podem entrar em modos monofásicos através da não utilização de sinais de semicondutores ou então com configuração de defasagem angular entre os braços dos lados primário e secundário [15].

Este estudo compara a performance e a eficiência dos modos monofásicos dos conversores DAB3 com as modulações SPS e triangular para aplicações em baixa potência.

Objetivos

O objetivo principal deste trabalho é analisar a performance de conversores DAB3 em modos monofásicos, utilizando-se as modulações SPS e triangular para os as configurações YY e Y Δ . Os objetivos específicos deste trabalho são os seguintes:

- Estudar as zonas de comutação suave dos modos monofásicos equivalentes das configurações DAB3 YY e Y Δ DAB com modulações triangular e SPS;
- Analisar as perdas dos modos monofásicos equivalentes das configurações DAB3 YY e Y Δ DAB com as modulações triangular e SPS;
- Obter gráficos de eficiência dos modos monofásicos equivalentes dos DAB3 e Y Δ DAB com as modulações SPS e triangular;

Metodologia

A pesquisa baseia-se na comparação de eficiência e regiões de comutação suave dos modos monofásicos dos DAB3 YY e Y Δ DAB com modulação SPS e triangular. Resultados analíticos de níveis de potência, nível de corrente eficaz no indutor de dispersão e regiões de comutação suave são obtidos para os respectivos modos e modulações.

A análise aborda também a comparação de resultados de simulação e resultados analíticos em relação a níveis de perda de comutação, perdas de condução, perdas totais, eficiência e níveis de corrente eficaz no indutor de dispersão.

Com o uso dos modos monofásicos dos conversores DAB3 YY e Y Δ DAB e da modulação triangular, propõe-se a utilização destas configurações com o objetivo de reduzir níveis de perdas e melhorar a eficiência energética.

Resultados e Discussão

Este estudo compara a eficiência e perdas dos modos monofásicos dos conversores DAB3 entre as modulações SPS e triangular. A contribuição principal deste trabalho foi a obtenção de diagramas de comutação suave, o que requereu o desenvolvimento de equacionamento referente a níveis de potência, corrente no indutor de dispersão e também os valores de razões cíclicas para operação das chaves do conversor, para os braços primário e secundário dos conversores DAB analisados.

Os resultados de simulação e analíticos mostram que os modos monofásicos com modulação triangular possuem menores níveis de perdas e níveis de corrente eficaz do indutor de dispersão quando se comparando com os modos monofásicos com modulação SPS.

Considerações Finais

Com o estudo realizado nesta dissertação se propõem os seguintes estudos futuros:

- Equações de valor eficaz da corrente do indutor de dispersão nos seguintes modos monofásicos equivalentes: YY-11-SPS, YY-11-Triangular, Y Δ – 10 – SPS, Y Δ – 10–Triangular, Y Δ – 01 – SPS e Y Δ – 01–Triangular;

- Estimaco de Perdas, com tempos de subida e descida, para o seguintes modos monofsicos equivalentes: YY-11-SPS, YY-11-Triangular, $Y\Delta - 10 - SPS$, $Y\Delta - 10 - \text{Triangular}$, $Y\Delta - 01 - SPS$, $Y\Delta - 01 - \text{Triangular}$;
- Anlise de modos monofsicos equivalentes para a modulao EPS, realizando-se comparaes de regio de comutao suave e nveis de perdas entre as modulaes e respectivos modos monofsicos entre as seguintes configuraes: SPS, triangular e EPS;

Palavras-chave: Comutao Suave, Conversor DAB, Eficincia Energtica, Modulao Triangular.

Abstract

According to the type of modulation technique applied to the DAB converter, there is a specific range of soft-switching and, as a consequence, different levels of conduction losses, switching losses, and efficiency. Aiming to compare the soft-switching range and its conditions of the triangular and SPS modulations, it is realized a literature review regarding the current levels in the leakage inductor of the transformer, operation principles, soft-switching range, and its constraints. To obtain the enhancement of efficiency for single-phase modes of the three-phase YY and YD DAB converters, the results mentioned above for the single-phase modes with triangular and SPS modulations. With these results, diagrams of soft-switching constraints of these two modulation techniques and their single-phase modes are obtained. As the triangular modulation is known for its high efficiency for low-power applications, levels of conduction losses, switching losses, total losses, and efficiency are obtained with the loss model of the PLECS software in the PLECS environment. Then, with the obtained simulation results of efficiency and losses, the single-phase modes with triangular and SPS modulations results are compared. Different types of modulation techniques applied to the DAB converter have a specific range of soft-switching, which results in different levels of conduction losses, switching losses, and efficiency. To compare the soft-switching range and conditions of the triangular and SPS modulations, a literature review was carried out related to the current levels in the leakage inductor of the transformer, operation principles, soft-switching range, and its constraints. To improve efficiency for single-phase modes of the three-phase YY and YD DAB converters, the results mentioned above for the single-phase modes with triangular and SPS modulations were evaluated. Diagrams of soft-switching constraints of these two modulation techniques and their single-phase modes were obtained using the results. The triangular modulation is known for its high efficiency for low-power applications. Therefore, levels of conduction losses, switching losses, total losses, and efficiency were obtained with the loss model of the PLECS software in the PLECS environment. Subsequently, simulation results of efficiency and losses with the single-phase modes of triangular and SPS modulations were compared to theoretical losses and efficiency, validating simulation results with theoretical values. It is concluded that the single-phase modes of YY and $Y\Delta$ with triangular modulation have lower losses than those with SPS modulation for low-power applications.

Key-words: Soft-switching, DAB Converter, Energy Efficiency, Triangular Modulation.

List of Figures

Figure 1.1 – Electrification index of the transport systems	2
Figure 1.2 – OBCs classification	2
Figure 1.3 – Two stages OBC	2
Figure 2.1 – Components of isolated bidirectional converter	9
Figure 2.2 – Isolated DC-DC single-phase bidirectional DAB converter	9
Figure 2.3 – Isolated DC-DC three-phase bidirectional DAB converter	9
Figure 2.4 – Voltage and current waveforms for primary and secondary sides	10
Figure 2.5 – Single-phase DAB converter - first stage of operation	12
Figure 2.6 – Second step of operation of single-phase DAB converter - SPS modulation	13
Figure 2.7 – DAB converter - soft-switching conditions with SPS modulation	15
Figure 2.8 – Voltage and current waveforms in the leakage inductor for $V_i > nV_o$ for triangular modulation - ($t_1 = T_1, t_2 = T_1 + T_2$)	15
Figure 2.9 – Voltage and current waveforms in the leakage inductor for $V_i < nV_o$ triangular modulation	17
Figure 2.10 – Soft-switching capability of DAB converter - triangular modulation. . .	18
Figure 2.11 – Soft-switching limits - triangular and SPS modulations $d = 0.75$	18
Figure 2.12 – RMS level of current of leakage inductor of the transformer.	19
Figure 3.1 – Three-phase transformer configurations	21
Figure 3.2 – Schematic of the YY-11 DAB converter single-phase mode with SPS modulation	23
Figure 3.3 – Schematic of the YY-00 DAB converter single-phase mode with SPS modulation	25
Figure 3.4 – Schematic of the Y Δ -10 DAB converter, single-phase mode with SPS modulation	27
Figure 3.5 – Schematic of the Y Δ -01 DAB converter single-phase mode with SPS modulation	28
Figure 3.6 – Soft-Switching Limits for YY and Y Δ Single-Phase and Three-Phase DAB Converters with SPS DAB Converters	36
Figure 4.1 – Schematic of the Y Δ three-phase DAB converter in the PLECS software. .	39
Figure 4.2 – Schematic of the YY Three-phase DAB converter in the PLECS software. .	40
Figure 4.3 – Conduction losses of the C3M0120090D MOSFET and body Diode	42
Figure 4.4 – Conduction losses of the SCT3060AW7 MOSFET and body diode - VG-0 . .	42
Figure 4.5 – Conduction losses of the SCT3060AW7 MOSFET and body diode - VG-18	43
Figure 4.6 – Turn-on losses C3M0120090D	43

Figure 4.7 – Turn-on losses SCT3060AW7	44
Figure 4.8 – Turn-off losses C3M0120090D	44
Figure 4.9 – Turn-off losses SCT3060AW7	45
Figure 4.10–Average Blocks.	45
Figure 4.11–Conduction Losses for DAB YY and $Y\Delta$ with SPS and triangular modulations.	47
Figure 4.12–Switching losses for DAB YY and $Y\Delta$ with SPS and triangular modulations.	48
Figure 4.13–Total losses for DAB YY and $Y\Delta$ with SPS and triangular modulations.	49
Figure 4.14–Efficiency for losses for DAB YY and $Y\Delta$ with SPS and triangular modulations.	50
Figure 4.15–Efficiency - analytical results - YY-00 - SPS and triangular modulations.	54

List of Tables

Table 2.1 – Single-stage isolated bidirectional DC-DC converters summary	6
Table 2.2 – Single-phase and three-phase DAB topologies comparisons	7
Table 4.1 – Simulation parameters initialization	38
Table 4.2 – V_o Configurations with different d	46
Table 4.3 – I_{Lkrms} values for YY-00 for both SPs and triangular modulations - d = 0.75	51
Table 4.4 – Losses and Efficiency - YY-00 - SPS - d=0.5	53
Table 4.5 – Losses and efficiency - YY-00 - triangular - d = 0.5	53
Table 4.6 – Losses and efficiency - YY-00 - SPS - d=0.75	53
Table 4.7 – Losses and efficiency - YY-00 - triangular - d = 0.75	53
Table C.1–Y Δ -10 - SPS - d = 0.5 - DAB- PLECS	73
Table C.2–Y Δ -10 - triangular modulation - DAB - d =0.5 - DAB- PLECS	73
Table C.3–Y Δ -01 - SPS - d = 0.5 - DAB- PLECS	73
Table C.4–Y Δ -01 - triangular modulation - DAB - d = 0.5 - DAB- PLECS	74
Table C.5–Y Δ - SPS - three-phase - d = 0.5 - DAB- PLECS	74
Table C.6–YY-00 - SPS - d= 0.5 - DAB - PLECS	74
Table C.7–YY-00 - triangular modulation - DAB - d= 0.5 - DAB- PLECS	74
Table C.8–YY-11 - SPS - d=0.5 - DAB - PLECS	75
Table C.9–YY-11 - triangular modulation - DAB - d=0.5 - DAB - PLECS	75
Table C.10–YY - SPS - three-phase - d = 0.5 - DAB - PLECS	75
Table C.11–Y Δ -10 - SPS - d =0.75 - DAB - PLECS	75
Table C.12–Y Δ -10 - triangular modulation - d = 0.75 - DAB - PLECS	76
Table C.13–Y Δ -01 - SPS - d = 0.75 - DAB - PLECS	76
Table C.14–Y Δ -01 - triangular modulation - DAB - d = 0.75 - PLECS	76
Table C.15–Y Δ - three-phase - SPS - d = 0.75 - DAB - PLECS	76
Table C.16–YY-00 - SPS - d=0.75 - DAB - PLECS	77
Table C.17–YY-00 - triangular modulation - d =0.75 - DAB - PLECS	77
Table C.18–YY-11 - SPS - d = 0.75 - DAB - PLECS	77
Table C.19–YY-11 - triangular modulation - DAB - d=0.75 - DAB - PLECS	77
Table C.20–YY - SPS - three-phase - d =0.75 - DAB - PLECS	78
Table C.21–Y Δ -10 - SPS - d = 1.25 - DAB - PLECS	78
Table C.22–Y Δ -10 - triangular modulation - DAB - d =1.25 - PLECS	78
Table C.23–Y Δ -01 - SPS - d = 1.25- DAB - PLECS	78
Table C.24–Y Δ -01 - triangular modulation - DAB - d = 1.25 - PLECS	79
Table C.25–Y Δ - three-phase - SPS - d = 1.25 - DAB- PLECS	79
Table C.26–YY-00 - SPS - d=1.25 - DAB - PLECS	79

Table C.27–YY-00 - triangular modulation - $d = 1.25$ - DAB - PLECS	80
Table C.28–YY-11 - SPS - $d = 1.25$ - DAB - PLECS	80
Table C.29–YY-11 - triangular modulation - $d=1.25$ - DAB - PLECS	80
Table C.30–YY - SPS - three-phase - $d =1.25$ - DAB - PLECS	81
Table C.31–Y Δ -10 - SPS - $d= 1.5$ - DAB - PLECS	81
Table C.32–Y Δ -10 - triangular modulation - DAB - $d = 1.5$ - PLECS	81
Table C.33–Y Δ -01 - SPS - $d = 1.5$ - DAB - PLECS	82
Table C.34–Y Δ -01 - triangular modulation - DAB - $d =1.5$ - PLECS	82
Table C.35–Y Δ - SPS - three-phase - $d =1.5$ - DAB - PLECS	82
Table C.36–YY-00 - SPS - $d=1.5$ - DAB - PLECS	83
Table C.37–YY-00 - triangular modulation - $d= 1.5$ - DAB - PLECS	83
Table C.38–YY-11 - SPS - $d = 1.5$ - DAB - PLECS	83
Table C.39–YY-11 - triangular modulation - $d=1.5$ - DAB - PLECS	83

List of abbreviations and acronyms

AC	Alternating Current
AC-DC	Alternating Current-Direct Current
BEV	Battery Electric Vehicle
BMS	Battery Management System
DAB	Dual Active Bridge
DC	Direct Current
DC-DC	Direct Current-Direct Current
DHB	Dual Half-Bridge Converter
DPS	Dual Phase-Shift Modulation
EPS	Extended Phase-Shift
ESS	Energy Storage System
EV	Electric Vehicle
EVs	Electric Vehicles
HFCV	Hydrogen Fuel Cell Vehicle
HS	Hard Switching
ICEV	Conventional Internal
IGBT	Insulated Gate Bipolar Transistor
INEP	Power Electronics Institute
LLC	LLC Resonant Converter
LUT	Look-up Table
MOSFET	Metal Oxide Semiconductor Field Effect Transistor
OBC	Onboard Charger
PFC	Power Factor Correction
PGEEL	Graduate Programme in Electrical Engineering

PHEVs	Plug-in Hybrid Electric Vehicle
PLECS	Simulation Platform for Power Electronic Systems
PWM	Pulse Width Modulation
PMSM	Permanent-Magnet Synchronous Motor
RMS	Root Mean Square
SEP	Electric Power Systems
SPS	Single Phase-Shift Modulation
TPS	Triple Phase-Shift Modulation
UFSC	Federal University of Santa Catarina
V2H	Vehicle-to-Home
V2G	Vehicle-to-Grid
V2L	Vehicle-to-Load
V2P	Vehicle-to-Person
V2V	Vehicle-to-Vehicle
	Combustion Engine Vehicle
WTW	Well to Wheel
ZCS	Zero Current Switching

List of symbols

f_s	Switching Frequency [Hz]
ω_s	Switching Frequency [rad/s]
V_{in}	Input Voltage [V]
V_o	Output Voltage [V]
V_{T1}	Primary Input Voltage - Square Waveform [V]
V_{T2}	Secondary Voltage Reflected to the Primary - Square Waveform [V]
L_k	Leakage Inductance of the Transformer [H]
I_L	Leakage Inductor Current [A]
θ	Conduction Angle of the Inductor Current [rad]
δ	Displacement Angle of the Phase-Shift [rad]
m	Modulation Index
P	Operating Power [W]
d	Duty Cycle

CONTENTS

1	INTRODUCTION	1
1.1	OBJECTIVES	4
1.1.1	Main Objective	4
1.1.2	Specific Objectives	4
1.2	WORK STRUCTURE	4
2	BIDIRECTIONAL DC-DC CONVERTERS	6
2.0.1	DAB Converter	7
2.1	SINGLE-PHASE DAB CONVERTER WITH SPS AND TRIANGULAR MODULATIONS	10
2.1.1	DAB Converter with Single Phase-Shift Modulation	10
2.1.1.1	Leakage Inductor Current Levels	11
2.1.2	Single-Phase DAB Converter with triangular Modulation	14
2.1.2.1	Leakage Inductor Current Levels	16
2.1.2.2	Soft-switching limits	17
2.1.2.3	Soft-switching constraints of SPS and triangular Modulations for Single-Phase DAB Converter	17
2.2	CHAPTER OVERVIEW	19
3	YY AND $Y\Delta$ SINGLE-PHASE MODES OF THREE-PHASE DAB CONVERTERS	20
3.1	YY THREE-PHASE DAB CONVERTER WITH SPS MODULATION	22
3.1.1	Power Flow	22
3.1.2	Soft-Switching Limits	22
3.2	$Y\Delta$ THREE-PHASE DAB CONVERTER WITH SPS MODULATION	22
3.2.1	Soft-Switching Limits	22
3.3	SINGLE-PHASE OPERATION OF THE THREE-PHASE THE DAB CONVERTER	23
3.3.1	Single-Phase Operation of the YY and YD Three Phase DAB Converters with Single-Phase Shift Modulation	24

3.3.1.1	YY Three-Phase DAB Converter in Single-Phase Operation with SPS Modulation	24
3.3.2	YY-11 Mode with SPS Modulation	24
3.3.3	YY-00 Mode with SPS Modulation	25
3.3.3.1	YD Three-Phase DAB Converter in Single-Phase Operation with SPS Modulation	26
3.3.4	YΔ-01 Single-Phase Mode with SPS Modulation	27
3.3.5	Single-Phase Operation of the YY and YD Three Phase DAB Converters with Triangular Modulation	28
3.3.5.1	YY Three-Phase DAB Converter in Single-Phase Operation with Triangular Modulation	29
3.3.6	YY-11 Single-Phase Mode with Triangular Modulation	29
3.3.7	YY 00 Single-Phase Mode with Triangular Modulation	31
3.3.7.1	YD Three-Phase DAB Converter in Single-Phase Operation with Triangular Modulation	32
3.4	SOFT-SWITCHING LIMITS DIAGRAMS	35
3.5	CHAPTER OVERVIEW	37
4	SIMULATION ANALYSIS AND RESULTS	38
4.1	TRANSFORMER AND LEAKAGE INDUCTANCE	41
4.1.1	MOSFET Switches, Antiparallel diodes, and Losses	41
4.1.2	Losses Estimation	41
4.1.3	Gate Signal Generation	45
4.1.4	Output Voltage	45
4.1.5	Analytical and Simulation Results Analysis	46
4.1.6	Simulation Results	46
4.1.7	Conduction Losses	47
4.1.8	Switching Losses	47
4.1.9	Total Losses	48
4.1.10	Efficiency	49
4.1.11	Equations Results vs Simulated Results	50
4.1.12	RMS Current	50
4.1.13	Losses - Calculated vs. Simulated	50
4.1.14	Chapter Overview	52
5	CONCLUSION	55
5.1	CONTRIBUTIONS AND FUTURE WORK	56
5.1.1	Contributions of Master Thesis	56
5.1.2	Future Work	57
	BIBLIOGRAPHY	58
APPENDIX A	POWER FLOW EQUATIONS DEVELOPMENT FOR TRIANGULAR MODULATION	62

APPENDIX B	MATLAB CODES	64
APPENDIX C	PLECS DATA - EFFICIENCY AND LOSSES .	73
APPENDIX D	LOSSES CALCULUS MATLAB CODE	85

The transportation industry is accountable for 25% of the world's greenhouse gas emissions, making it a significant contributor to the increase in emissions. After a century of the dominance of the oil industry, specialists believe that electric vehicles, such as pure electric vehicles and plug-in hybrid electric vehicles, can potentially revolutionize the demand for energy in the transportation sector [1].

Electric vehicles are considered a promising technological solution for transportation, and many governments have proposed goals to phase out diesel and gas vehicles by 2050 [16]. The motors of electric vehicles (EVs) are more efficient than those of internal combustion engine vehicles (ICEVs). However, the overall energy efficiency of electric cars should be evaluated considering their wheel-to-wheel efficiency (WTW) [17].

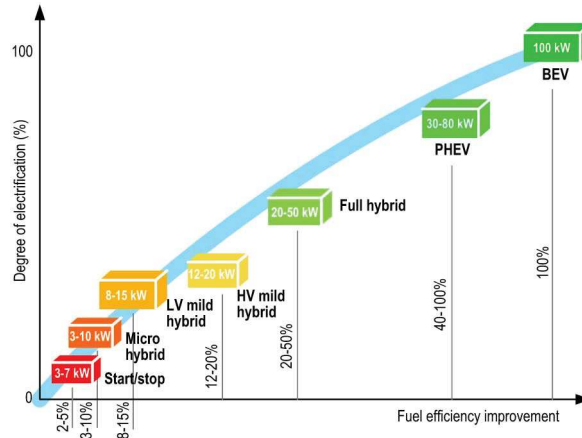
Gasoline-powered Internal Combustion Engine Vehicles (ICEVs) have a total efficiency that varies between 11% and 27%. Diesel ICEVs, on the other hand, have an efficiency ranging from 25% to 37%. For Compressed Natural Gas Vehicles (CNGVs), the efficiency varies between 13% and 22%. When renewable energy sources are used, the overall efficiency of electric vehicles increases from 40% to 70% [17]. Energy storage systems (ESSs), electric machines, and static converters are alternative technologies that offer high efficiency [18].

Developing powertrain systems for high-performance vehicles is related to architecture, design, control systems, and software, resulting in increased efficiency and economic benefits [18].

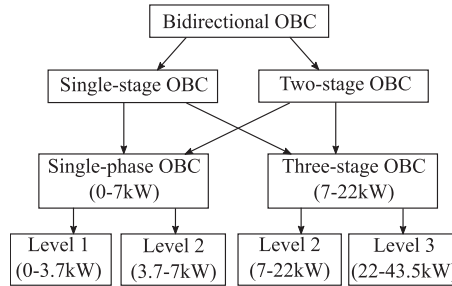
Electric vehicles are becoming more popular because of their ability to emit low levels of greenhouse gases or none at all and their reduced reliance on petroleum. There are different types of electric vehicles, such as pure electric vehicles (BEV), plug-in hybrid electric vehicles (PHEVs), and fuel cell electric vehicles (FCEVs) [2].

Figure 1.1 shows the relationship between the energy efficiency of different electric vehicles and the electrification index of the transport system [18].

With the electrification of transport systems, the demand for high power density and energy efficiency onboard chargers (OBC) is increasing [3]. Meanwhile, OBCs can be classified into one or two stages based on their power level, as shown in Figure 1.2 [4]. The focus of this Master's thesis is on the two-stage Onboard Charger (OBC). Figure 1.3 illustrates the configuration of a circuit with two stages. The first stage, known as AC-DC, is responsible for the correction of the power factor PFC [5].

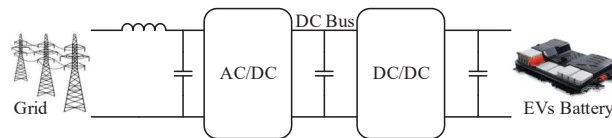
Figure 1.1 – Electrification index of the transport systems .

Source: [18].

Figure 1.2 – OBCs classification .

Source: [4].

In addition, the DC-DC section stabilizes the DC bus and controls battery current to enable various charge and discharge modes according to BMS requirements [5].

Figure 1.3 – Two stages OBC .

Source: [5].

According to [6], isolated battery chargers frequently employ converters such as DAB, LLC Resonant, and Full-Bridge with Phase-Shift. Due to its high efficiency, bidirectional power flow, and galvanic isolation, the DAB converter is the most widely used among these different circuit topologies, as mentioned in [7].

The bidirectional capacity of electric vehicles enables Vehicle-to-Grid (V2G) operation. V2G can help electric power systems attenuate energy demand peaks, while Vehicle-to-Home (V2H) or Vehicle-to-Load (V2L) can supply energy during power system outages. Furthermore, the bidirectional capacity enables Vehicle-to-Vehicle (V2V) operation, which can supply energy in emergencies [4].

The DAB converter regulates the output voltage by modulating power switches.

The converter can be controlled by the following characteristics [8]:

- phase displacement (δ) between two H-Bridges;
- configuration of the duty cycles of the switches;
- configuration of the switching frequency;

Literature frequently discusses the following DAB modulation techniques.

- Use of Single Phase-Shift (SPS) modulation, which involves a phase displacement between the primary and secondary [8].
- Extended Phase Shift (EPS) uses three-level modulation in DAB primary and two-level modulation in DAB secondary terminal [19];
- Dual Phase-Shift (DPS) operates a three-level modulation with the same duty cycle and a phase shift between primary and secondary [19]. Dual-phase-shift modulation is an improvement over extended phase-shift modulation. This modulation offers several benefits, such as lower current spike levels, higher converter efficiency, and reduced output capacitance. Although it is possible to control the voltage level on the primary and secondary bridges, there is no closed-form solution to its application, making it more complex to control [20].
- Triple Phase Shift (TPS), where there are different duty cycles for each bridge of the converter, and there is a third order freedom degree [19];

To eliminate reactive power and reduce conduction loss, EPS, DPS, and TPS modulation techniques can be used [9]. Modulation of SPS, EPS, and DPS can be considered to be exceptional cases of TPS [10].

Research groups have discussed the use of triangular and trapezoidal modulation techniques together, which provide efficient operation for the DAB converter [11, 12].

In trapezoidal modulation, two voltage displacements are applied to the transformer terminals and two internal displacements are applied to each arm of the bridge converters [12].

The term "triangular modulation" refers to the current waveform of the inductor in the DAB converter [12]. The soft-switching zone for triangular modulation has a more comprehensive range than single-phase shift and trapezoidal modulations in the DAB converter [13].

Meanwhile, in the study presented by [14], the limits of the soft-switching power have the following configuration: $P_{tri} < P < P_{trap}$, meaning that the triangular modulation is suitable for low-power applications. The DAB3 can enter single-phase mode by not using switch signals or by using a phase shift configuration between the primary and secondary arms [15].

These modulations can increase converter reliability or be used for low-power operation, improving efficiency [21]. This study compares the performance and efficiency of the single-phase modes of DAB3 with SPS and triangular modulations for low-power applications. DAB converters experience two main categories of losses. Transformer and inductor losses account for about 20% of the total losses, while switching losses account for 35% [22].

1.1 OBJECTIVES

The first step is to review the DC-DC converter topologies discussed in the literature to analyze the efficiency, performance, and losses of DAB converters that use SPS and triangular modulations. After that, the modulation schemes are studied in terms of their working principle, switching losses, conduction losses, converter efficiency, and inductor current value. The study investigates the properties of single-phase DAB converters with SPS and triangular modifications. It also examines YY and Y Δ DAB Converters with triangular and SPS modulations and their equivalent single phase modes.

Switching conduction losses, efficiency, and RMS values are obtained using PLECS software models and validated analytically.

1.1.1 Main Objective

The primary goal of this work is to analyze the performance of DAB converters that use SPS and triangular modulations in the single-phase equivalent modes of YY and Y Δ DAB converters.

1.1.2 Specific Objectives

The specific objectives of this work are the following:

- Study the soft-switching zones of single-phase equivalent modes for YY and Y Δ DAB Converters with single-phase shift and triangular modulations ;
- Analyze losses of the DAB converter operating with single-phase equivalent modes of YY and Y Δ DAB Converters with single-phase shift and triangular modulations.;
- Evaluate efficiency graphs of the DAB converter using single-phase equivalent modes of YY and Y Δ DAB converters with single-phase shift and triangular modulations through applying PLECS.

1.2 WORK STRUCTURE

This thesis consists of five chapters. Chapter 2 provides an overview of DC-DC converters, modulation techniques, their applications, and research objectives. Also, in Chapter 2, the single phase DAB converter's leading properties and working principles

are presented. The study of SPS and triangular modulations for their operations is also discussed.

Chapter 3 presents the single-phase modes of the YY and Y Δ DAB converters for the triangular and SPS modulations. The working principle and soft-switching constraints are studied.

In Chapter 4, the thermal properties of PLECS models are presented, including an analysis of their inductors, transformers, switches, signal generation, and output voltage configuration. In addition, in Chapter 4, the results from PLECS the losses model regarding switching losses, conduction losses, total losses, and efficiency are presented. Moreover, this chapter presents the analytical results of the leakage inductor efficiency, losses, and RMS current, where the analytical and simulation results are compared.

Finally, in Chapter 5 the conclusions, contributions and prospective studies of this master thesis are presented.

Non-isolated converters have a direct path for power flow. In contrast, isolated converters have a high-frequency transformer to isolate the direct power flow between the primary and secondary sides of the converter [23].

Non-isolated bidirectional converters have simpler circuitry and are less susceptible to EMI but lack galvanic isolation. This makes them compatible with weight and size requirements. Meanwhile, the isolated topologies have sections for DC-AC and AC-DC conversion, occurring sequentially, ensuring a high voltage gain due to the presence of the high frequency transformer [23].

They can be classified as one-stage or two-stage configurations for studying isolated bidirectional converters with high voltage gain, which require galvanic isolation. Figure 2.1 shows the single-stage isolated bidirectional converter configuration [14]. Among the isolated bidirectional converter topologies presented in Table 2.1, the DAB has characteristics such as bidirectional power flow, high-power density, simple implementation of soft-switching capabilities, and compatibility with cascaded and parallel configurations [24].

The DAB converter can achieve soft switching only when the voltage ratio is equal to one, as presented in [25], resulting in low switching losses [26].

Table 2.1 – Single-stage isolated bidirectional DC-DC converters summary

	Flyback, Forward, Cuk converter topologies.	Dual Active Bridge Without Resonance	Dual Bridge Converters	Active Resonant Converters
Advantages	Simple circuitry, low number of switches	Effective converter utilization, low semiconductor switching losses, compatibility with high-power applications	Low losses, capability utilization switches	increased of switches
Drawbacks	Low utilization of transformer and switch capacities.			Increased number of power components

Source: [27].

In this chapter, the principles behind the DAB converter will be reviewed. In

addition, their topology variations and modulation techniques will be covered.

2.0.1 DAB Converter

The Dual Active Bridge converter was created in the 1990s by [25]. It is specifically designed for high power uses that require efficient performance, buck-boost functionality, and the ability to transfer power in both directions [28].

The DAB converter consists of two full bridges connected by a high-frequency transformer [29]. The transformer provides galvanic isolation and is responsible for the conversion of voltage [30]. In addition, a leakage inductor facilitates power transfer between the primary and secondary bridges [29].

When the voltage gain is not equal to one, the DAB converter cannot achieve soft switching, resulting in a lower efficiency [31].

Figures 2.2 and 2.3 display variations in topology for the single-phase and three-phase configurations of the DAB Converter.

Table 2.2 summarizes the comparison between the three-phase and single-phase configurations [27].

Table 2.2 – Single-phase and three-phase DAB topologies comparisons .

	Three-Phase	Single-Phase
Advantages	Low semiconductor stresses, low capacitor ripple current	Low quantity of passive elements, uniform currents through the semiconductors, ZVS or ZCS capability, high-density of power density, simple transformer design
Drawbacks	High number of active components, elevated switching and conduction losses, complexity of the design of three-phase transformers	High output current ripple, and compatibility with applications in the low to mid power range

Source: [27, 32].

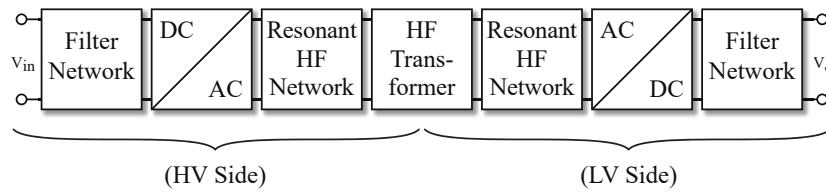
Research suggests that when the voltage-gain ratio is not equal to unity and the DAB converter operates at a low load, it loses soft-switching capability. This results in lower efficiency due to higher switching losses [20]. The DAB3 can operate in single phase mode, using switch signals or with a phase shift configuration between the primary and secondary arms of the converter [15]. These configurations may enhance converter efficiency or increase reliability in low power mode [21]. To improve efficiency, it is recommended to use three-level modulation techniques in the single-phase mode of three-phase DAB [15].

There are three parameters that can be utilized to regulate the power flow between the primary and secondary sides in DAB Converter operation techniques. These parameters include the phase shift between the secondary and primary square voltages (δ), the duty

cycles of the square waveforms on each side(D_1 and D_2) and the switching frequency (f_s) [33].

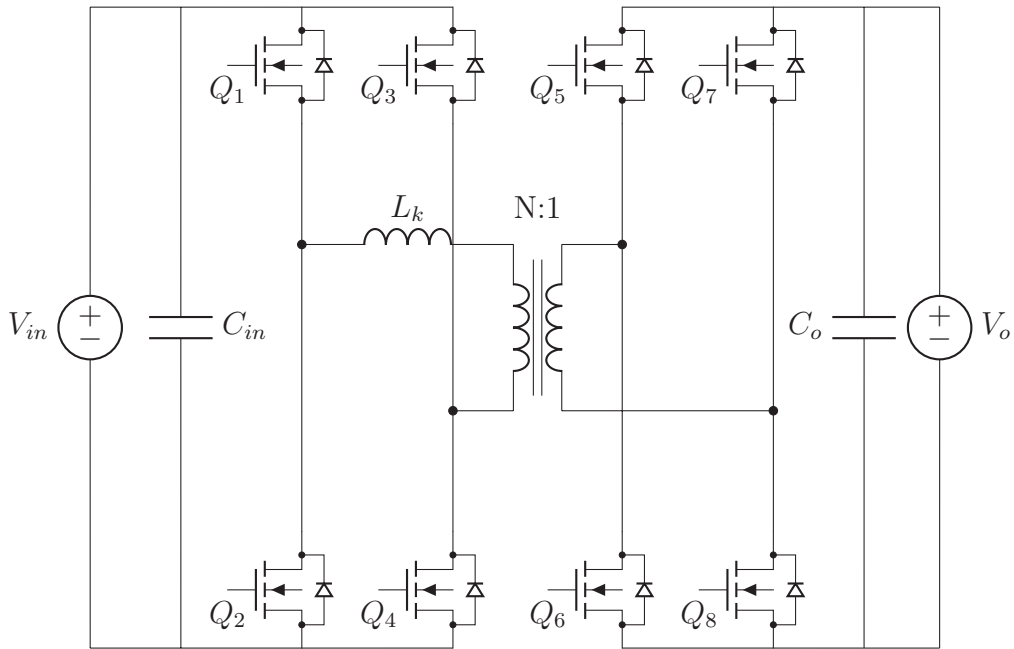
In this thesis, only the phase shift and duty cycle of the bridges are analyzed, where the following modulations are studied: the single phase shift modulation (SPS) and the triangular modulation.

Figure 2.1 – Components of isolated bidirectional converter



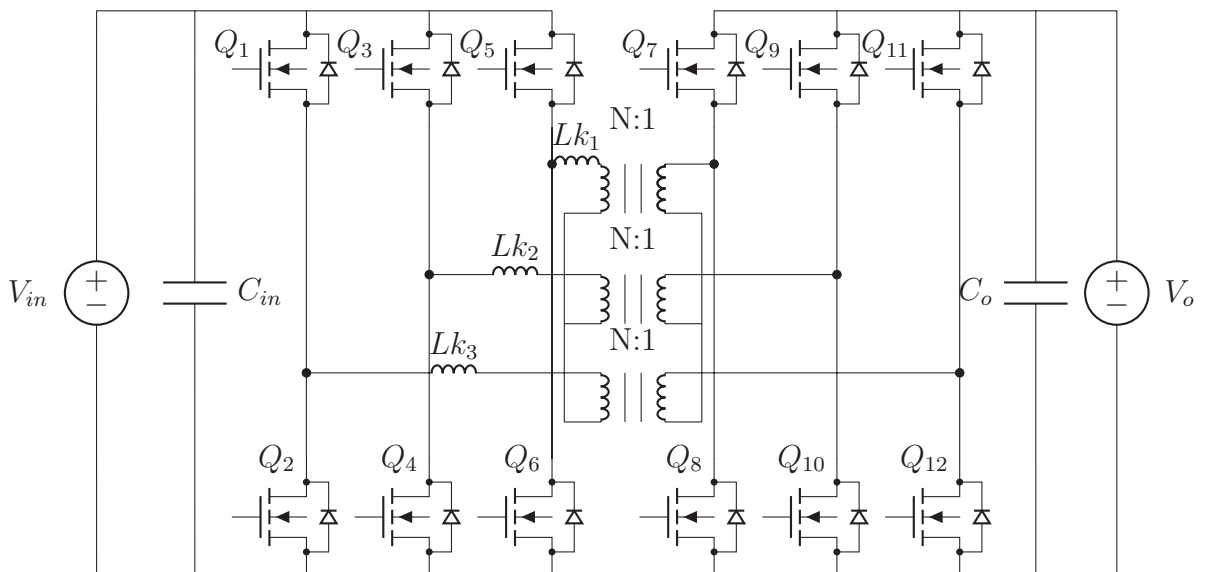
Source: [14].

Figure 2.2 – Isolated DC-DC single-phase bidirectional DAB converter .



Source: [25].

Figure 2.3 – Isolated DC-DC three-phase bidirectional DAB converter .



Source: [25].

2.1 SINGLE-PHASE DAB CONVERTER WITH SPS AND TRIANGULAR MODULATIONS

This section reviews SPS and triangular modulations for a single-phase DAB topology. The following chapters cover single-phase modes of three-phase DAB converters.

The SPS modulation technique uses square waveforms to control the power transfer between the primary and secondary sides of a transformer. Unlike other types of waveform, square waveforms do not have clamping intervals. Instead, their phase shift is what regulates the power flow.

In triangular current mode modulation, square voltage waveforms with clamping intervals are applied to the secondary [11]. The voltage and current equations for both modulations and their soft-switching capabilities are analyzed mathematically to compare conduction losses, switching losses, and efficiency.

2.1.1 DAB Converter with Single Phase-Shift Modulation

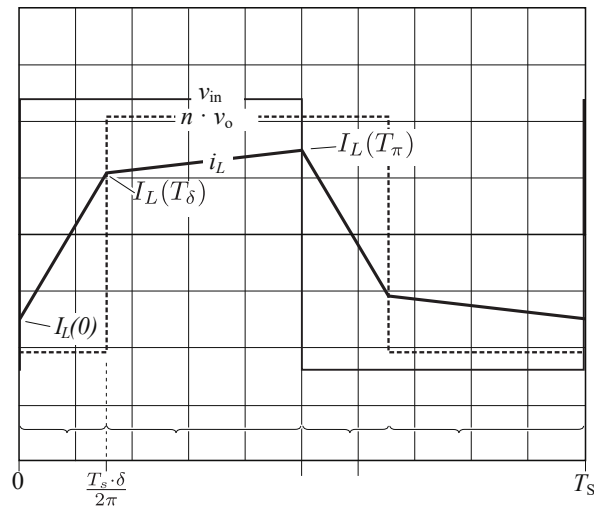
From [28], the power flow in the SPS modulation can be derived as shown in 2.2. To determine the phase-shift angle for a given power, use 2.3, where 2.1 defines the voltage gain ratio.

When considering only positive values of δ , the phase-shift angle falls within the range of $0 \leq \delta \leq \frac{\pi}{2}$ [33]. Using this result, it is possible to estimate the maximum leakage inductance with 2.4 [14, 25].

$$d = \frac{V_o n}{V_{in}} \quad (2.1)$$

$$P = \frac{V_{in}^2 d \delta (\pi - |\delta|)}{\omega_s \pi L_k} \quad (2.2)$$

Figure 2.4 – Voltage and current waveforms for primary and secondary sides .



Source: [14].

$$\delta = \frac{\pi \pm \sqrt{\pi^2 - \frac{4\pi\omega_s L_k P}{V_{in}^2 d}}}{2} \quad (2.3)$$

$$L \leq \frac{V_{in}^2 d}{8f_s P_{max}} \quad (2.4)$$

2.1.1.1 Leakage Inductor Current Levels

Two voltage square waveforms are applied to the DAB converter terminals, as shown in Figure 2.4.

$$\frac{dI_{L_k}(t)}{dt} = \frac{V_{t_1}(t) - V'_{t_2}(t)}{L_k} \quad (2.5)$$

In Figure 2.4, two square voltage waves are applied to the transformer's primary and secondary sides, generating a current waveform denoted as I . As the waveform exhibits half-symmetry, it is only necessary to consider one half-cycle of the I_{L_k} signal [28].

The equations 2.6 and 2.7, represent, respectively, the current in the periods $0 - \delta$ and $\delta - \pi$, assuming $I_{L_k}(0) = -I_{L_k}(\pi)$. Meanwhile, the Figure 2.5a presents the operation of current behavior during the beginning and end of the period $0 - \delta$, where it is shown that the body diodes of the switches Q_1, Q_4 are conducting current, ensuring the ZVS operation for the primary bridge [19]. Also, from Figure 2.4, it is possible to obtain 2.6.

$$I_{L_k}(\theta) = \frac{(V_{in} + V'_o)\theta}{\omega_s L_k} + I_{L_k}(0) \quad (2.6)$$

Furthermore, Figure 2.6 describes the operation of the current in the second stage of operation of the DAB converter, where the end of this stage represents the half-cycle period of the operation of the DAB converter. Using the current behavior in Figure 2.6 is obtained (2.7) for the $\delta - \pi$ period. Meanwhile, from the behavior of the current for the period $0 - \pi$, it is noticed that $I_{L_k}(\pi) = -I_{L_k}(0)$, resulting in (2.8).

$$I_{L_k}(\theta) = \frac{(V_{in} - V'_o)(\theta - \delta)}{\omega_s L_k} + I_{L_k}(\delta) \quad (2.7)$$

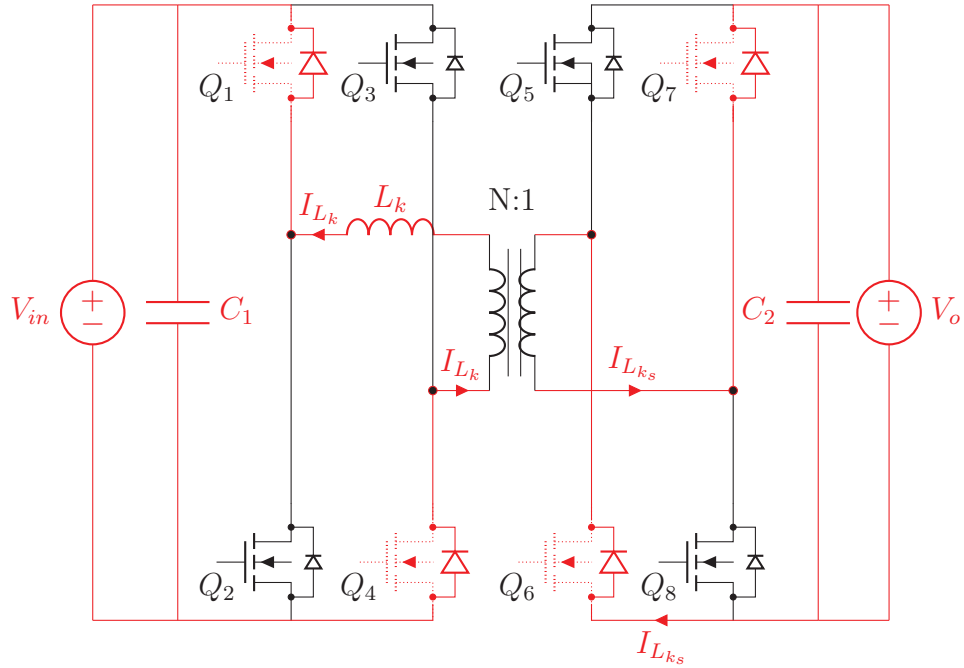
$$I_{L_k}(0) = -\frac{(2V'_o\delta + V_{in}\pi - V'_o\pi)}{2\omega L_k} \quad (2.8)$$

Using previous equations of phase-shift, power flow, and levels of current of the leakage inductors, and using the results from [27], derived the equation 2.9, for RMS level of leakage inductor current for SPS modulation.

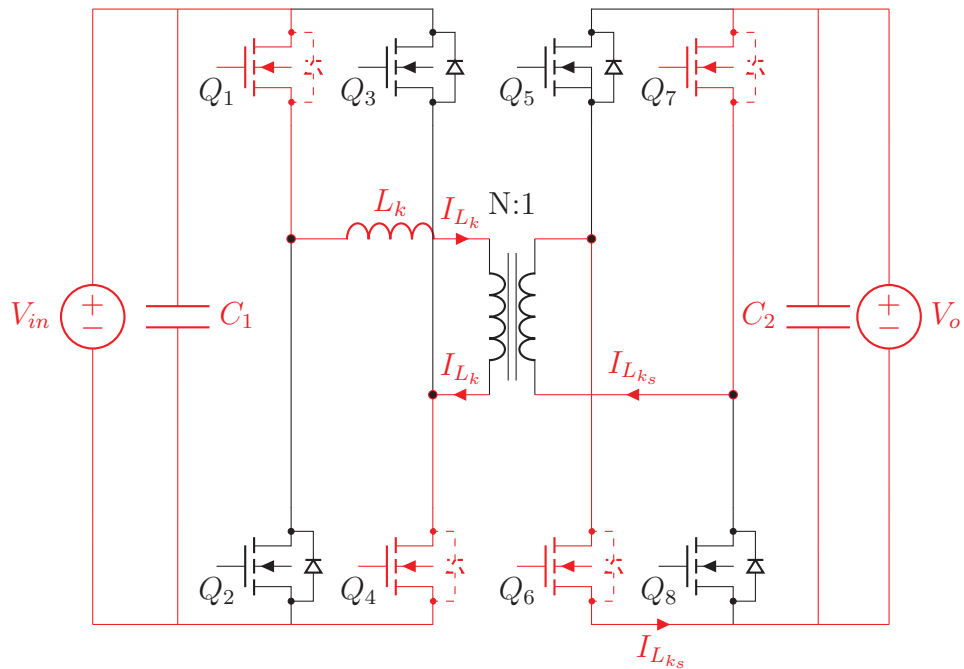
$$I_{L_{krms\ sps}} = Vp \cdot \frac{1}{f_s} \cdot (-3(8(\delta)^3 d - 12(\delta)^2 d - d^2 + 2 \cdot d - 1))^{(1/2)} / (12 \cdot L_k) \quad (2.9)$$

By examining equation 2.8 and Figure 2.5a, it is possible to derive constraints for the current values in the switches of both the primary and secondary bridges. These constraints

Figure 2.5 – Single-phase DAB converter - first stage of operation .

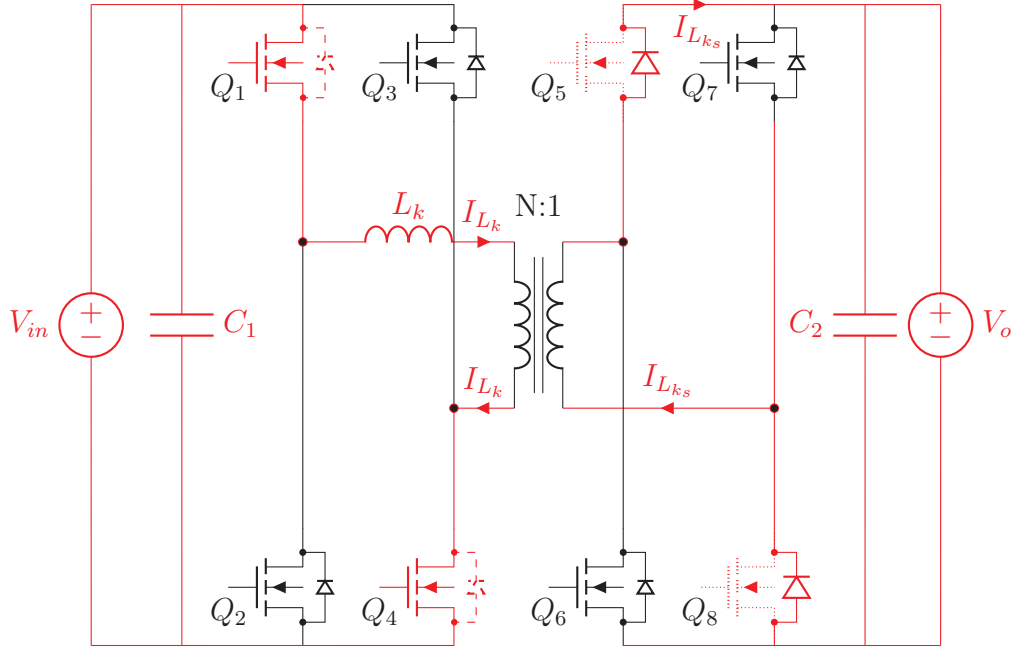


(a) First Step of Beginning Stage



(b) Last Step of Beginning Step

Source: [19].

Figure 2.6 – Second step of operation of single-phase DAB converter - SPS modulation .

Source: [19].

are described in equation 2.10 for the primary bridge and in equation 2.11 for the secondary bridges [19].

$$\begin{aligned}
 I_{Q_{1-4}}(0 - \delta) &= \frac{(V_{in} + V'_o)\theta}{\omega_s L_k} + I_{L_k}(0) \\
 I_{Q_{1-4}}(\delta - \pi) &= \frac{(V_{in} - V'_o)(\theta - \delta)}{\omega_s L_k} + I_{L_k}(\delta) \\
 I_{Q_{1-4}}(\pi - (\delta + \pi)) &= -\frac{(V_{in} + V'_o)(\theta - \pi)}{\omega_s L_k} - I_{L_k}(0) \\
 I_{Q_{1-4}}((\delta + \pi) - 2\pi) &= -\frac{(V_{in} - V'_o)(\theta - (\delta + \pi))}{\omega_s L_k} - I_{L_k}(\delta)
 \end{aligned} \tag{2.10}$$

$$\begin{aligned}
 I_{Q_{7-6}}(0 - \delta) &= \frac{(V_{in} + V'_o)\theta}{\omega_s L_k} + I_{L_k}(0) \\
 I_{Q_{7-6}}(\delta - \pi) &= \frac{(V_{in} - V'_o)(\theta - \delta)}{\omega_s L_k} + I_{L_k}(\delta) \\
 I_{Q_{7-6}}((\pi) - (\delta + \pi)) &= \frac{(V_{in} + V'_o)\theta - \pi}{\omega_s L_k} + I_{L_k}(0) \\
 I_{Q_{7-6}}((\delta + \pi) - 2\pi) &= \frac{(V_{in} - V'_o)(\theta - (\delta - \pi))}{\omega_s L_k} + I_{L_k}(\delta)
 \end{aligned} \tag{2.11}$$

To achieve soft-switching on the primary side of the bridge, it is necessary to ensure that the current $I_{L_k}(0)$ is equal to zero. This ensures that the switches Q_1 and Q_4 can conduct currents through the anti-parallel diodes with soft switching. This analysis leads to the inequality shown in Equation 2.12. By further considering the voltage gain (d), it is possible

to obtain Equation 2.14 ($d > 1$) to achieve soft-switching conditions on the primary side. Furthermore, the utilization of the results obtained from equation 2.11 requires that the current $I_{Lk}(\delta)$ be greater than zero to ensure that the current flow aligns with the behavior depicted in Figure 2.6, resulting in equation 2.13. Additionally, by applying the voltage gain (d), the soft-switching constraint is derived for the secondary bridge as shown in equation 2.15 ($d < 1$).

$$-\frac{(2V_o'\delta + V_{in}\pi - V_o'\pi)}{2\omega L_k} < 0 \quad (2.12)$$

$$(V_{in} + V_o)\frac{(\delta)}{\omega L_k} - \frac{(2V_o\delta + V_{in}\pi - V_o\pi)}{2\omega L_k} \quad (2.13)$$

$$\delta > \frac{\pi(d-1)}{2d} \quad (2.14)$$

$$\delta > \frac{\pi(1-d)}{2} \quad (2.15)$$

Furthermore, by using the equations presented in 2.15 and 2.14 within the power flow equation 2.2, it becomes feasible to derive a soft switching zone diagram for the single-phase DAB converter that operates with SPS modulation. This diagram illustrates the relationship between the operating power of the DAB converter, the inductor, and the switching frequency, as described in the investigation carried out [15]. Figure 2.7 depicts the resulting soft switching diagram.

2.1.2 Single-Phase DAB Converter with triangular Modulation

The triangular modulation is named after the triangular form of the current inducing the leakage in the transformer [33]. Two bridges produce two three-level square waveforms with the desired duty cycle values of the waveforms [34].

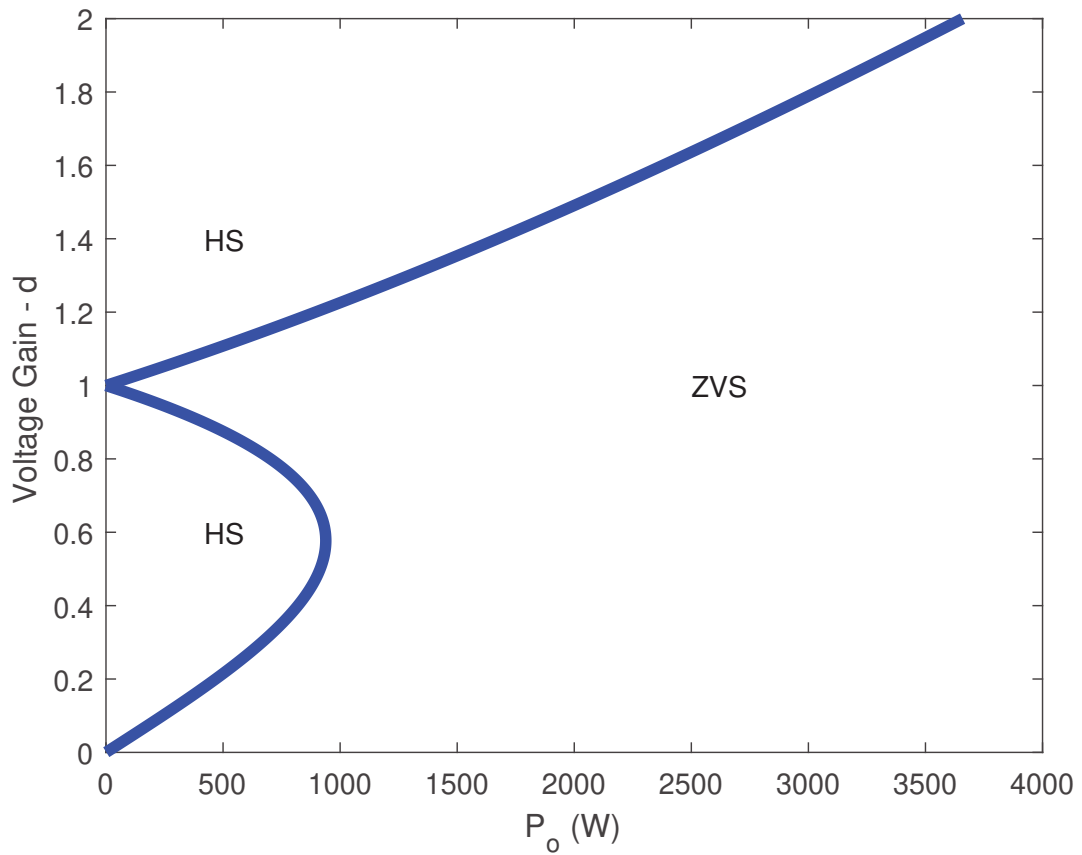
According to [14], the triangular modulation has a few advantages over the SPS modulation. First, it reduces the RMS transformer induction current. Lastly, it reduces switching losses, as mentioned in [34].

Power flow regulation is achieved by adjusting the phase shift between the voltages of the three levels and their corresponding duty cycles. This relationship can be observed in equation 2.16 when the input voltage, V_{in} , is greater than nV_o . The specific value of the phase shift is determined by equation 2.17. The conduction times, T_1 and T_2 , which are illustrated in Figure 2.8, can be calculated using equations 2.18 and 2.19 respectively [14].

$$P = \frac{\delta^2 d^2 V_{in}^2}{\pi^2 f_s L_k (1-d)} \quad (2.16)$$

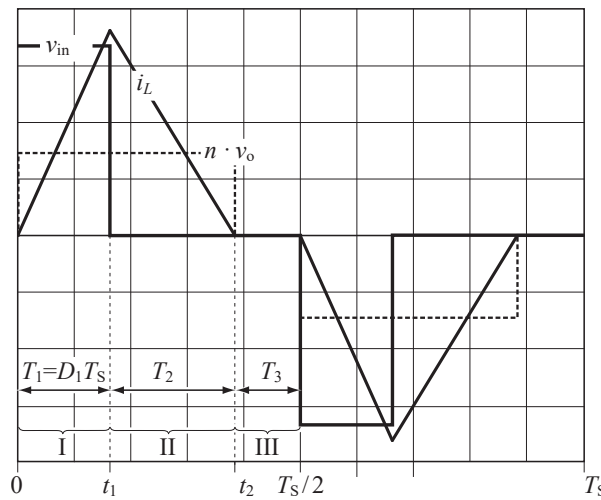
$$\delta = \pi \sqrt{\frac{P f_s L_k (1-d)}{d^2 V_{in}^2}} \quad (2.17)$$

Figure 2.7 – DAB converter - soft-switching conditions with SPS modulation .



Source: From the author.

Figure 2.8 – Voltage and current waveforms in the leakage inductor for $V_i > nV_o$ for triangular modulation - ($t_1 = T_1$, $t_2 = T_1 + T_2$) .



Source : [14].

$$T_1 = \frac{\delta d}{\pi f_s (1 - d)} \tag{2.18}$$

$$T_2 = \frac{\delta}{\pi f_s} \tag{2.19}$$

$$T_3 = \frac{T_s}{2} - T_1 - T_2 \quad (2.20)$$

The regulation of power flow in the circuit is achieved by adjusting the phase shift between the three-level voltages and the corresponding duty cycles. This relationship can be represented by equation 2.21 when the input voltage (V_{in}) is lower than nV_o [14]. The phase shift under the same conditions can be calculated using the equation 2.22. Conduction times (T_1 and T_2) can be determined using equations 2.23 and 2.24, respectively, as illustrated in Figure 2.8 [14].

$$P = \frac{\delta^2 V_{in}^2 d}{\pi^2 f_s L_k (d-1)} \quad (2.21)$$

$$\delta = \frac{\pi}{V_{in}} \sqrt{\frac{P f_s L_k (d-1)}{d}} \quad (2.22)$$

$$T_1 = \frac{\delta}{\pi f_s} \quad (2.23)$$

$$T_2 = \frac{\delta}{\pi f_s (d-1)} \quad (2.24)$$

$$T_3 = \frac{T_s}{2} - T_2 - T_1 \quad (2.25)$$

2.1.2.1 Leakage Inductor Current Levels

By examining Figure 2.8, one can obtain formulas for the current of the leakage inductor in the case where $V_{in} > nV_o$. The current values within the intervals $0 \leq t \leq T_1$ and $T_1 \leq t \leq T_2$ can be calculated using equation 2.26 [14]. By using the results obtained from Equation 2.26, it can be employed the idea of the root mean square (RMS) value of a variable to calculate the RMS value of the current flowing through the leakage inductor of the single-phase DAB converter. A detailed explanation of this is provided in 2.27, where it was used the software Mathcad to the respective derivation.

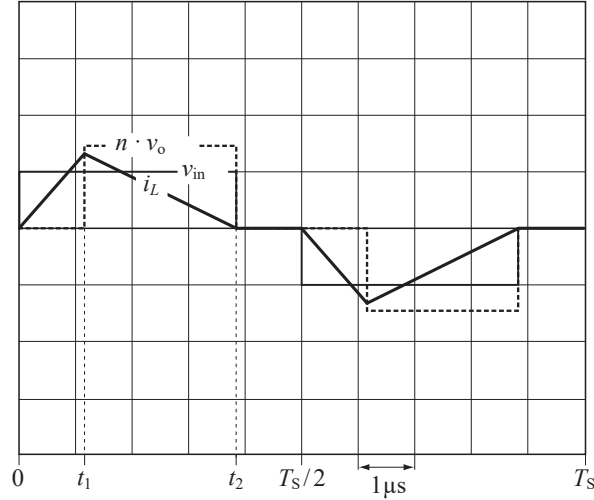
$$\begin{cases} I_{L_k}(t) = \frac{V_{in}(1-d)t}{L_k}, & \text{if } 0 \leq t \leq t_1 \\ I_{L_k}(t) = I_{L_k}(t_1) - \frac{dV_{in}(t-t_1)}{L_k} & \text{if } t_1 \leq t \leq t_2 \end{cases} \quad (2.26)$$

$$I_{L_{krms\ tri}} = \sqrt{\frac{\int_0^{T_s} I_{L_k}^2(t) dt}{T_s}} = \frac{\sqrt{3} \sqrt{2 \cdot \left(\left(\frac{V_p^2 \delta^3 d^2}{L_k^2 f_s^2} \right) + \left(\frac{V_p^2 \delta^3 d^3}{L_k^2 f_s^2 (1-d)} \right) \right)}}{3\pi^{\frac{3}{2}}} \quad (2.27)$$

To examine the leakage inductor's current levels when the input voltage (V_{in}) is greater than the output voltage (nV_o), please consult Figure 2.9. The findings are subsequently outlined in Equation 2.28.

$$\begin{cases} I_{L_k}(t) = \frac{(|V_{in}|t)}{L_k} + I_{L_k}(0), & \text{if } 0 \leq t \leq T_1 \\ I_{L_k}(t) = \frac{-|V_{in}(1-d)|(t-T_1)}{L_k} + \frac{V_{in}T_1}{L_k}, & \text{if } T_1 \leq t \leq T_2 \end{cases} \quad (2.28)$$

Figure 2.9 – Voltage and current waveforms in the leakage inductor for $V_i < nV_o$ triangular modulation .



Source : [14].

2.1.2.2 Soft-switching limits

The triangular modulation equations consist of three conduction times: T_1 , T_2 , and T_3 . Among these, T_3 represents the conduction time at which the current flowing through the transformer leakage inductor reaches zero.

To optimize power flow, set the conduction time T_3 to zero. Using this outcome in equations 2.21 and 3.29, the result is obtained 2.29.

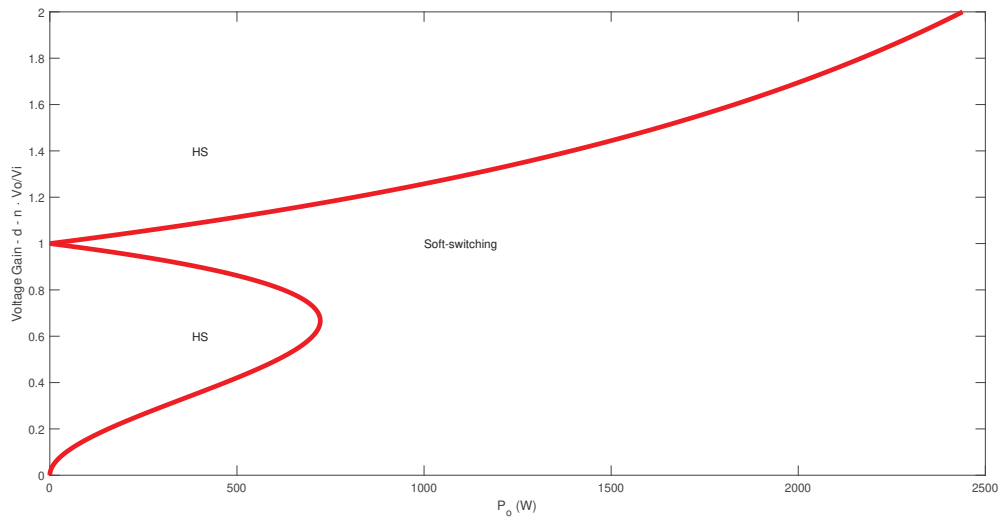
The derivation of these equations is explained in Appendix A, which provides the boundaries of soft-switching for triangular modulation. The detailed step-by-step derivation of these results can be found in Appendix A, where the Mathcad software was used for the respective development.

$$P_{max} = \begin{cases} \frac{(dV_{in})^2(1-d)}{4f_s L_k}, & \text{if } V_{in} > nV_o \\ \frac{V_{in}^2(d-1)}{4f_s L_k d}, & \text{if } V_{in} < nV_o \end{cases} \quad (2.29)$$

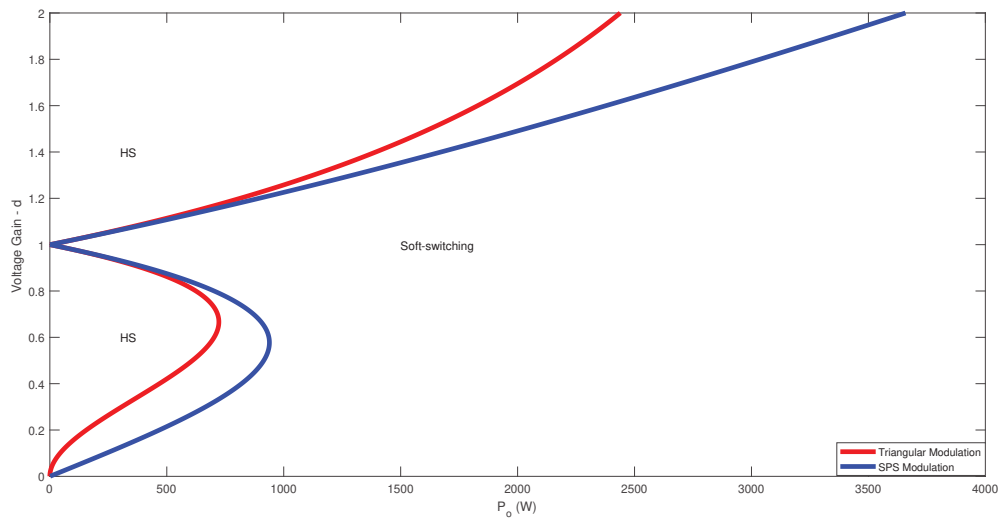
A diagram was generated that illustrates the voltage gain values of the output power using the results of equation 2.29, a diagram illustrating the voltage-gain values of the output power. This diagram is depicted in Figure 2.10.

2.1.2.3 Soft-switching constraints of SPS and triangular Modulations for Single-Phase DAB Converter

[34] notes that using SPS modulation results in a significant amount of reactive power when the voltage operating point deviates from the nominal operating point. Moreover, the shape of the transformer current cannot be controlled because of its dependence on both input and output voltage and phase shift.

Figure 2.10 – Soft-switching capability of DAB converter - triangular modulation.

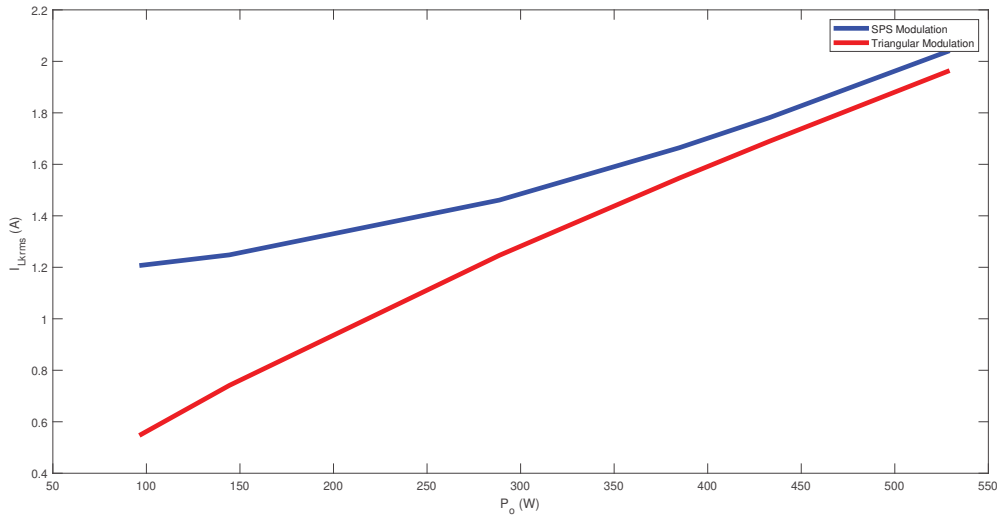
Source: From the author.

Figure 2.11 – Soft-switching limits - triangular and SPS modulations $d = 0.75$.

Source: From the author.

Meanwhile, according to [34], applying three-level voltages to the leakage inductance of a transformer can reduce reactive power and switching losses. In Figure 2.11, it can be seen that triangular modulation has a more extensive soft-switch range compared to SPS modulation. This analysis refers to the losses of SPS versus triangular modulation. As per [20], SPS modulation has a wide soft-switching zone when operating in a unity voltage ratio. However, when operating away from the unitary voltage gain, SPS modulation incurs high conduction and switching losses.

As depicted in Figure 2.11, the Single-Phase DAB converter modulated with the triangular technique has a broader range of soft-switching applicable for low-power operations. Figure 2.11 shows that although triangular modulation has a more expansive

Figure 2.12 – RMS level of current of leakage inductor of the transformer.

Source: From the author.

soft-switching zone, it uses a three-level voltage configuration over the transformer. In contrast, the SPS modulation uses a two-level variable.

As shown in Figure 2.12, the application of triangular modulation for the DAB converter results in a reduction in the RMS value of the current of the leakage inductor and is expected to lead to a decrease in conduction losses when the SPS modulation is compared to the triangular modulation, in their application to single-phase DAB converters.

2.2 CHAPTER OVERVIEW

To summarize, the SPS modulation is simple to use, requiring only one variable level to operate the power flow from the primary side to the secondary side. Additionally, when applied to the DAB converter, the SPS modulation has a wide soft-switching zone when the voltage-ratio gain is near unity.

However, it has a drawback when used in low-power applications. It loses the capability of soft-switching when the voltage-gain ratio is not near the unity zone, resulting in a high level of reactive power.

Also, it was noticed that for low-power applications of single-phase DAB converters, the configuration that employs triangular modulation reduces conduction losses.

Therefore, the triangular and SPS modulations are used for different configurations of DAB converters to reduce switching and conduction losses, as well as levels of reactive power for low-power operating points of DAB converters.

YY and Y Δ Single-Phase Modes of Three-Phase DAB Converters

As mentioned earlier, the DAB converter can be implemented in either a three-phase or single-phase configuration. These configurations are shown in Figures 2.2 and 2.3, respectively.

The input and output capacitor filters in three-phase DAB converters have a ratio of three times the switching frequency. This helps to decrease the filtering stresses experienced by the DC link capacitors. Moreover, the power flow is divided by a factor of 1/3, leading to reduced reactive power levels and lower switch turn-off losses [35].

The DAB Converter, introduced by [25] and illustrated in Figure 2.3, utilizes SPS modulation. Each semiconductor in each arm of the half-bridge experiences a 180-degree phase shift. Additionally, there is a phase shift (δ) between the arms on the primary and secondary sides.

According to [15], in the three-phase DAB converter, when SPS modulation is used, there is a phase displacement, δ , responsible for the power flow between the three-phase bridges of the primary and secondary. As per the citation, the Single-Phase DAB's SPS modulation has a simple configuration, a limited region of soft-switching, and a high level of reactive power when operating away from the unitary voltage gain.

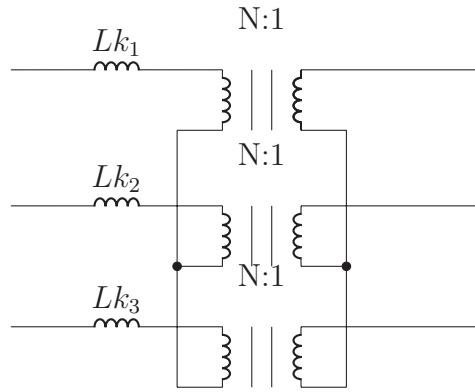
The three-phase DAB converter presented by [25] is known as the YY configuration due to the winding configuration of the transformer of the respective three-phase DAB converter [35].

The transformer of the three-phase DAB converter can have the following configurations: YY, Y Δ and $\Delta - \Delta$. When comparing the YY and $\Delta - \Delta$ configurations, they perform equally, noticing that $\Delta - \Delta$ has $\sqrt{3}$ reduction in winding current [35].

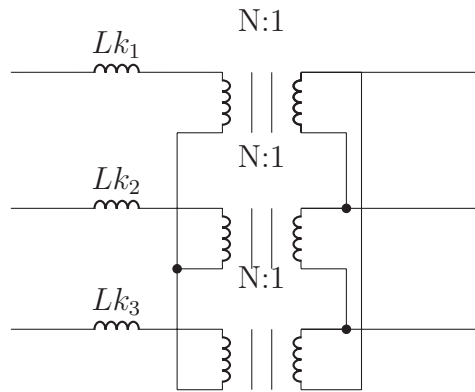
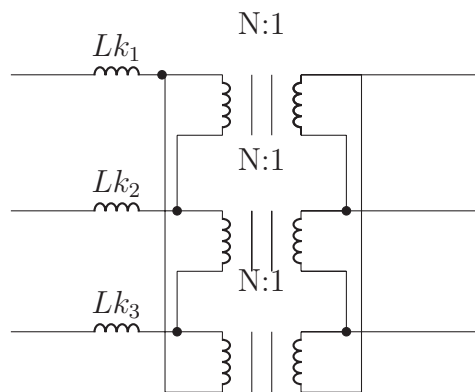
Among the topologies of the three-phase DAB converter, the Y- Δ topology has the best overall performance. It is particularly effective in the power range 50% - 80% and results in lower current stresses in the switches, transformer, and filter capacitors [35].

In addition, there is the availability to operate the DAB3 converter in a single-phase operation, where this is obtained through the non-utilization of some of the controlling signals of the switches or the control of the phase shift of the DAB3 converter [15].

According to [15, 21], this operation can result in persistence of the failure mode or can be used as an operation mode of low-power configurations, aiming to enhance the

Figure 3.1 – Three-phase transformer configurations .

(a) YY three-phase transformer.

(b) Y Δ three-phase transformer .(c) $\Delta\Delta$ three-phase transformer .

Source: [35].

converter's efficiency.

Chapter 2 studies the SPS and triangular modulations for the single-phase DAB converter with respect to power transmission, current levels in the leakage inductor, and soft-switching capabilities.

This chapter reviews the single-phase modes for the YY and YΔ DAB Converters with the SPS modulation, as well as the application of the single-phase modes for triangular modulation in the YY and YΔ Three-Phase DAB Converters.

3.1 YY THREE-PHASE DAB CONVERTER WITH SPS MODULATION

3.1.1 Power Flow

The derivations in [25] describe the transmission power for the SPS modulation of the YY DAB converter described by 3.1.

$$P(\delta) = \begin{cases} \frac{d\delta V_{in}^2}{2\pi f_s Lk} \left(\frac{2}{3} - \frac{\delta}{2\pi} \right), & \text{if } 0 \leq \delta \leq \frac{\pi}{3} \\ \frac{d\delta V_{in}^2}{2\pi f_s Lk} \left(1 - \left(\frac{\delta}{\pi} \right) - \frac{\pi}{18\delta} \right), & \text{if } \frac{\pi}{3} < \delta \leq \frac{\pi}{2} \end{cases} \quad (3.1)$$

3.1.2 Soft-Switching Limits

The soft-switching conditions for the YY Three-Phase DAB Converter are presented in 3.2 and 3.3 [25].

$$d < \begin{cases} \frac{1}{1 - \frac{3\delta}{2\pi}}, & \text{if } 0 \leq \delta \leq \frac{\pi}{3} \\ \frac{1}{\frac{3}{2} - \frac{3\delta}{\pi}}, & \text{if } \frac{\pi}{3} < \delta \leq \frac{\pi}{2} \end{cases} \quad (3.2)$$

$$d > \begin{cases} 1 - \frac{3\delta}{2\pi}, & \text{if } 0 \leq \delta \leq \frac{\pi}{3} \\ \frac{3}{2} - \frac{3\delta}{\pi}, & \text{if } \frac{\pi}{3} < \delta \leq \frac{\pi}{2} \end{cases} \quad (3.3)$$

3.2 YΔ THREE-PHASE DAB CONVERTER WITH SPS MODULATION

The analysis of soft-switching constraints for the YΔ Three-Phase DAB Converter is presented in 3.4, for the SPS modulation [25].

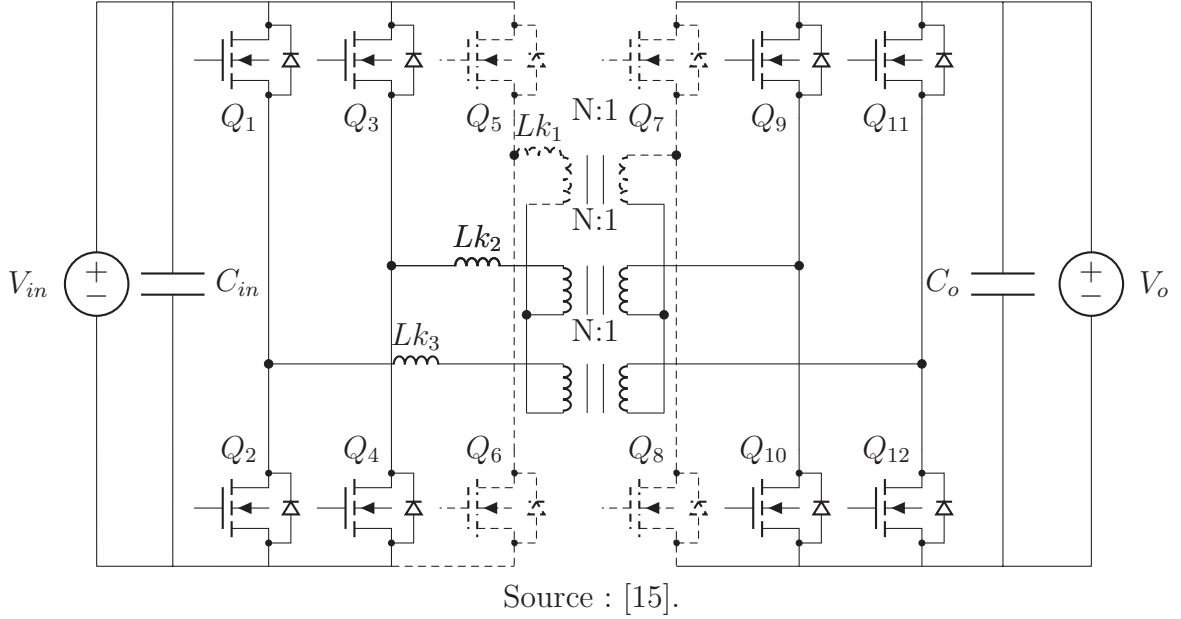
$$P(\delta) = \begin{cases} \frac{dV_{in}^2 \delta}{2\sqrt{3}\pi f_s Lk}, & \text{if } 0 \leq \delta \leq \frac{\pi}{6} \\ \frac{dV_{in}^2}{2\sqrt{3}\pi f_s Lk} \left(\frac{3}{2} \left(\delta - \frac{\delta^2}{\pi} \right) - \frac{\pi}{24} \right), & \text{if } \frac{\pi}{6} < \delta \leq \frac{\pi}{2} \end{cases} \quad (3.4)$$

3.2.1 Soft-Switching Limits

Additionally, [36] presents the soft switching conditions for the YΔ converter, which are shown in 3.5 and 3.6.

$$d_p < \begin{cases} \frac{2\sqrt{3}}{3}, & \text{if } 0 \leq \delta \leq \frac{\pi}{6} \\ \frac{4\sqrt{3}\pi}{9\pi - 18\delta}, & \text{if } \frac{\pi}{6} < \delta \leq \frac{\pi}{2} \end{cases} \quad (3.5)$$

Figure 3.2 – Schematic of the YY-11 DAB converter single-phase mode with SPS modulation .



$$d_s > \begin{cases} \frac{\sqrt{3}}{2}, & \text{if } 0 \leq \delta \leq \frac{\pi}{6} \\ \frac{\sqrt{3}(3\pi-6\delta)}{4\pi}, & \text{if } \frac{\pi}{6} < \delta \leq \frac{\pi}{2} \end{cases} \quad (3.6)$$

3.3 SINGLE-PHASE OPERATION OF THE THREE-PHASE THE DAB CONVERTER

As described in this thesis, the DAB3 can be operated in a single-phase mode to enhance efficiency in low-power operations. The topologies analyzed in this chapter are YY and YΔ DAB3 Converters that can operate with SPS or Triangular Modulations. For the YY DAB3 configuration, there are the configurations YY-11, which consists of the non-utilization of one arm of switches of the primary and secondary bridges of the DAB3 Converter, described in Figure 3.2, and also YY-00, where two arms of the primary and secondary bridges of the DAB Converter operate in parallel, described in Figure 3.3 [15]. Meanwhile, for the YΔ configuration two configurations are expected, one named YΔ 10, described in Figure 3.4 which means that one arm of the primary bridge is not used and that two arms of the secondary bridge of the DAB3 YΔ are operated in parallel and receive the same command. In addition, a second configuration, named YΔ 01, is predicted in Figure 3.5, meaning that two arms of the primary bridge operate in parallel and receive the same command and that one of the arms of the secondary is not used.

3.3.1 Single-Phase Operation of the YY and YD Three Phase DAB Converters with Single-Phase Shift Modulation

3.3.1.1 YY Three-Phase DAB Converter in Single-Phase Operation with SPS Modulation

In this section, the power flow equations, the leakage inductor current levels and the soft switching conditions for the single-phase modes YY-11 and YY-00 of the DAB3 YY are derived for SPS modulation [15]. In the first single-phase mode (YY-11), each branch of the primary and secondary bridges is maintained open, as shown in Figure 3.2. Meanwhile, each branch of the secondary and primary bridges received a single command to operate in the second single-phase mode, as shown in Figure 3.3.

3.3.2 YY-11 Mode with SPS Modulation

The YY-11 converter, with SPS modulation, has a single-phase mode that maintains one arm of the input bridge and one arm of the output bridge. This mode is shown in Figure 3.2. In this single-phase mode, the equivalent inductance is $L_{eq} = 2Lk$, and the transformer gain is maintained as in the DAB3 YY [15].

The configuration for the YY-11 DAB converter is also shown in Figure 3.2. As shown in Figure 3.2, the leakage inductor of one of the phases has been cut off from the primary to the secondary side, not allowing current to flow in one of the leakage inductors. To analyze the power flow equations, phase-shift angle, leakage inductor current, and soft-switching constraints, the equivalent inductance [25] and transformer are used in the equations of the single-phase DAB converter. This results in the following equations: 3.7 for power flow, 3.8 for phase shift, 3.9 for leakage inductor current levels, 3.11 for initial current and 3.12 for soft-switching constraints [25].

$$P = V_{in}^2 d \delta \frac{(\pi - |\delta|)}{2\omega_s \pi Lk} \quad (3.7)$$

$$\delta = \frac{\pi \pm \sqrt{\pi^2 - \frac{8\pi\omega_s Lk P}{V_{in}^2 d}}}{2} \quad (3.8)$$

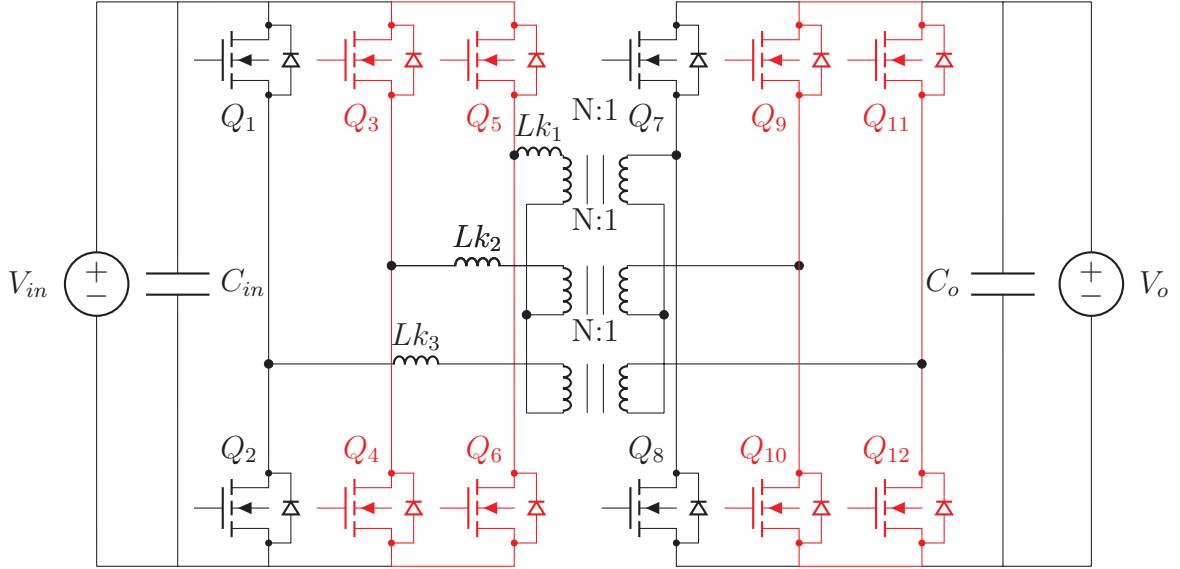
$$\begin{cases} I_{Lk}(\theta) = \frac{(V_{in} + V_o')\theta}{2\omega_s Lk} + I_{Lk}(0), & \text{if } 0 \leq \theta \leq \delta \\ I_{Lk}(\theta) = \frac{V_{in} - V_o'(\theta - \delta)}{2\omega_s Lk} + I_{Lk}(\delta), & \text{if } \delta \leq \theta \leq \pi \end{cases} \quad (3.9)$$

$$I_{Lk}(\pi) = -I_{Lk}(0) \quad (3.10)$$

$$I_{Lk}(0) = -\frac{2V_o'\delta + V_{in}\pi - V_o'\pi}{4\omega_s Lk} \quad (3.11)$$

$$\begin{cases} \delta > \frac{\pi(d-1)}{2d}, & \text{if } d > 1 \\ \delta > \frac{\pi(1-d)}{2}, & \text{if } d < 1 \end{cases} \quad (3.12)$$

Figure 3.3 – Schematic of the YY-00 DAB converter single-phase mode with SPS modulation .



Source: [15].

3.3.3 YY-00 Mode with SPS Modulation

Based on Figure 3.3 [15], the YY-00 single-phase mode of DAB3 YY, with SPS modulation, involves the unified command signaling of two arms of the primary and secondary bridges. Red switches are operated in parallel, meaning they have the same current stress ($L_{k_1} = L_{k_2} = L_{k_3}$) in each arm of the half-bridges and receive the same command simultaneously. As in one of the phases of the Δ secondary side of the DAB Converter that is shortcircuited, the primary voltage is also shortcircuited, blocking in this way the path of current in the antiparallel diodes of the switches Q_3 and Q_4 . In the secondary of the DAB converter presented, Figure 3.3 presents the following components:

- Q_1 - Q_{12} : Semiconductors Switches;
- Lk_1, Lk_2, Lk_3 : Leakage Inductors of the YY three-phase.
- C_{in} : Input capacitor.
- C_o : Output capacitor.
- $N : 1$: Primary turn-ratio.

The equivalent inductor has an inductance of $L_{eq} = 1.5Lk$. The transformer gain of the YY-00 single-phase mode is maintained. Using the equivalent inductance, transformer gain, and equations from [25], it can be obtained the following:

- 3.13 for power flow;
- 3.14 for phase-shift;

- 3.15 for the leakage inductor current levels;
- 3.16 for initial current;
- 3.17 for the soft-switching constraints;

$$P = \frac{V_{in}^2 d \delta (\pi - |\delta|)}{\frac{3}{2} \omega_s \pi Lk} \quad (3.13)$$

$$\delta = \frac{\pi \pm \sqrt{\pi^2 - \frac{6\pi\omega_s Lk P}{V_{in}^2 d}}}{2} \quad (3.14)$$

$$\begin{cases} I_{Lk}(\theta) = \frac{(V_{in} + V'_o)(\theta)}{\frac{3}{2} \omega_s Lk} + I_{Lk}(0), & \text{if } 0 \leq \theta \leq \delta \\ I_{Lk}(\theta) = \frac{(V_{in} - V'_o)(\theta - \delta)}{\frac{3}{2} \omega_s Lk} + I_{Lk}(\delta), & \text{if } \delta \leq \theta \leq \pi \end{cases} \quad (3.15)$$

$$I_{Lk}(0) = -\frac{2V'_o \delta + V_{in} \pi - V'_o \pi}{3\omega_s Lk} \quad (3.16)$$

$$\begin{cases} \delta > \frac{\pi(d-1)}{2d}, & \text{if } d > 1 \\ \delta > \frac{\pi(1-d)}{2}, & \text{if } d < 1 \end{cases} \quad (3.17)$$

3.3.3.1 YD Three-Phase DAB Converter in Single-Phase Operation with SPS Modulation

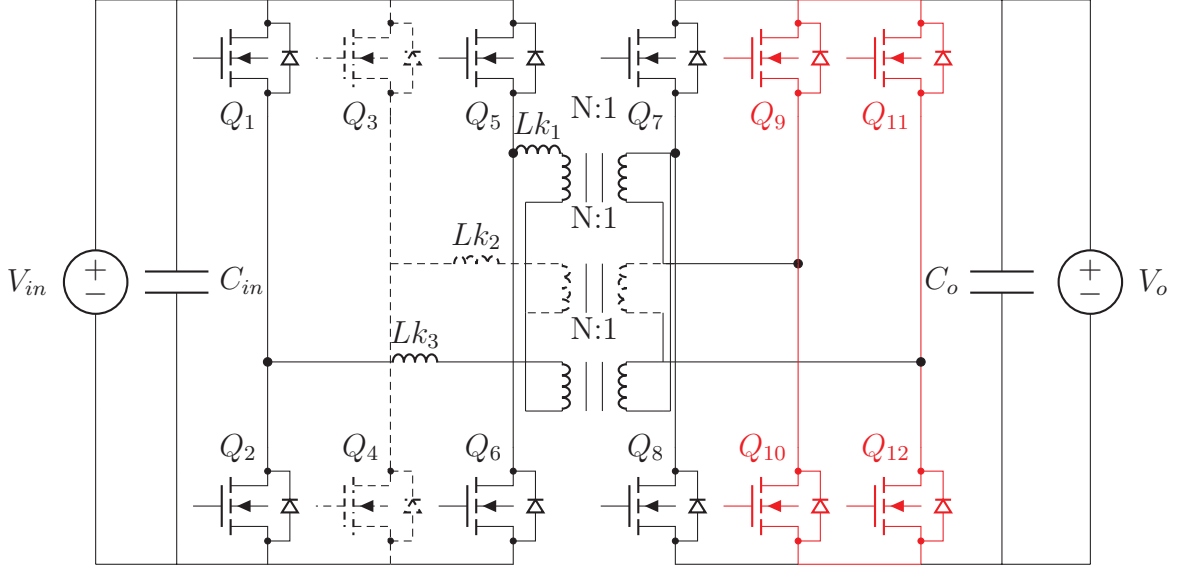
The DAB3 YΔ, with SPS modulation, configuration can be used in both three-phase and single-phase modes to improve energy efficiency [15]. One of the arms of the converter on the Y-side is kept open in the DAB3 YΔ 10 single-phase mode, while two arms on the Δ side are operated in parallel as shown in Figure 3.4. This configuration increases the efficiency of the converter [15].

The Y-Δ equivalent inductance is $L_{eq} = 2Lk$ and the transformer gain is $\frac{\sqrt{3}n}{2}$ [15]. With these properties and the equations from [25] for the DAB converter, the following results can be derived:

- 3.18 for power flow;
- 3.19 for phase-shift;
- 3.21 for leakage inductor current levels;
- 3.22 for initial current;
- 3.23 for soft-switching constraints;

$$P = \frac{V_{in}^2 d \sqrt{3} \delta (\pi - |\delta|)}{3\omega_s Lk \pi} \quad (3.18)$$

Figure 3.4 – Schematic of the YΔ-10 DAB converter, single-phase mode with SPS modulation .



Source: [15].

$$\delta = \frac{\pi \pm \sqrt{\pi^2 - \frac{4\sqrt{3}\pi\omega_s LkP}{V_{in}^2 d}}}{2} \quad (3.19)$$

$$I_{Lk}(\theta) = \frac{(V_{in} + \frac{2\sqrt{3}V'_o}{3})(\theta)}{2\omega_s Lk} + I_{Lk}(0) \quad (3.20)$$

$$\begin{cases} I_{Lk}(\theta) = \frac{(V_{in} + \frac{2\sqrt{3}V'_o}{3})(\theta)}{2\omega_s Lk} + I_{Lk}(0), & \text{if } 0 \leq \theta \leq \delta \\ I_{Lk}(\theta) = \frac{(V_{in} - \frac{2\sqrt{3}V'_o}{3})(\theta - \delta)}{2\omega_s Lk} + I_{Lk}(\delta), & \text{if } \delta \leq \theta \leq \pi \end{cases} \quad (3.21)$$

$$I_{Lk}(0) = -\frac{((V'_o 2\frac{\sqrt{3}}{3})(2\delta - \pi) + V_{in}\pi)}{4\omega_s Lk} \quad (3.22)$$

$$\begin{cases} \delta > \frac{\pi(d2\sqrt{3}-3)}{4\sqrt{3}d}, & \text{if } d > 1 \\ \delta > \pi \frac{(1-2\frac{\sqrt{3}d}{3})}{2}, & \text{if } d < 1 \end{cases} \quad (3.23)$$

3.3.4 YΔ-01 Single-Phase Mode with SPS Modulation

Meanwhile, when both arms on the Y side are operated in parallel and one arm of the Δ is kept open, as shown in Figure 3.5 [15]. According to the configuration, the equivalent inductor can be determined using the Equation $L_{eq} = 1.5Lk$. Additionally, the transformer gain of the configuration is $\frac{2n}{\sqrt{3}}$ as stated in [15]. By combining these properties with the equations provided in [25], the following equations can be obtained for the single-phase mode of the DAB converter:

- 3.24 for the power flow;
- 3.25 for the phase-shift;

3.3.5.1 YY Three-Phase DAB Converter in Single-Phase Operation with Triangular Modulation

This study focuses on single phase modes in terms of power flow, leakage inductor current levels, and soft-switching constraints to study the YY DAB converter for triangular modulation.

In Chapter 2, equations were derived for soft-switching constraints, transmission power, and conduction times for the Single-Phase DAB Converter with Triangular modulation. Previous discussions have also covered the single-phase modes of YY and YΔ DAB converters for SPS modulation.

As a central contribution to this Master thesis, this study analyzes and provides equations for the single-phase modes of the three-phase DAB converters operating with triangular modulation. The configuration of parallel half-bridges used in the results of the SPS modulation can be applied to the triangular modulation. However, instead of equivalent single-phase modes with SPS modulation, this study presents the results of equations of equivalent modes with triangular modulation.

Therefore, the following sections present the equations and working principles of the single-phase equivalent modes of the YY and YΔ DAB converters.

3.3.6 YY-11 Single-Phase Mode with Triangular Modulation

In YY-11's single-phase mode, the converter maintains the transformer gain of the SPS modulation and has an equivalent inductance of $2Lk$ for the triangular modulation. The previous sections show the working principles for the single-phase DAB Converter with Triangular Modulation. As shown in the single-phase YY-11 mode, there is an equivalent single-phase DAB converter with the equivalent inductance of $2Lk$, and using this inductance in the single-phase DAB converter with triangular modulation, from [14], the following results apply when $V_{in} > nV_o$:

- 3.29, for power flow with $V_{in} > nV_o$.
- 3.30, for phase-shift with $V_{in} > nV_o$.
- 3.31, for conduction time T_1 with $V_{in} > nV_o$.
- 3.32, for conduction time T_2 with $V_{in} > nV_o$.
- 3.33, half-period conduction time T_3 .

$$P = \frac{\delta^2 d^2 V_{in}^2}{2\pi^2 f_s Lk(1-d)} \quad (3.29)$$

$$\delta = \pi \sqrt{\frac{P f_s Lk(1-d)}{2d^2 V_{in}^2}} \quad (3.30)$$

$$T_1 = \frac{\delta d}{\pi f_s (1-d)} \quad (3.31)$$

$$T_2 = \frac{\delta}{\pi f_s} \quad (3.32)$$

$$T_3 = \frac{T_s}{2} - T_2 - T_1 \quad (3.33)$$

It is possible to obtain the relations regarding the levels of current in the leakage inductor, presented in Equation 3.34, using the results from power flow equations, phase-shift, and conduction times.

$$\begin{cases} I_{Lk}(t) = \frac{V_{in}(1-d)t}{2Lk}, & \text{if } 0 \leq t \leq T_1 \\ I_{Lk}(t) = I_{Lk}(T_1) - \frac{dV_{in}(t-T_1)}{2Lk} & \text{if } T_1 \leq t \leq T_2 \end{cases} \quad (3.34)$$

When using the equations from [14] and the equivalent results for YY-11 single-phase configuration, the equation 3.35 represents the soft-switching limit for the YY-11 single-phase mode with triangular modulation.

$$P_{max} = \frac{(dV_{in})^2(1-d)}{8f_s Lk} \quad (3.35)$$

Furthermore, for the same equivalent inductance and transformer gain, the resulting power flow, phase-shift, and conduction times can be obtained for $V_{in} < nV_o$, using the following conclusions:

- 3.36 for the power flow with $V_{in} < nV_o$;
- 3.37 for the phase-shift with $V_{in} < nV_o$;
- 3.38 for the T_1 conduction time with $V_{in} < nV_o$;
- 3.39 for the T_2 conduction time with $V_{in} < nV_o$.
- 3.40 for half period with $V_{in} < nV_o$.

$$P = \frac{\delta^2 V_{in}^2 d}{2\pi^2 f_s Lk (d-1)} \quad (3.36)$$

$$\delta = \frac{\pi}{V_{in}} \sqrt{2 \frac{P f_s Lk (d-1)}{d}} \quad (3.37)$$

$$T_1 = \frac{\delta}{\pi f_s} \quad (3.38)$$

$$T_2 = \frac{\delta}{\pi f_s (d-1)} \quad (3.39)$$

$$T_3 = \frac{T_s}{2} - T_2 - T_1 \quad (3.40)$$

With the results of equivalencies for the YY-11 and the equations derived from [34], using $T_3 = 0$, the relations of leakage inductor current levels for the single-phase mode with triangular modulation are presented in Equation (3.41).

$$\begin{cases} I_{Lk}(t) = \frac{|V_{in}|t}{2Lk} + I_{Lk}(0), & \text{if } 0 \leq t \leq T_1 \\ I_{Lk}(t) = \frac{-|V_{in}(1-d)|(t-T_1)}{2Lk} + \frac{V_{in}T_1}{2Lk}, & \text{if } T_1 \leq t \leq T_2 \end{cases} \quad (3.41)$$

Aiming to obtain soft-switching constraints for YY-11 single-phase mode with triangular modulation and $V_{in} < nV_o$, utilizing the results from [14], is concluded the relation 3.42.

$$P_{max} = \frac{V_{in}^2(d-1)}{8f_s Lk d} \quad (3.42)$$

3.3.7 YY 00 Single-Phase Mode with Triangular Modulation

In the YY-00 single-phase mode, the equivalent inductance is $L_{eq} = 1.5Lk$, and the transformer gain is the same as the DAB3 YY with SPS modulation when analyzed for the triangular modulation. This was stated in [15]. Combining the results from [15] and [14], can be obtained the equations for power flow (3.43), phase-shift (3.44), T_1 conduction time (3.45), T_2 conduction time (3.46), and T_3 for half period (3.47). These results are applicable when $V_{in} > nV_o$.

$$P = \frac{2\delta^2 d^2 V_{in}^2}{3\pi^2 f_s Lk(1-d)} \quad (3.43)$$

$$\delta = \pi \sqrt{\frac{2P f_s Lk(1-d)}{3d^2 V_{in}^2}} \quad (3.44)$$

$$T_1 = \frac{\delta d}{\pi f_s(1-d)} \quad (3.45)$$

$$T_2 = \frac{\delta}{\pi f_s} \quad (3.46)$$

$$T_3 = \frac{T_s}{2} - T_2 - T_1 \quad (3.47)$$

Aiming to analyze the current levels of the leakage inductor, was utilized the equations presented in [14]. Additionally, was employed the equivalency results for the YY-00 single-phase mode with triangular modulation, where the mathematical relations, using $T_3 = 0$, are given in 3.48.

$$\begin{cases} I_{Lk}(t) = \frac{2V_{in}(1-d)t}{3Lk}, & \text{if } 0 \leq t \leq T_1 \\ I_{Lk}(t) = I_{Lk}(T_1) - \frac{2dV_{in}(t-T_1)}{3Lk} & \text{if } T_1 \leq t \leq T_2 \end{cases} \quad (3.48)$$

The soft-switching constraint of the single-phase YY-11 mode can be obtained, as

shown in 3.49.

$$P_{max} = \frac{(dV_{in})^2(1-d)}{6f_s Lk} \quad (3.49)$$

Based in the results of equivalency for the YY-00 single-phase mode, the results from [15] and [14], it is possible to obtain the following relations: 3.50, for power flow, 3.51, for phase-shift, 3.52, for T_1 conduction time, 3.53 for T_2 conduction time, T_3 , for half period time, and 3.55, for leakage inductor current levels, for $V_{in} < nV_o$.

$$P = \frac{2\delta^2 V_{in}^2 d}{3\pi^2 f_s Lk (d-1)} \quad (3.50)$$

$$\delta = \frac{\pi}{V_{in}} \sqrt{\frac{2P f_s Lk (d-1)}{3d}} \quad (3.51)$$

$$T_1 = \frac{\delta}{\pi f_s} \quad (3.52)$$

$$T_2 = \frac{\delta}{\pi f_s (d-1)} \quad (3.53)$$

$$T_3 = \frac{T_s}{2} - T_2 - T_1 \quad (3.54)$$

$$\begin{cases} I_{Lk}(t) = \frac{2|V_{in}|t}{3Lk} + I_{Lk}(0), & \text{if } 0 \leq t \leq T_1 \\ I_{Lk}(t) = \frac{-2|V_{in}(1-d)|(t-T_1)}{3Lk} + \frac{2V_{in}T_1}{3Lk}, & \text{if } T_1 \leq t \leq T_2 \end{cases} \quad (3.55)$$

Moreover, the soft-switching constraints for YY-00 single-phase mode with triangular modulation can be obtained using the results from [14], using $T_3 = 0$, as shown in 3.56.

$$P_{max} = \frac{V_{in}^2 (d-1)}{6f_s Lkd} \quad (3.56)$$

3.3.7.1 YΔ Three-Phase DAB Converter in Single-Phase Operation with Triangular Modulation

Aiming to obtain equations for power flow and soft-switching constraints of the single-phase modes of the YΔ Three-Phase DAB Converter, with Triangular Modulation, the configurations of the YΔ – 10 and YΔ – 01 are applied to analyze single-phase modes of the YΔ Three-Phase DAB Converter.

In the YΔ – 10 single-phase configuration, when the triangular modulation is applied, the equivalent inductance of the single-phase equivalent mode can be calculated using the relation $L_{eq} = 2Lk$, while the transformer gain can be calculated as $\frac{\sqrt{3}n}{2}$. Using these values and the results for triangular modulation from [14], can be derived the following equations: 3.57 for power flow, 3.58 for phase-shift, 3.59 for the conduction time of T_1 , and 3.60 and 3.61 for the conduction times of T_2 and T_3 , respectively. These results

are applicable only when $V_{in} > nV_o$.

$$P = \frac{\delta^2 (d^{\frac{2\sqrt{3}}{3}})^2 V_{in}^2}{2\pi^2 f_s Lk (1 - d^{\frac{2\sqrt{3}}{3}})} \quad (3.57)$$

$$\delta = \pi \sqrt{\frac{P f_s 2Lk (1 - d^{\frac{2\sqrt{3}}{3}})}{(d^{\frac{2\sqrt{3}}{3}})^2 V_{in}^2}} \quad (3.58)$$

$$T_1 = \frac{\delta d^{\frac{2\sqrt{3}}{3}}}{\pi f_s (1 - d^{\frac{2\sqrt{3}}{3}})} \quad (3.59)$$

$$T_2 = \frac{\delta}{\pi f_s} \quad (3.60)$$

$$T_3 = \frac{T_s}{2} - T_2 - T_1 \quad (3.61)$$

Furthermore, the equations for leakage inductor current levels and soft-switching constraints are derived in 3.62 and 3.63, respectively, using equivalency results, $T_3 = 0$ and relations from [14].

$$\begin{cases} I_{Lk}(t) = \frac{V_{in}(1-d^{\frac{2\sqrt{3}}{3}})t}{2Lk}, & \text{if } 0 \leq t \leq T_1 \\ I_{Lk}(t) = I_{Lk}(T_1) - \frac{d^{\frac{2\sqrt{3}}{3}}V_{in}(t-T_1)}{2Lk} & \text{if } T_1 \leq t \leq T_2 \end{cases} \quad (3.62)$$

$$P_{max} = \frac{(d^{\frac{2\sqrt{3}}{3}}V_{in})^2(1 - d^{\frac{2\sqrt{3}}{3}})}{8f_s Lk} \quad (3.63)$$

The following conclusions are obtained for the YΔ 10 configuration with triangular modulation when using the equivalency for the YΔ and applying the s from [15] and [14] for the $V_{in} < nV_o$ configuration: (3.64) for power flow, (3.65) for phase-shift, (3.66) for conduction time T_1 , (3.67) for conduction time T_2 , and T_3 for half-period time.

$$P = \frac{\delta^2 V_{in}^2 d^{\frac{2\sqrt{3}}{3}}}{2\pi^2 f_s Lk (d^{\frac{2\sqrt{3}}{3}} - 1)} \quad (3.64)$$

$$\delta = \frac{\pi}{V_{in}} \sqrt{2 \frac{P f_s Lk (d^{\frac{2\sqrt{3}}{3}} - 1)}{d^{\frac{2\sqrt{3}}{3}}}} \quad (3.65)$$

$$T_1 = \frac{\delta}{\pi f_s} \quad (3.66)$$

$$T_2 = \frac{\delta}{\pi f_s (d^{\frac{2\sqrt{3}}{3}} - 1)} \quad (3.67)$$

$$T_3 = \frac{T_s}{2} - T_2 - T_1 \quad (3.68)$$

To analyze leakage inductor current levels and soft-switching constraints, using the equivalency of the YΔ 10 single-phase mode with the triangular modulation for $V_{in} < nV_o$ and $T_3 = 0$, are obtained the (3.69) and (3.70), that are related to leakage inductor current levels and soft-switching constraints, respectively.

$$\begin{cases} I_{Lk}(t) = \frac{|V_{in}|t}{2Lk} + I_{Lk}(0), & \text{if } 0 \leq t \leq T_1 \\ I_{Lk}(t) = \frac{-|V_{in}(1-d\frac{2\sqrt{3}}{3})|(t-T_1)}{2Lk} + \frac{V_{in}T_1}{2Lk}, & \text{if } T_1 \leq t \leq T_2 \end{cases} \quad (3.69)$$

$$P_{max} = \frac{V_{in}^2(d\frac{2\sqrt{3}}{3} - 1)}{8f_s Lk d\frac{2\sqrt{3}}{3}} \quad (3.70)$$

In the YΔ-01 single-phase mode, when the triangular modulation is analyzed, the equivalent inductance is calculated as $L_{eq} = 1.5Lk$ and the transformer gain is determined as $\frac{2}{\sqrt{3}}n$. This applies to both the $V_{in} > nV_o$ and $V_{in} < nV_o$ configurations that are studied.

For the $V_{in} > nV_o$ configuration, the following relationships are obtained using the equivalency and equations from [14] and [15]: (3.71) for power flow, (3.72) for phase-shift, (3.73) for the T_1 conduction time, (3.74) for the T_2 conduction time, and T_3 for half period.

$$P = \frac{2\delta^2(d\frac{\sqrt{3}}{2})^2V_{in}^2}{3\pi^2f_sLk(1-d\frac{\sqrt{3}}{2})} \quad (3.71)$$

$$\delta = \pi \sqrt{\frac{2Pf_sLk(1-d\frac{\sqrt{3}}{2})}{3(d\frac{\sqrt{3}}{2})^2V_{in}^2}} \quad (3.72)$$

$$T_1 = \frac{\delta d\frac{\sqrt{3}}{2}}{\pi f_s(1-d\frac{\sqrt{3}}{2})} \quad (3.73)$$

$$T_2 = \frac{\delta}{\pi f_s} \quad (3.74)$$

$$T_3 = \frac{T_s}{2} - T_2 - T_1 \quad (3.75)$$

Aiming to analyze the levels of leakage inductor current and the soft-switching constraints for the DAB converter's YΔ 01 single-phase mode and $T_3 = 0$, are obtained the following results: (3.76) for leakage inductor current levels, and (3.77) for soft-switching constraints.

$$\begin{cases} I_{Lk}(t) = \frac{2V_{in}(1-d\frac{\sqrt{3}}{2})t}{3Lk}, & \text{if } 0 \leq t \leq T_1 \\ I_{Lk}(t) = I_{Lk}(T_1) - \frac{2d\frac{\sqrt{3}}{2}V_{in}(t-T_1)}{3Lk} & \text{if } T_1 \leq t \leq T_2 \end{cases} \quad (3.76)$$

$$P_{max} = \frac{(d\frac{\sqrt{3}}{2}V_{in})^2(1-d)}{6f_sLk} \quad (3.77)$$

In the YΔ 01 single-phase mode of the DAB converter, if the input voltage (V_{in}) is less than

the output voltage (nV_o), can be derived equations to calculate the power flow, phase-shift, and conduction times. The one for power flow is given by (3.78), the phase-shift is given by (3.79), the T_1 conduction time is given by (3.80), the T_2 conduction time is given by (3.74), and the one for half period is given by (3.82).

$$P = \frac{2\delta^2 V_{in}^2 d \frac{\sqrt{3}}{2}}{3\pi^2 f_s Lk (d \frac{\sqrt{3}}{2} - 1)} \quad (3.78)$$

$$\delta = \frac{\pi}{V_{in}} \sqrt{\frac{2P f_s Lk (d \frac{\sqrt{3}}{2} - 1)}{3d \frac{\sqrt{3}}{2}}} \quad (3.79)$$

$$T_1 = \frac{\delta}{\pi f_s} \quad (3.80)$$

$$T_2 = \frac{\delta}{\pi f_s (d \frac{\sqrt{3}}{2} - 1)} \quad (3.81)$$

$$T_3 = \frac{T_s}{2} - T_2 - T_1 \quad (3.82)$$

Furthermore, it is possible to obtain equations related to the current levels of the leakage inductor using Equation 3.83 and $T_3 = 0$. Soft-switching constraints can be obtained with Equation 3.84 using the single-phase triangular modulation equations from [14].

$$\begin{cases} I_{Lk}(t) = \frac{2|V_{in}|t}{3Lk} + I_{Lk}(0), & \text{if } 0 \leq t \leq T_1 \\ I_{Lk}(t) = \frac{-2|V_{in}(1-d\frac{\sqrt{3}}{2})|(t-T_1)}{3Lk} + \frac{2V_{in}T_1}{3Lk}, & \text{if } T_1 \leq t \leq T_2 \end{cases} \quad (3.83)$$

$$P_{max} = \frac{V_{in}^2 (d \frac{\sqrt{3}}{2} - 1)}{6f_s Lk d \frac{\sqrt{3}}{2}} \quad (3.84)$$

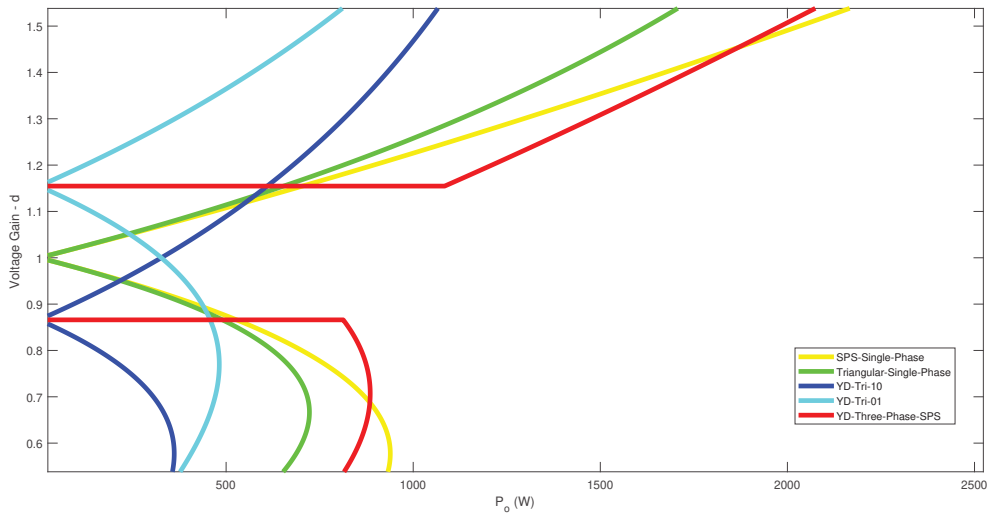
3.4 SOFT-SWITCHING LIMITS DIAGRAMS

It is possible to obtain soft-switching diagrams for the three-phase and single-phase modes of YY and YΔ DAB converters using the equations from this chapter. These diagrams help analyze the soft-switching range for different modulations used in single-phase and three-phase configurations of the DAB converter.

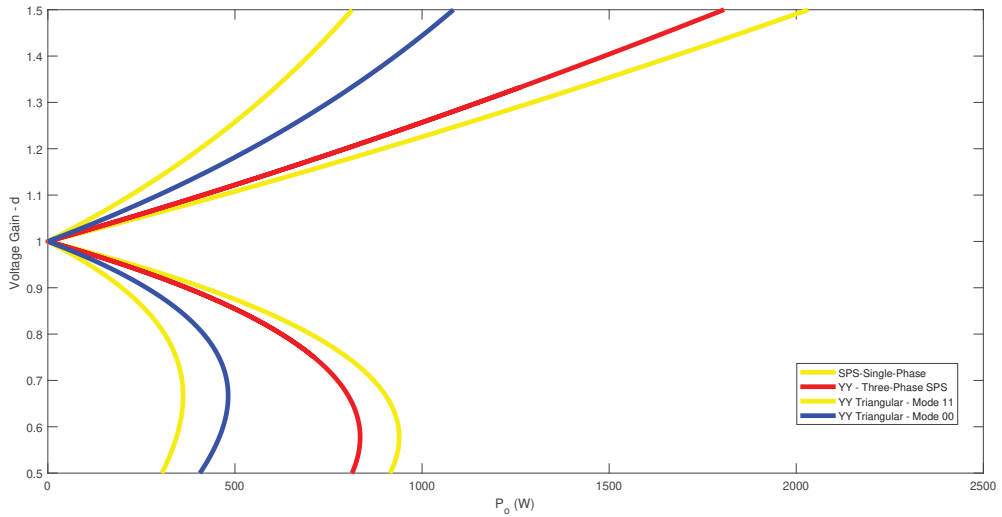
Regarding triangular modulation with YΔ configurations, Figure 3.6a depicts the soft-switching diagram showing the normalized output power. The figure also analyses the single-phase configuration for triangular modulation, single-phase modes of the YΔ configuration with triangular modulation, and three-phase YΔ configuration with SPS modulation.

For the YΔ DAB converter, with Figure 3.6a, it is possible to notice that the single-phase modes should operate when the power is less than 500 W, where the three-phase DAB converter cannot operate with ZVS with a gain near unity.

Figure 3.6 – Soft-Switching Limits for YY and YΔ Single-Phase and Three-Phase DAB Converters with SPS DAB Converters



(a) Soft-switching limits of the YD DAB converter with triangular modulations.



(b) Soft-switching limits of YY DAB converter operating with SPS and triangular modulations.

Source: From the author.

Soft-switching diagrams were obtained for the YY DAB configuration, which presents the soft-switching range for the YY3 DAB converter with SPS modulation and the single-phase modes of YY3 DAB with triangular modulation.

Meanwhile, for the YY DAB Converter, it is possible to notice that for output power less than 500 W, the Three-Phase DAB Converter has an extension of soft-switching capabilities

3.5 CHAPTER OVERVIEW

. The objective is to analyze the soft-switching constraints of the SPS modulation for the three-phase DAB converter (YY and Y Δ) and the single-phase modes of YY and Y Δ converters with triangular modulation. Analyzing the soft switching ranges of Figures 3.6a and 3.6b, it is possible to notice that the soft switching range is more comprehensive for the Y Δ single-phase modes when compared to YY single-phase modes with triangular modulation.

As a final analysis, for all single-phase modes of YY and Y Δ , there is an enlargement in the soft switching range when comparing the three-phase SPS modulated DAB converters with the single-phase modes with triangular modulation. This result of a more comprehensive soft-switching range shall be verified by the level of switching losses, which will be analyzed in the upcoming chapters. To obtain a power range for the single-phase modes YY and Y Δ , it is verified that there is an improvement in the soft-switching range within the power range of 0-500 W for the different configurations of single-phase modes.

The previous chapters, Chapter 2 and Chapter 3, discussed the simulation of single-phase modes such as YY, Y Δ , SPS, and Triangular modulations. These modes can be simulated using the software PLECS.

Table 4.1 contains the parameters used in the PLECS simulations, and are described in the following subsections. The voltage gain values presented in Table 4.1 are chosen according to distance to the point where $d = 1$, the values of $d = 0.75$ and $d = 1.25$ are selected as near unity and $d = 0.5$ and $d = 1.5$ as away from unity, which means that for values away from unity there is a narrower soft switching. as shown by zone [36].

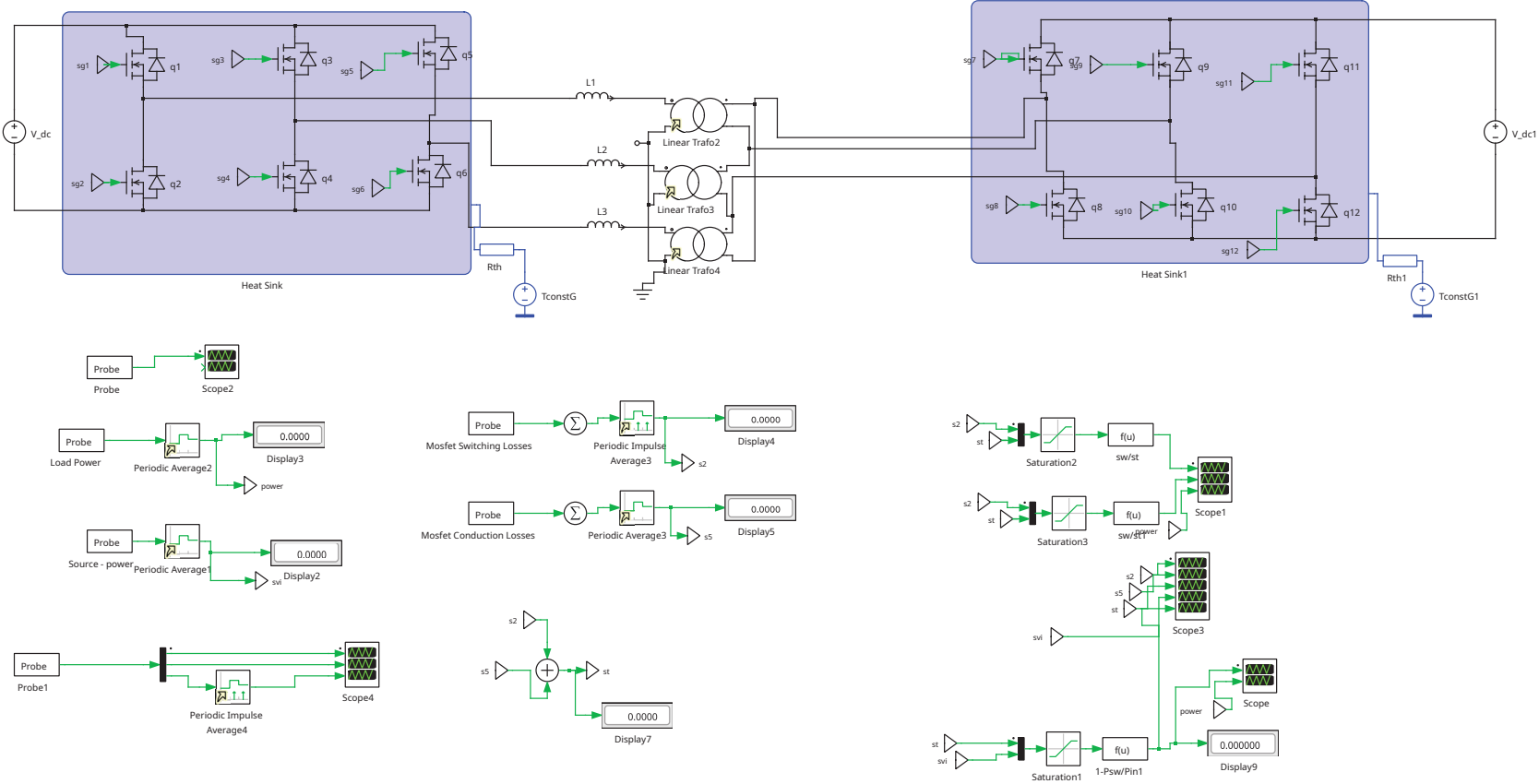
Figures 4.1 and 4.2 present schematic models of the Y Δ and YY DAB converters using PLECS.

Table 4.1 – Simulation parameters initialization

Description	Variable	Value
Input Voltage	V_{in}	400 [V]
Voltage Gain	d	0.5,0.75,1.25,1.5
Maximum Input Power	P	1,00 kV
Switching Frequency	f_s	100kHz
Transformer YY and YD gain	n	0.37
Leakage Inductance $S_{W_{1-6}}$	L_1, L_2, L_3 C3M0120090D	MOSFETs SIC 900 V/23A
MOSFETs SIC 650 V/38A	$S_{W_{7-12}}$	SCT3060AW7
On-Resistance $R_{DS(on)}$ Primary Side	R_{on_p}	120 m Ω
On-Resistance $R_{DS(on)}$ Secondary Side	R_{on_s}	60 m Ω

Source: From the author.

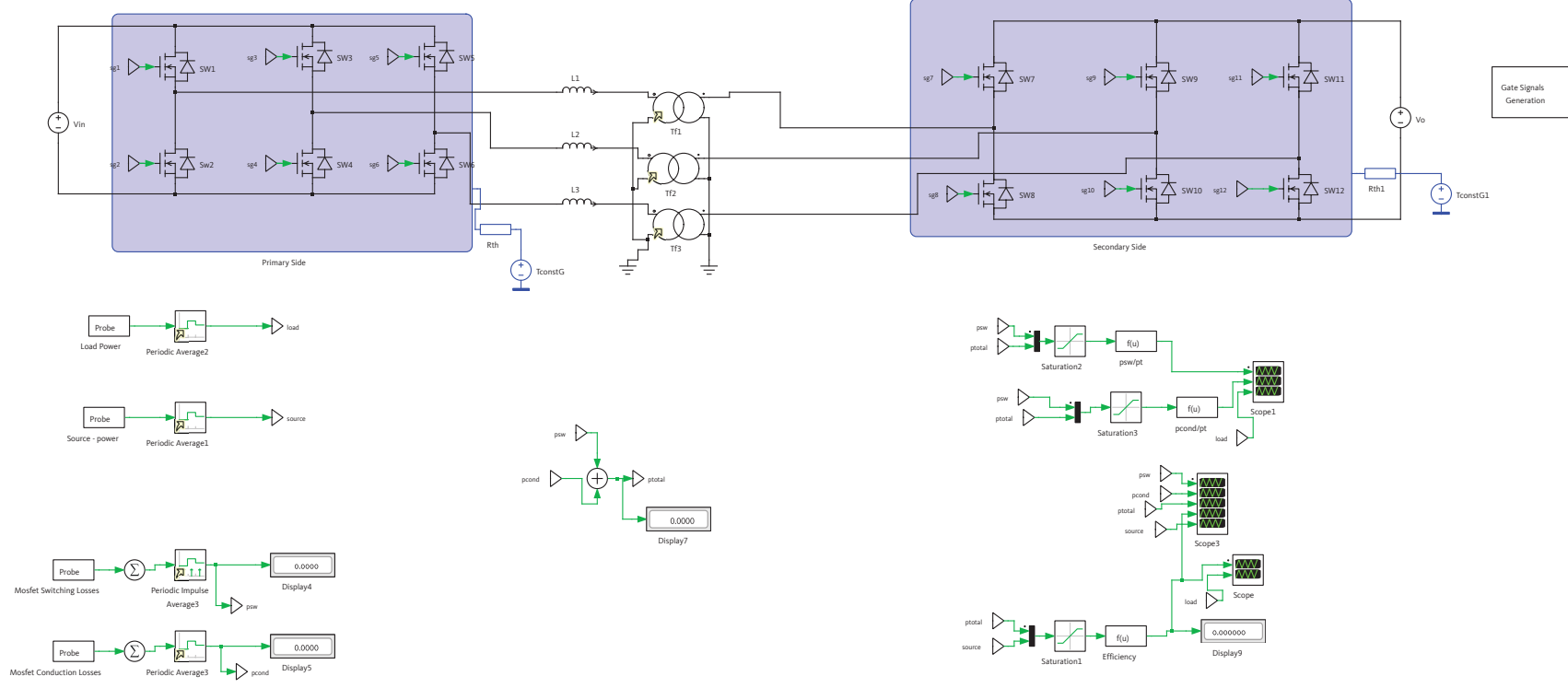
Figure 4.1 – Schematic of the $Y\Delta$ three-phase DAB converter in the PLECS software.



Sub

Source: From the author.

Figure 4.2 – Schematic of the YY Three-phase DAB converter in the PLECS software.



Source: From the author.

4.1 TRANSFORMER AND LEAKAGE INDUCTANCE

In YY and Y Δ DAB converters, the transformer is ideally operating without any core or winding losses. The transformer is a combination of an ideal single-phase transformer and a leakage inductance corresponding to each phase, whether in YY or Y Δ configuration.

Leakage inductance is a crucial component of the Dual-Active Bridge Converter, as it enables power flow. Proper sizing of the inductor is essential for the behavior of the model. A large leakage inductance can result in undesired reactive power and circulating current. Moreover, if the leakage inductance is too high, it can cause problems with the operation of the converter. In addition, if the leakage inductance is too small, the soft switchability capabilities of the topology are limited [33]. In this model, the leakage inductance of $82 \mu H$ is used for each phase, as per [15].

4.1.1 MOSFET Switches, Antiparallel diodes, and Losses

To obtain conduction and switching losses of MOSFET switches, the thermal model or PLECS model must be attached to each MOSFET component, where the data from 4.1 are assigned to each element of the *PLECS*[®]. The current script cannot handle the switching of MOSFETs and antiparallel diodes. Therefore, the thermal model for these components must be assigned manually based on the datasheet information. Alternatively, the thermal library file can automatically incorporate the thermal model. [27]. The method that employs automatic import from the thermal library is used to obtain high-accuracy losses for MOSFET switches [37, 38, 39].

The MOSFET's intrinsic body diode is utilized as an antiparallel diode in the circuit, while the thermal description is automatically imported from the datasheet.

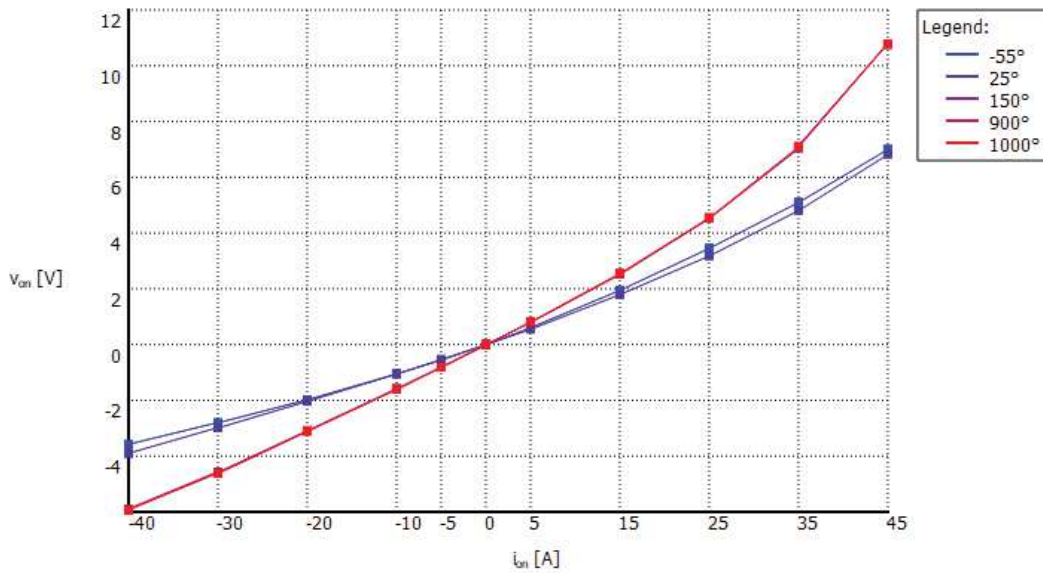
4.1.2 Losses Estimation

When importing data from the Thermal Library, it is possible to estimate conduction and switching losses using probes. To read the results of the probe, the periodic average block is used for conduction losses, while the Periodic Impulse Average Block is used to obtain the switching losses [27]. There are different types of losses in a power converter:

- primary and secondary conduction losses (Figures 4.3 and 4.4, respectively);
- primary and secondary switching turn-on losses (Figures 4.6 and 4.7, respectively.);
- primary and secondary switching turn-off losses (Figures 4.8 and 4.9, respectively);

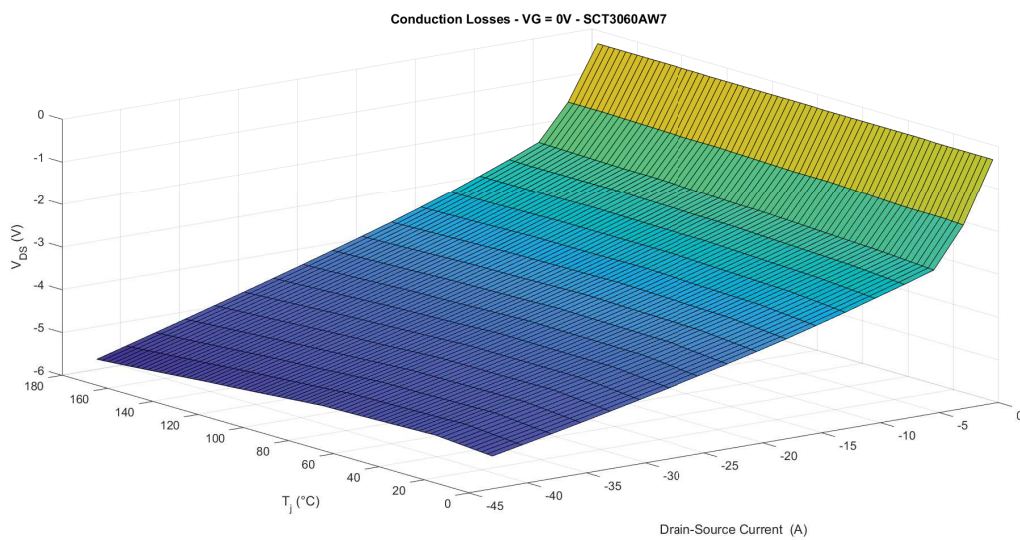
Figure 4.10 shows the structure used in PLECS to obtain the switching and conduction losses. These losses result in the total average losses of the converter, which can be in YY or Y Δ configurations.

Figure 4.3 – Conduction losses of the C3M0120090D MOSFET and body Diode

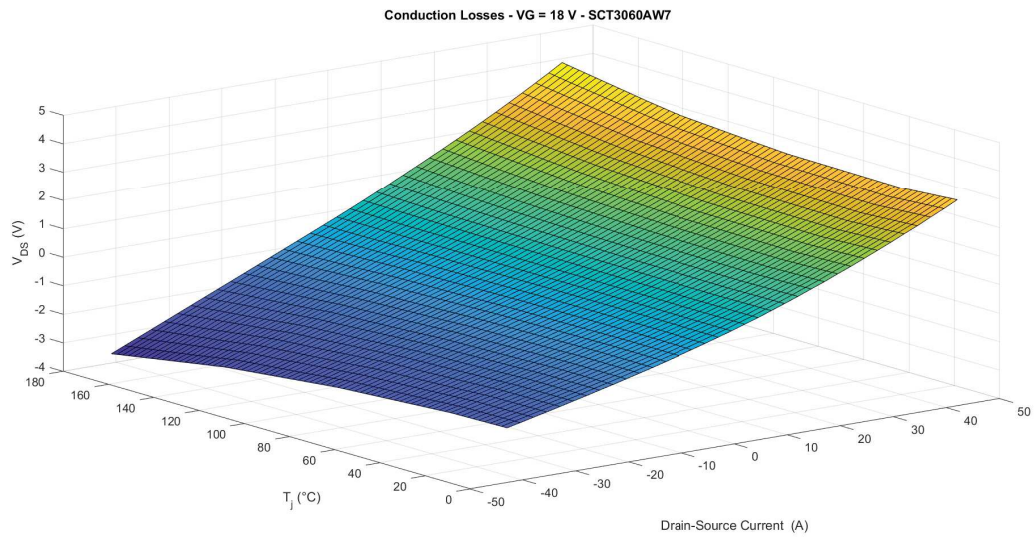


Source: [38].

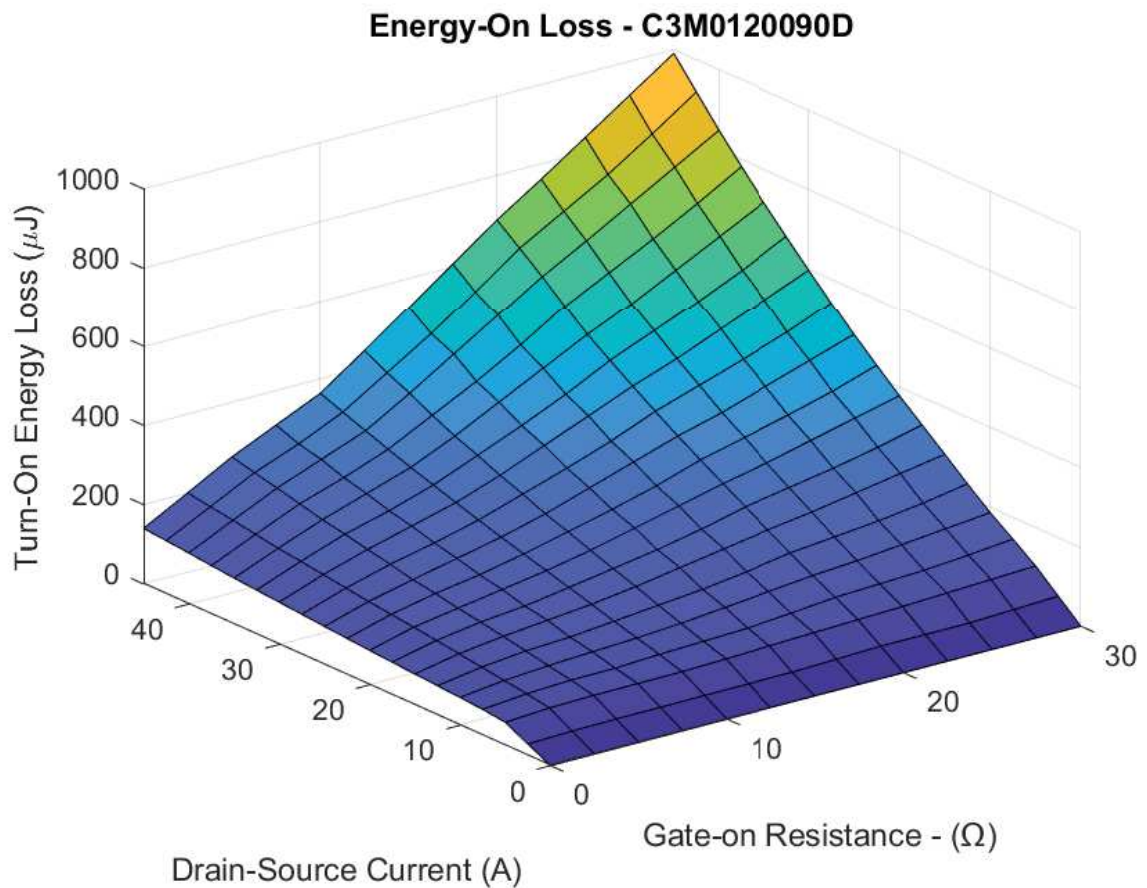
Figure 4.4 – Conduction losses of the SCT3060AW7 MOSFET and body diode - VG=0 .



Source: [39].

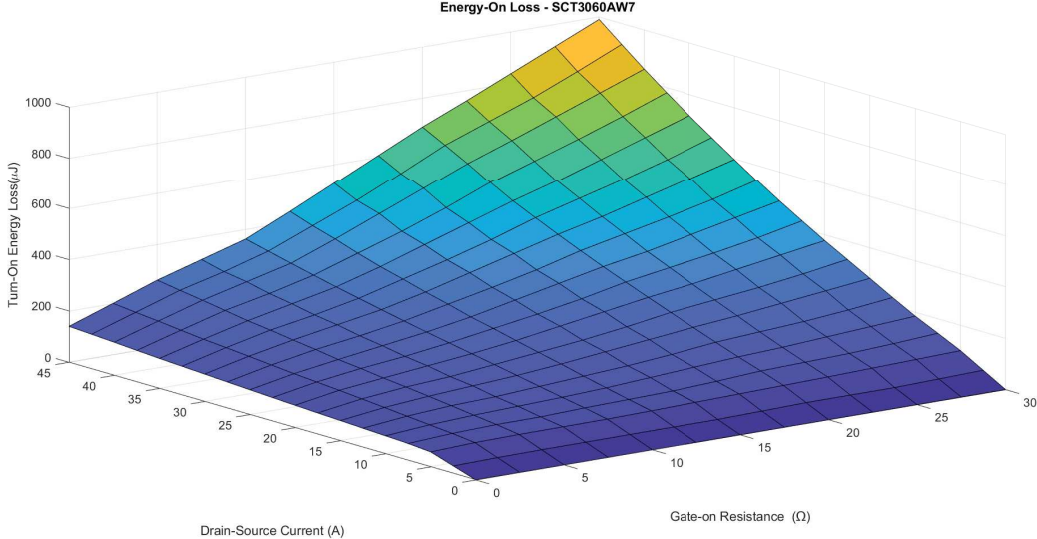
Figure 4.5 – Conduction losses of the SCT3060AW7 MOSFET and body diode - VG-18 .

Source: [39].

Figure 4.6 – Turn-on losses C3M0120090D .

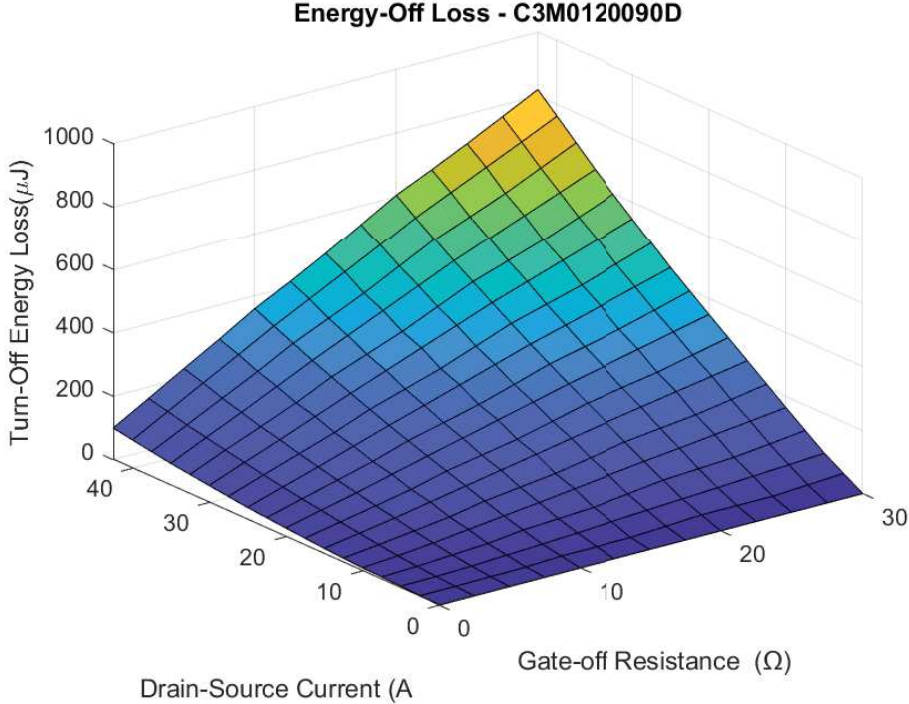
Source: [38].

Figure 4.7 – Turn-on losses SCT3060AW7 .

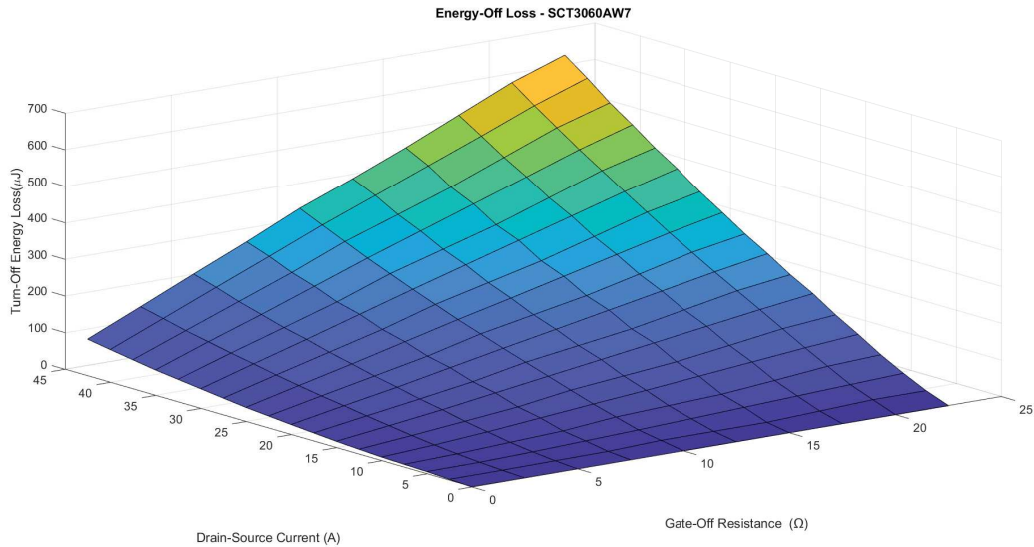


Source: [39].

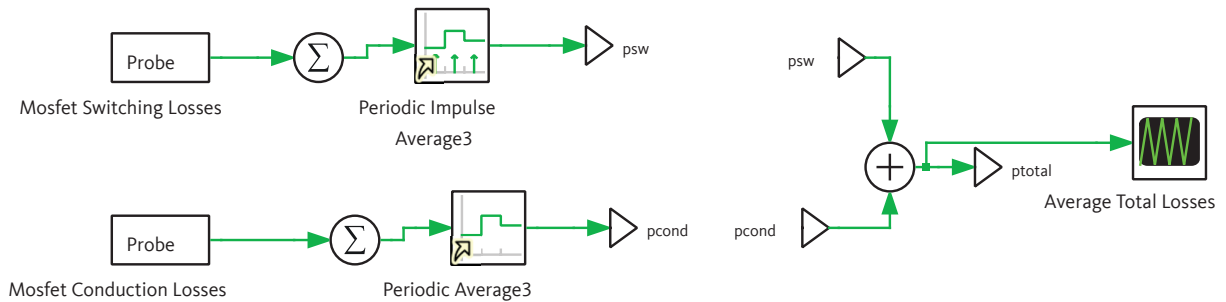
Figure 4.8 – Turn-off losses C3M0120090D .



Source: [38].

Figure 4.9 – Turn-off losses SCT3060AW7 .

Source: [39].

Figure 4.10 – Average Blocks.

Source: From the author.

4.1.3 Gate Signal Generation

A subsystem generates the necessary gate signals for the various modulations used in the circuit. This subsystem utilizes a triangular waveform, which can vary its duty cycle and phase-shift angle. The duty cycle is controlled by comparing a DC value, while the phase shift can be adjusted as required. The resulting signal controls the MOSFETs on the primary and secondary sides.

4.1.4 Output Voltage

As the configurations of the DAB3 YY in a single-phase mode do not arbitrate any voltage gain for the single-phase equivalent circuit, to obtain the voltage gain of $d = 0.5, 0.75, 1.25,$ and 1.5 , the output voltage is controlled by the output voltage. Meanwhile, as mentioned in Chapter 3, the single-phase modes of the DAB3 $Y\Delta$ arbitrate a different level of transformer gain, thus obtaining the values of $d = 0.5, 0.75, 1.25,$ and 1.5 , are necessary different levels of output voltage, when comparing to the DAB3 YY single-phase modes. The voltage levels for DAB3 YY and DAB 3 $Y\Delta$ are shown in Table 4.2.

Table 4.2 – V_o Configurations with different d

Voltage Gain (d)	V_o YY DAB [V]	V_o Y Δ [V]	V_o YY-11 [V]	V_o YY-00 [V]	V_o Y Δ – α [V]	V_o Y Δ – β [V]
0.5	74	74	74	74	64.1	85.44
0.75	111	111	111	111	96.12	128.17
1.25	185	185	185	185	160.21	213.62
1.5	222	222	222	222	192.25	256.34

Source: From the author.

4.1.5 Analytical and Simulation Results Analysis

The power flow results, the current levels of the leakage inductor, the phase shift and the soft switching constraints of DAB3YY and DAB3Y Δ , were studied with SPS and triangular modulation in single phase modes.

Therefore, it is necessary to analyze the simulation results of the DAB modeling presented in previous sections, together with the relevant modulations discussed in Chapters 2 and 3 using *PLECS*[®].

The operating points are related to the operating input power (P_{in}), and for *PLECS*[®], they fall within the range of [540W - 96E]. The transformer voltage gain of d is set to [0.5, 0.75, 1.25, 1.5], while the power operating points are available for the respective single-phase mode and modulation.

According to [33], the triangular modulation is suitable for low-power applications. Additionally, as demonstrated in the soft-switching restrictions of Chapter 3, triangular modulation makes it possible to achieve soft-switching over a broader input power range when the voltage gain is not near unity. Thus, triangular modulation is used for those operating points that align with the equations defining the power flow of various single-phase modes of the DAB configurations YY and Y Δ .

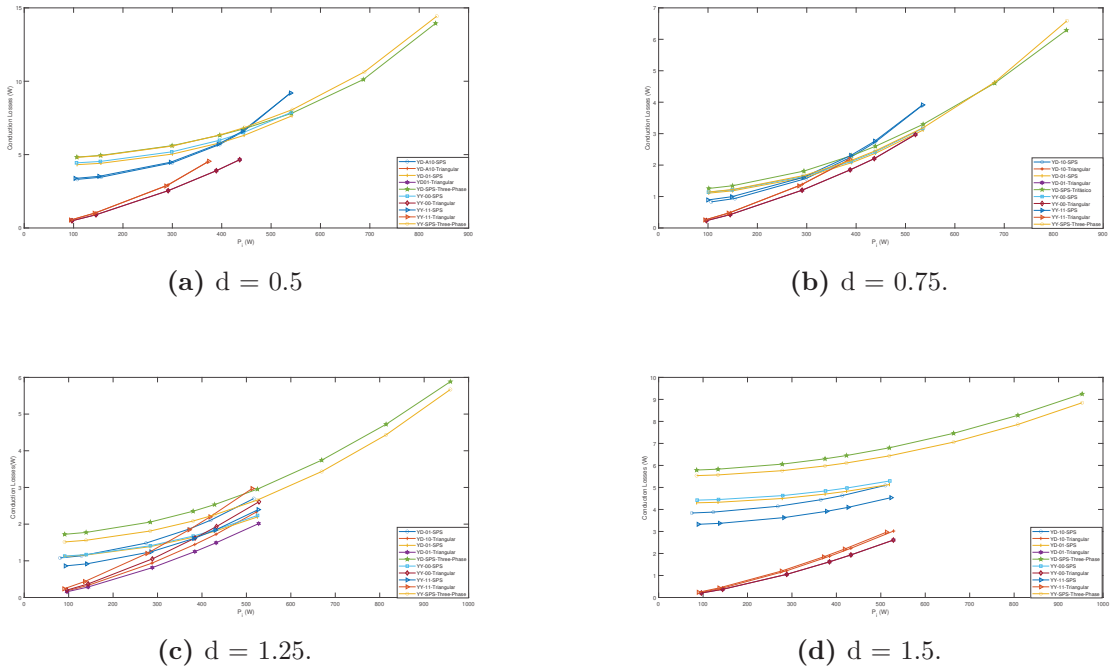
The input power and voltage transformer gain obtained are then used in conjunction with the results from Chapters 2 and 3 while taking into account the following properties:

- Conduction Losses [W];
- Switching Losses [W];
- Total Losses [W];
- Efficiency [%];
- $I_{Lk_{rms}}$ [A];

4.1.6 Simulation Results

Converter specifications for *PLECS* were presented in previous sections. Results for conduction losses, switching losses, total losses, and efficiency are obtained for the

Figure 4.11 – Conduction Losses for DAB YY and $Y\Delta$ with SPS and triangular modulations.



Source: From the author.

three-phase and single-phase variations of the DAB converter.

4.1.7 Conduction Losses

Using the average block, described in Figure 4.10, the conduction losses for the desired operating points with a voltage gain of 0.5, 0.75, 1.25, and 1.5 can be obtained.

Meanwhile, Figure 4.11a indicates that the $Y\Delta$ -01-Triangular and YY-00-Triangular configurations produce the lowest levels of conduction losses up to 430 W.

The YY-00-Triangular mode exhibits the lowest conduction losses, as shown in Figure 4.11b.

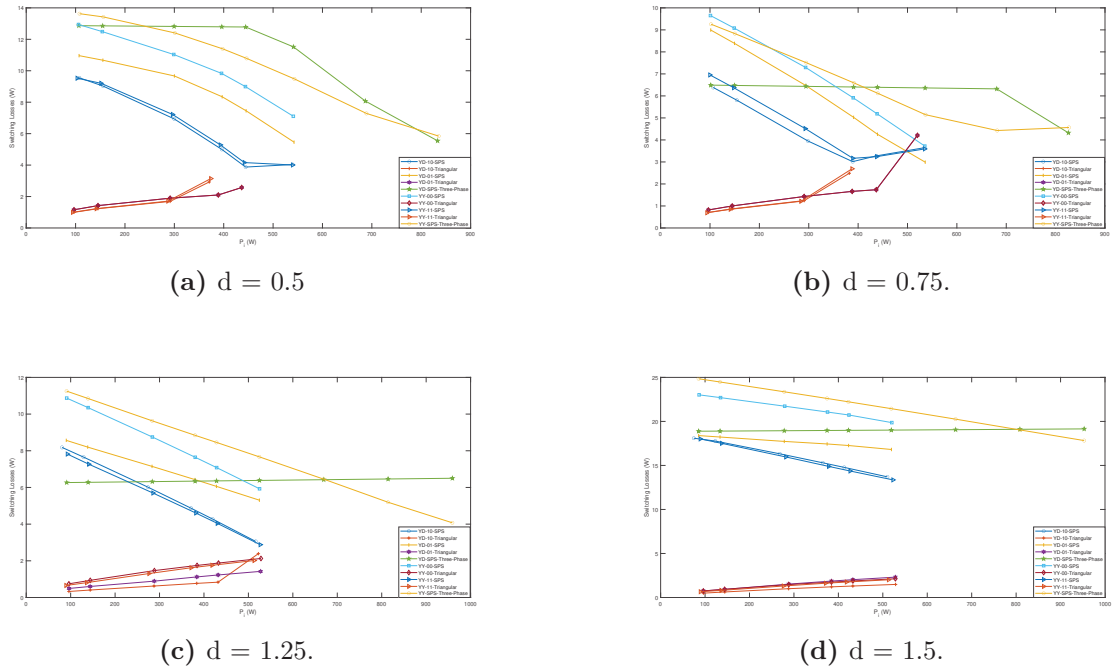
After analyzing the conduction losses, it was found that the $Y\Delta$ -Triangular configuration has the lowest level of conduction losses across the entire range of input power, as shown in Figure 4.11c.

For the $d=1.5$ voltage gain, the conduction losses of YY and $Y\Delta$ DAB configurations are shown. The YY-00-Triangular and $Y\Delta\beta$ configurations exhibit the lowest levels of conduction losses for the entire range of input power.

4.1.8 Switching Losses

After analyzing the conduction losses, it is necessary to study the switching losses for the same modulation schemes and DAB configurations. The switching losses for the voltage gains of $d = 0.5, 0.75, 1.25$ and 1.5 are then examined.

Figure 4.12 – Switching losses for DAB YY and $Y\Delta$ with SPS and triangular modulations.



Source: From the author.

Looking at the switching losses for a voltage gain of $d = 0.5$ in Figure 4.12a, it can be seen that the single phase modes of the YY and $Y\Delta$ DAB converter configurations with triangular modulation have the lowest level of switching losses among the different configurations and modulations.

In contrast, for the voltage gain of $d = 0.75$ shown in Figure 4.13b, the single-phase modes of the YY and $Y\Delta$ DAB configurations with triangular modulation have the lowest levels of switching losses for low input power within the range of 100W-440W.

Moreover, Figure 4.12c shows the lowest switching losses levels for the range of 100W-530W for the single phase modes of YY and $Y\Delta$ with triangular modulation when the voltage gain is varied to $d = 1.25$.

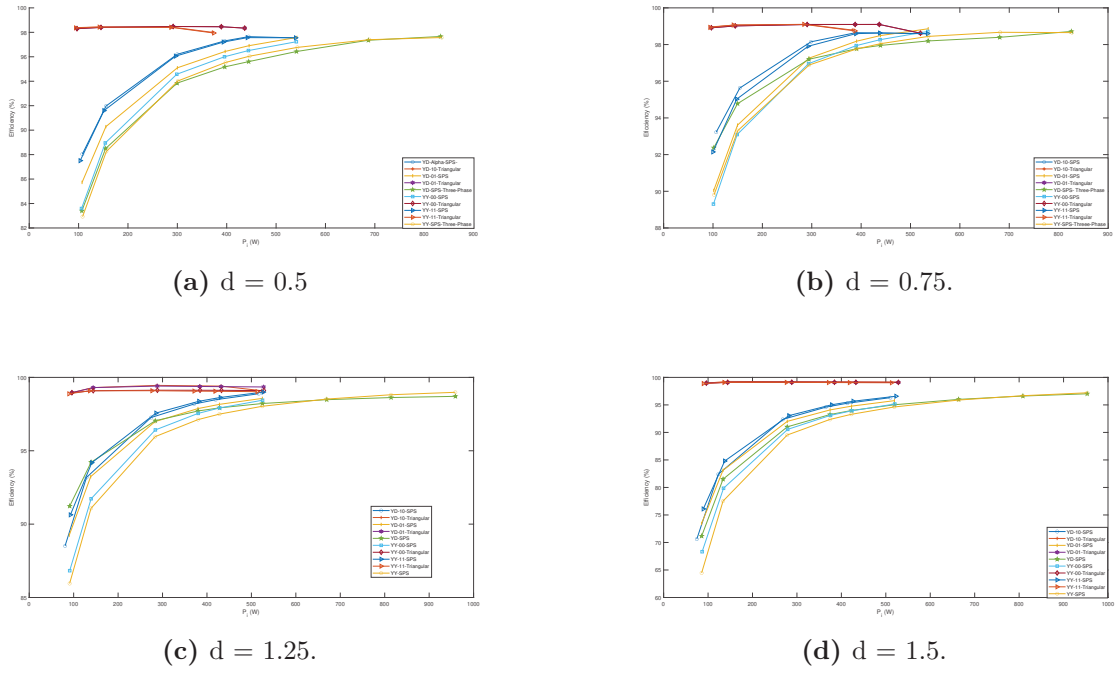
Furthermore, for the voltage gain of $d = 1.5$ and the input power range of 100W-500W, the single-phase modes of YY and $Y\Delta$ show the lowest levels of switching loss.

4.1.9 Total Losses

By analyzing the conduction and switching losses, it is possible to determine the total losses for different configurations of the YY and $Y\Delta$ DAB converter with SPS and triangular modulations.

Looking at Figure 4.13a it can be seen that the single-phase modes of YY and $Y\Delta$ Three-Phase DAB configurations with triangular modulation for the input power range of 100W-430W exhibit the lowest total loss. This indicates that a more comprehensive soft-switching range leads to lower losses for the 100W-430W range.

Figure 4.14 – Efficiency for losses for DAB YY and Y Δ with SPS and triangular modulations.



Source : From the author.

4.1.11 Equations Results vs Simulated Results

4.1.12 RMS Current

As discussed by [27], an equation was derived to calculate the RMS current of the leakage inductor (L_k) for the SPS modulation of a single-phase DAB converter. Using the equivalency of $L_{eq} = 1.5L_k$ for the YY-00 single-phase mode, the 4.1 can be obtained.

$$I_{Lk_{rms}} = V_p \cdot T_s \cdot (-3(8(\delta)^3d - 12(\delta)^2d - d^2 + 2 \cdot d - 1))^{(1/2)} / (12 \cdot Lk) \quad (4.1)$$

It is possible to compare the analytical and simulation results for the leakage current RMS value of the single-phase DAB and YY-00 DAB with SPS and Triangular modulations using the results 2.27, 4.1, and the data presented in Table 4.3, with $d = 0.75$.

After analyzing the data presented in Table 4.3, it can be concluded that the single-phase mode YY-00 of the YY DAB Converter experiences a lower level of RMS current for the same power and voltage as compared to the leakage inductor of the single-phase equivalent mode.

4.1.13 Losses - Calculated vs. Simulated

This subsection of losses is described for the output power range of 96W-439 W, with $d = 0.5$ and $d = 0.75$, for the YY-00-SPS and YY-00-Triangular single-phase modes of the YY DAB Converter. From the simulation with the configurations of YY-00-SPS

Table 4.3 – $I_{Lk_{rms}}$ values for YY-00 for both SPS and triangular modulations - d = 0.75

$I_{Lk_{RMS}}$ Simulated (A)	SPS analytical results (A)	SPS $I_{Lk_{RMS}}$ Triangular Simulated (A)	$I_{Lk_{RMS}}$ Triangular - analytical results (A)	Output Power (W)
1.20571	1.2067903	0.547453	0.5469	96.4344
1.2459	1.248212325	0.742122	0.7413	144.519
1.45668	1.461202748	1.249390	1.2466	289.313
1.65964	1.664598893	1.55054	1.5467	385.899
1.77648	1.781457767	1.6944	1.6897	434.395
2.03654	2.041324042	1.96735	1.9641	516.895

Source: From the author.

with d=0.5, it is possible to obtain levels of conduction losses and switching losses. The conduction losses are obtained with (4.2), where $R_{DS_{on}}$ is the Drain-Source resistor of the MOSFET used in the *PLECS*[®] model for the primary and secondary sides of the equivalent single-phase modes of YY and Y Δ DAB converters with SPS and Triangular modulations.

$$P_{cond} = R_{DS_{on}} \cdot I_{SW_{RMS}}^2 \quad (4.2)$$

The switching losses can be calculated using (4.3). The variables involved in the calculation are t_{on} for the rise time, t_f for the fall time, V_{DS} for the Drain-Source Voltage, I_{DS} for the Maximum Drain-Source Current and f_s for the switching frequency. These values are taken from the single-phase equivalent mode of the YY-00 DAB Converter.

$$P_{SW} = \frac{(t_{on} \cdot V_{DS} \cdot I_{DS} + t_{off} \cdot I_{DS} \cdot V_{VDS}) \cdot f_s}{2} \quad (4.3)$$

In addition, the gate resistance for the MOSFETs on the primary side is 12 Ω , while the secondary side has a gate resistance of 10 Ω for the same components.

As the YY-00 single-phase equivalent mode uses MOSFETs in parallel, it is necessary to calculate the conduction and switching losses for two types of MOSFETs on each side. The equations are applied primarily to YY-00-SPS and YY-00-Triangular with d=0.5 and d=0.75, respectively. ZVS is present on both the primary and secondary sides, and the switching losses are calculated using 4.4.

The switching losses for the primary and secondary sides are obtained by applying this equation to the six switches on the YY-00-SPS, YY-00-Triangular, primary, and secondary sides of the YY DAB Transformer. The results of the maximum current in the drain-source obtained from the simulations of YY-00-SPS and YY-00-Triangular are used to calculate the switching losses for the primary and secondary sides.

$$P_{SW} = \frac{(t_{off} \cdot I_{DS} \cdot V_{VDS}) \cdot f_s}{2} \quad (4.4)$$

The YY DAB Converter has two configurations, YY-00-SPS and YY-00-Triangular, and can be used in the equations for switching and conduction losses to calculate their efficiency for voltage gains of $d=[0.5-0.75]$.

Tables 4.4 and 4.5 show both configurations' switching losses, conduction losses, and efficiency values. Also, it can be concluded that the YY-00-SPS configuration has higher switching losses for the same power level than the YY-00-Triangular configuration. Additionally, the YY-00-Triangular configuration with $d=0.5$ has lower conduction losses than the YY-00-SPS configuration.

It can be seen from Figure 4.12a that for low power with the YY-00-SPS configuration, there is a loss of the ZVS configuration, resulting in high switching loss levels. Furthermore, it can be referred to Figure 4.11a to see that the lower level of conduction losses for the YY-00 triangular configuration results from the lower level of RMS value of the current of the leakage inductor of the equivalent single-phase DAB converter.

It is important to note that when the voltage gain is away from unity, the behaviors of YY-00-SPS and YY-00-Triangular configurations are according to the expected. The YY-00-Triangular configuration has lower switching and conduction losses than the YY-00-SPS, resulting in higher efficiency.

For $d=0.75$, the levels of switching losses of the YY-00-SPS configuration are lower than those of the YY-00-SPS configuration with $d=0.5$ due to the proximity to unity, closer to the soft-switching capability region. When the values of switching losses and conduction losses are compared for the YY-00-SPS and YY-00-Triangular, the values of switching losses for the SPS configuration are higher than for the triangular configuration due to the soft-switching diagram of 3.6b. This shows us that the YY-00-Triangular modulation has a broader spectrum of soft-switching capabilities, resulting in lower switching loss levels.

Using the results from 4.3, it can be verified that the YY-00-Triangular configuration has a lower level of RMS current of the leakage inductor of the equivalent single phase than the YY-00-SPS with the same voltage gain, resulting in a lower level of conduction losses. Although YY-00-SPS, with $d = 0.75$, has a lower level of losses than YY-00-SPS, with $d = 0.5$, the efficiency of YY-00-Triangular, with $d = 0.75$, is higher than the YY-00-SPS, with $d=0.75$, due to lower switching and conduction losses, as expected from the soft-switching diagram of 3.6b.

4.1.14 Chapter Overview

This subsection presents the analysis and comparison of switching losses, conduction losses, and efficiency for the single-phase equivalent modes of the YY and $Y\Delta$ DAB converters under SPS and triangular modulations.

The variables used in the analysis and comparison of the losses and efficiency levels were the switching losses, the conduction losses, and the RMS value of the current inductor

Table 4.4 – Losses and Efficiency - YY-00 - SPS - d=0.5

Switching Losses(W)	Conduction Losses(W)	P_o	Efficiency (%)
16.4786602	4.8485547	99	82.27565149
15.6777118	5.0487834	149	87.78829718
13.0879036	6.0527016	293	93.86795411
11.1612585	7.1241235	390	95.52142135
9.21839	7.810000648	439	96.26593615

Source: From the author.

Table 4.5 – Losses and efficiency - YY-00 - triangular - d = 0.5

Switching Losses (W)	Conduction Losses (W)	$P_o(W)$	Efficiency (%)
0.9012663	0.4696164	99	98.63418287
1.1063032	0.8630057	149	98.69555674
1.5784985	2.4429076	293	98.64608879
1.8291740	3.7680137	390	98.58512955
2.40997	4.538705985	439	98.44182228

Source: From the author.

Table 4.6 – Losses and efficiency - YY-00 - SPS - d=0.75

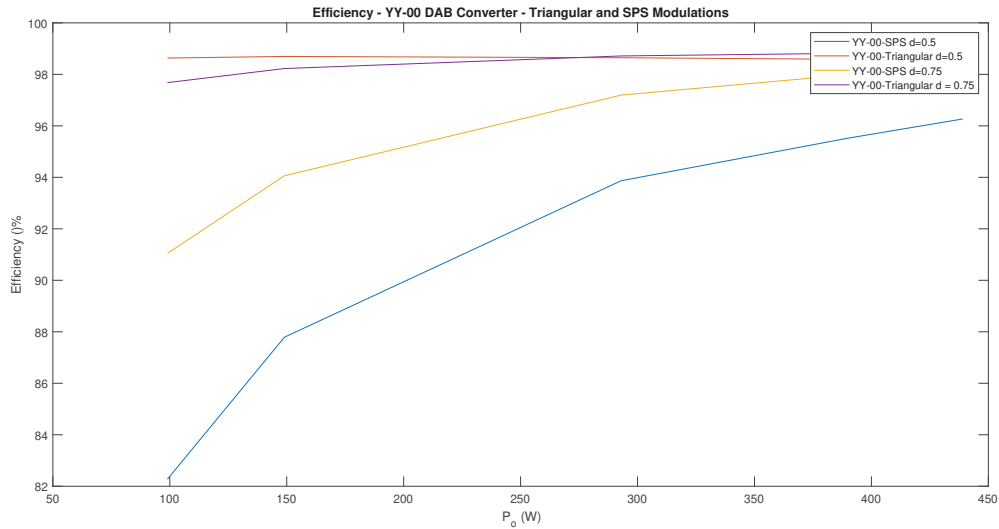
Switching Losses (W)	Conduction Losses (W)	$P_o(W)$	Efficiency (%)
8.49407	1.2414	99	91.04663971
8.0681	1.3413	149	94.06008614
6.59377	1.8620	293	97.19503707
5.6049	2.4302	390	97.98130898
5.08732	2.7860	439	98.23812587

Source: From the author.

Table 4.7 – Losses and efficiency - YY-00 - triangular - d = 0.75

Switching Losses (W)	Conduction Losses (W)	$P_o(W)$	Efficiency (%)
2.1171	0.2353	99.0000	97.6790
2.2594	0.4316	149.0000	98.2260
2.5907	1.2233	293.0000	98.7150
2.7692	1.8952	390.0000	98.8181
2.8508	2.2691	439.0000	98.8472

Source: From the author.

Figure 4.15 – Efficiency - analytical results - YY-00 - SPS and triangular modulations.

Source: From the author.

of the equivalent DAB converter in single phase. The simulation and analytical results showed that for the same configuration and voltage-rain, the triangular modulation has a lower level of RMS current of the leakage inductor of the single-phase equivalent DAB converter.

Furthermore, it was observed that, for voltage gains away from the unity, the SPS configuration causes higher switching losses. The soft-switching diagrams for the equivalent modes YY-SPS and YY-Triangular indicated that when the triangular modulation is applied, there is an expected more comprehensive soft-switching range and a lower level of switching losses, values that were obtained from simulations and analytical results.

Thus, based on the results of switching losses and conduction losses, it was concluded that for the single-phase mode of YY-00 with triangular and SPS modulations, the version with triangular modulation has a higher level of efficiency for low-power applications due to lower values of switching losses and conduction losses.

The analysis of single-phase modes with triangular and SPS modulations can be performed for all variations YY and $Y\Delta$ discussed in previous chapters regarding switching losses, conduction losses, and efficiency. They are expected to behave similarly to single-phase equivalent modes.

This Master Thesis aimed to study and compare the performance in efficiency, switching losses, conduction losses, and RMS level of current of the leakage current of Single-Phase Mode of DAB3 Converters.

Initially, the study and comparison of Single-Phase Modes of DAB Converters between SPS and DPS modulations aimed to study the applications of different modulations to achieve a whole range for soft-switching conditions when the voltage gain is different from the unity.

The DPS modulation does not have a closed analytical form. Optimization strategies would be required optimization to obtain duty cycle values for the DAB Converter's primary and secondary switches to obtain a more expansive soft-switching zone than the SPS modulation.

Also, as stated in Chapter 3, the single-phase mode of three-phase DAB converters has a single-phase mode that can be applied to increase efficiency in low-power applications.

As triangular modulation has a simple way to obtain the values of duty cycles to operate the switches and also has an enhanced level of efficiency and losses for power applications, the proposal was presented to compare levels of efficiency, losses, and RMS value of the current of the leakage current between the SPS and Triangular Modulation.

The literature contains closed-form solutions for power flow, duty cycle, power flow, and leakage inductance for SPS and triangular modulations. However, there is no analytical description of the RMS current of the buck mode for single-phase DAB converters for triangular modulation in single-phase DAB converters.

Mathcad software was used to get an analytical equation for the RMS value of leakage inductance between the triangular and SPS modulations to the single-phase DAB converter to compare the RMS value current of the leakage inductor.

The study developed by [15] studied the single-phase mode of DAB3 for SPS modulations, and one of the contributions of this Master thesis was the analytical forms of power flow, duty cycles, conduction times, and leakage inductance.

The main contribution of this Master Thesis was the soft-switching diagrams of YY and $Y\Delta$ DAB single-phase modes, which required the use of the developed equations to obtain the values of duty cycles to operate in the desired voltage gain and power operating point.

Finally, simulation results of switching losses, conduction losses, total losses, and

efficiency were presented for different single-phase modes of DAB3 with SPS and Triangular Modulations.

To prove the simulation results that indicate that the single-phase modes with Triangular Modulation provide a more expansive soft-switching zone, lower levels of losses, and lower level of RMS value of current of leakage inductor, analytical results of losses, efficiency, and RMS level of current of leakage current for the YY-00 single-phase mode with SPS and Triangular Modulations were obtained. This shows that for low power applications and single-phase mode configurations, the single-phase mode of DAB3 with triangular modulation has an enhanced performance compared to the single-phase modes of DAB3 with SPS modulation.

5.1 CONTRIBUTIONS AND FUTURE WORK

This section describes the main contributions of this Master's Thesis and possible further studies.

5.1.1 Contributions of Master Thesis

The main contributions of this Master's Thesis are:

- RMS Current Equation for Buck Configuration of single-phase mode DAB Converter with Triangular Modulation;
- YY-00 and YY-11 Single-Phase Mode Equations of Power Flow, Phase-shift and Soft-Switching Constraints for SPS Modulation;
- YY-00 and YY-11 Single-Phase Mode Equations of Power Flow, Phase-shift and Soft-Switching Constraints for Triangular Modulation;
- $Y\Delta - 10$ and $Y\Delta - 01$ Single-Phase Mode Equations of Power Flow, Phase-shift and Soft-Switching Constraints for Triangular Modulation;
- Simulations of evaluation of losses and efficiency for YY-00, YY-11, $Y\Delta - 10$ and $Y\Delta - 01$ for SPS and Triangular Modulations;
- Estimation of Losses, Efficiency, and RMS Current of Transformer, with rising and falling times for YY-00-SPS and YY-00-Triangular configurations;
- Article of Scientific Dissemination Magazine: L. Bellincanta de Souza, "IEEE PELS SBC in Brazil Organizes Tech Talk [Society News]," IEEE Power Electronics Magazine, vol. 7, n^o 3, p. 76–78, set. 2020, doi: 10.1109/MPEL.2020.3011779.

5.1.2 Future Work

Prospective studies derived from this Master's Thesis suggested the following topics:

- Equations of RMS value of transformer current of equivalent single-phase mode for YY-11-SPS, YY-11-Triangular, $Y\Delta - 10 - SPS$, $Y\Delta - 10 - Triangular$, $Y\Delta - 01 - SPS$, $Y\Delta - 01 - Triangular$ configurations of DAB3 Converters;
- Estimation of Losses, with rising and falling times of MOSFETs, and Efficiency, for YY-11-SPS, YY-11-Triangular, $Y\Delta - 10 - SPS$, $Y\Delta - 10 - Triangular$, $Y\Delta - 01 - SPS$, $Y\Delta - 01 - Triangular$
- Analysis of single-phase modes for EPS modulation and comparisons of the efficiency of single-phase modes for SPS, EPS, and Triangular Modulations

Bibliography

- [1] M. Muratori and T. Mai, “The shape of electrified transportation,” *Environmental Research Letters*, vol. 16, p. 011003, Jan. 2021.
- [2] M. A. Delucchi, C. Yang, A. F. Burke, J. M. Ogden, K. Kurani, J. Kessler, and D. Sperling, “An assessment of electric vehicles: technology, infrastructure requirements, greenhouse-gas emissions, petroleum use, material use, lifetime cost, consumer acceptance and policy initiatives,” *Philosophical Transactions of the Royal Society A: Mathematical, Physical and Engineering Sciences*, vol. 372, p. 20120325, Jan. 2014. Publisher: Royal Society.
- [3] Y. Park, S. Chakraborty, and A. Khaligh, “DAB Converter for EV Onboard Chargers Using Bare-Die SiC MOSFETs and Leakage-Integrated Planar Transformer,” *IEEE Transactions on Transportation Electrification*, vol. 8, pp. 209–224, Mar. 2022. Conference Name: IEEE Transactions on Transportation Electrification.
- [4] J. Yuan, L. Dorn-Gomba, A. D. Callegaro, J. Reimers, and A. Emadi, “A Review of Bidirectional On-Board Chargers for Electric Vehicles,” *IEEE Access*, vol. 9, pp. 51501–51518, 2021. Conference Name: IEEE Access.
- [5] B. Li, L. Jing, X. Wang, N. Chen, B. Liu, and M. Chen, “A Smooth Mode-Switching Strategy for Bidirectional OBC Base on V2G Technology,” in *2019 IEEE Applied Power Electronics Conference and Exposition (APEC)*, pp. 3320–3324, Mar. 2019. ISSN: 2470-6647.
- [6] S. Anwar, W. Zhang, F. Wang, and D. J. Costinett, “Integrated DC-DC converter design for Electric Vehicle powertrains,” in *2016 IEEE Applied Power Electronics Conference and Exposition (APEC)*, pp. 424–431, Mar. 2016.
- [7] P. Nayak, S. Mandal, Y. Gupta, A. Shukla, and S. Doolla, “Improving the Efficiency of the DAB Converter of an On-board EV Charger Using Different Modulation Techniques,” in *2020 IEEE International Conference on Power Electronics, Drives and Energy Systems (PEDES)*, pp. 1–6, Dec. 2020.
- [8] D. M. Lima, M. L. Heldwein, and N. Roqueiro, “Modelagem e controle do conversor Dual Active Bridge (DAB),” p. 192, 2019.

- [9] M. Yaqoob, K. H. Loo, and Y. M. Lai, “A Four-Degrees-of-Freedom Modulation Strategy for Dual-Active-Bridge Series-Resonant Converter Designed for Total Loss Minimization,” *IEEE Transactions on Power Electronics*, vol. 34, pp. 1065–1081, Feb. 2019. Conference Name: IEEE Transactions on Power Electronics.
- [10] H. Yu, L. Hang, X. Zheng, Z. He, Y. He, L. Shen, C. Shao, P. Zeng, Q. Wu, X. Yang, and H. Tao, “Globally Unified ZVS and Quasi-Optimal Minimum Conduction Loss Modulation of DAB Converters,” *IEEE Transactions on Transportation Electrification*, vol. 8, pp. 3989–4000, Sept. 2022. Conference Name: IEEE Transactions on Transportation Electrification.
- [11] F. Jauch and J. Biela, “Generalized modeling and optimization of a bidirectional dual active bridge DC-DC converter including frequency variation,” in *2014 International Power Electronics Conference (IPEC-Hiroshima 2014 - ECCE ASIA)*, pp. 1788–1795, May 2014. ISSN: 2150-6086.
- [12] D. Goldmann, S. Schramm, and H.-G. Herzog, “Triangular and Trapezoidal Modulation for Dual Active Bridge DC-DC Converters with Fast Switching Semiconductors,” in *2019 21st European Conference on Power Electronics and Applications (EPE '19 ECCE Europe)*, pp. P.1–P.10, Sept. 2019.
- [13] Y. Cui, R. Hou, P. Malysz, and A. Emadi, “Improved combined modulation strategy for dual active bridge converter in electrified vehicles,” in *2017 IEEE Transportation Electrification Conference and Expo (ITEC)*, pp. 101–107, June 2017.
- [14] F. Krismer, *Modeling and optimization of bidirectional dual active bridge DC-DC converter topologies*. Doctoral Thesis, ETH Zurich, 2010. Accepted: 2017-06-13T12:47:58Z.
- [15] L. M. Cúnico, *Estratégias de projeto e modulação para o conversor DAB trifásico*. PhD thesis, Federal University of Santa Catarina, 2021.
- [16] R. Zhang and S. Fujimori, “The role of transport electrification in global climate change mitigation scenarios,” *Environmental Research Letters*, vol. 15, p. 034019, Feb. 2020.
- [17] A. Albatayneh, M. N. Assaf, D. Alterman, and M. Jaradat, “Comparison of the Overall Energy Efficiency for Internal Combustion Engine Vehicles and Electric Vehicles,” *Environmental and Climate Technologies*, vol. 24, pp. 669–680, Jan. 2020.
- [18] B. Bilgin, P. Magne, P. Malysz, Y. Yang, V. Pantelic, M. Preindl, A. Korobkine, W. Jiang, M. Lawford, and A. Emadi, “Making the Case for Electrified Transportation,” *IEEE Transactions on Transportation Electrification*, vol. 1, pp. 4–17, June 2015. Conference Name: IEEE Transactions on Transportation Electrification.

- [19] A. L. Kirsten, “METODOLOGIA DE PROJETO DO CONVERSOR DAB APLICADO A TRANSFORMADORES DE ESTADO SÓLIDO,” p. 236, 2014.
- [20] W. W. A. G. Silva, *Estudo e implementação de um conversor bidirecional como interface na regulação de tensão em barramento c.c. e carregamento de baterias em um sistema nanorrede*. PhD thesis, 2013.
- [21] M. Berger, I. Kocar, H. Fortin-Blanchette, and C. Lavertu, “Open-Phase Fault-Tolerant Operation of the Three-Phase Dual Active Bridge Converter,” *IEEE Transactions on Power Electronics*, vol. 35, pp. 3651–3662, Apr. 2020.
- [22] S. M. Akbar, A. Hasan, A. J. Watson, and P. Wheeler, “FEA Based Transformer Loss Analysis for Dual Active Bridge DC–DC Converter Using Triple Phase Shift Modulation,” *IEEE Journal of Emerging and Selected Topics in Power Electronics*, vol. 10, pp. 4347–4360, Aug. 2022. Conference Name: IEEE Journal of Emerging and Selected Topics in Power Electronics.
- [23] S. A. Gorji, H. G. Sahebi, M. Ektesabi, and A. B. Rad, “Topologies and Control Schemes of Bidirectional DC–DC Power Converters: An Overview,” *IEEE Access*, vol. 7, pp. 117997–118019, 2019. Conference Name: IEEE Access.
- [24] N. HOU, W. SONG, Y. ZHU, X. SUN, and W. LI, “Dynamic and static performance optimization of dual active bridge DC-DC converters,” *Journal of Modern Power Systems and Clean Energy*, vol. 6, pp. 607–618, May 2018.
- [25] R. De Doncker, D. Divan, and M. Kheraluwala, “A three-phase soft-switched high-power-density DC/DC converter for high-power applications,” *IEEE Transactions on Industry Applications*, vol. 27, pp. 63–73, Jan. 1991. Conference Name: IEEE Transactions on Industry Applications.
- [26] G. Oggier, G. O. García, and A. R. Oliva, “Modulation strategy to operate the dual active bridge DC-DC converter under soft switching in the whole operating range,” *IEEE Transactions on Power Electronics*, vol. 26, pp. 1228–1236, Apr. 2011. Conference Name: IEEE Transactions on Power Electronics.
- [27] D. Krasniqi, “Dual Active Bridge Converter,” Master’s thesis, NTNU, 2021. Accepted: 2021-10-16T17:21:16Z.
- [28] G. G. Oggier, R. Leidhold, G. O. Garcia, A. R. Oliva, J. C. Balda, and F. Barlow, “Extending the ZVS operating range of dual active bridge high-power DC-DC converters,” in *2006 37th IEEE Power Electronics Specialists Conference*, pp. 1–7, June 2006. ISSN: 2377-6617.

- [29] T. Huisman, “A Dual Active Bridge DC-DC Converter for Automotive Applications: Design of a High Efficiency Bidirectional DAB Converter for the Lightyear One,” 2020.
- [30] F. Lin, “The dual active bridge converter design with artificial intelligence,” 2022. Accepted: 2022-12-20T04:32:23Z Publisher: Nanyang Technological University.
- [31] G. G. Oggier, G. O. García, and A. R. Oliva, “Switching Control Strategy to Minimize Dual Active Bridge Converter Losses,” *IEEE Transactions on Power Electronics*, vol. 24, pp. 1826–1838, July 2009. Conference Name: IEEE Transactions on Power Electronics.
- [32] D.-D. Nguyen, T.-T. Pham, T.-T. Le, S. Choi, and K. Yukita, “A Modulation Method for Three-Phase Dual-Active-Bridge Converters in Battery Charging Applications,” *Sustainability*, vol. 15, p. 5170, Jan. 2023. Number: 6 Publisher: Multidisciplinary Digital Publishing Institute.
- [33] V. Steub, “Study of Modulation Schemes for the Dual-Active-Bridge Converter in a Grid-Connected Photovoltaic Park,” p. 114, 2018.
- [34] F. Krismer, S. Round, and J. W. Kolar, “Performance optimization of a high current dual active bridge with a wide operating voltage range,” in *2006 37th IEEE Power Electronics Specialists Conference*, pp. 1–7, June 2006. ISSN: 2377-6617.
- [35] N. H. Baars, J. Everts, C. G. E. Wijnands, and E. A. Lomonova, “Performance Evaluation of a Three-Phase Dual Active Bridge DC–DC Converter With Different Transformer Winding Configurations,” *IEEE Transactions on Power Electronics*, vol. 31, pp. 6814–6823, Oct. 2016. Conference Name: IEEE Transactions on Power Electronics.
- [36] L. M. Cúnico and A. L. Kirsten, “Single-Phase Operating Modes for DC–DC Three-Phase Dual-Active-Bridge With Y Transformer,” *IEEE Journal of Emerging and Selected Topics in Power Electronics*, vol. 10, pp. 4845–4853, Aug. 2022. Conference Name: IEEE Journal of Emerging and Selected Topics in Power Electronics.
- [37] E. Ayerbe, “C3m0060065k silicon carbide power mosfet c3m tm mosfet technology n-channel enhancement mode,” 2020.
- [38] E. Ayerbe, “C3m0120090d silicon carbide power mosfet c3m tm mosfet technology n-channel enhancement mode,” 2020.
- [39] R. Co, “N-channel sic power mosfet,” 2022.

A Power Flow Equations Development for Triangular Modulation

The first equations obtained for the power flow of the triangular modulus are regarding when $V_{in} > nV_o$, described in A.1.

$$\begin{aligned}
 T_3 = \frac{T_s}{2} - T_2 - T_1 &= \frac{1}{2f_s} - \frac{\phi}{\pi f_s} - \frac{\phi(\frac{nV_o}{V_{in}-V_o})}{\pi f_s} = 0 \\
 \phi_{max} &= \frac{\pi(V_{in} - nV_o)}{2V_{in}} \\
 P &= \frac{\frac{\pi^2}{4}(1 - \frac{nV_o}{V_{in}})^2 V_{in} (nV_o)^2}{\pi^2 f_s L_k (V_{in} - nV_o)} \\
 P &= \frac{\phi^2 V_{in}^2 nV_o}{\pi^2 f_s L_k} \\
 P_{max} &= \frac{(nV_o)^2 (V_{in} - nV_o)}{4f_s L_k V_{in}} \\
 d &= \frac{nV_o}{V_{in}} \\
 P_{max} &= V_{in}^2 d^2 \frac{(1-d)}{4f_s L}
 \end{aligned}
 \tag{A.1}$$

Meanwhile, when $V_{in} < nV_o$ the results of power flow, conduction times and duty

cycles are described in A.2.

$$T_3 = \frac{T_s}{2} - \frac{\phi}{\pi f_s} - \frac{\pi}{\pi f_s (d-1)} = 0$$

$$\phi_{max} = \frac{\pi (d-1)}{2d}$$

$$P_{max} = \frac{\frac{\pi^2}{4} \left(\frac{d-1}{d}\right)^2 V_{in}^2 \frac{(d)}{d-1}}{\phi^2 f_s L}$$

$$P_{max} = V_{in}^2 \frac{(d-1)}{4f_s d L}$$

(A.2)

B

MATLAB Codes

```
1  \% Extraction of Conduction and Energy Losses of MOSFETs of Primary and Secondary
   Sides
   clear all
3  close all
   A = [0  0  0  0  0  0;
5  0  0  0  0  0;
   61.83  68.74  71.65  73.12  88  107.2;
7  71.27  83.66  93.5  107  150.5  195;
   79.33  98.32  113.3  140.5  213.5  290.6;
9  88.47  114.2  131.8  175.7  282.8  391.5;
   98.48  127.2  151.5  210.5  354.9  501.2;
11 108.5  142.4  173.8  246.5  429.2  614.8;
   118.4  155.3  195  284.3  509.9  735.2;
13 130.1  172.1  218.6  323.3  603.6  857.5;
   140.7  187.5  242  366.1  693.2  997.9]
15 A = A
   x = [0  2  3.9  10  20  30]
17 y = [-1  0  5.3  10.63  15.49  20.72  25.91  30.78  35.77  40.4  45.3]
   V = rand(11,6,10)
19 Z = 1:100:1000
   [xi,yi] = meshgrid(0:2.5:30, 0:2.5:45.3);
21 zi = griddata(x,y,A,xi,yi);
   surf(xi,yi,zi);
23 xlabel(' Gate-on Resistance - ( )')
   ylabel('Drain-Source Current (A)')
25 zlabel('Turn-On Energy Loss (\muJ)')
   title('Energy-On Loss - C3M0120090D')
27

29 Toff= [
   0  0  0  0  0  0;
31 0  0  0  0  0  0;
   6.44  6.68  8.95  21.97  47.55  74.62;
33 10.35  17.4  25.63  58.16  114.3  167.5;
   17.57  32.36  45.45  96.81  180  257.1;
35 27.74  49.9  68.4  137.7  248.2  350.3;
   39.11  67.76  93.69  181.5  321.3  447;
```

```

37 53.88 88.86 120.2 226.7 395.6 546;
   69.3 112.1 148.3 276 473.7 647.7;
39 88.2 136 181.7 327.9 553.7 755.4;
   107.7 162.2 215.6 379.2 636.3 858.8];
41 x = [0 2 3.9 10 20 30]';
   y = [-1 0 5.1 10.24 15.02 20.08 25.19 29.99 34.96 39.71 44.3]';
43 Z = 1:100:1000
   [xi,yi] = meshgrid(0:2.5:30, 0:2.5:45.3);
45 zi = griddata(x,y,Toff,xi,yi);
   figure
47 surf(xi,yi,zi);
   xlabel(' Gate-off Resistance ( )')
49 ylabel('Drain-Source Current (A)')
   zlabel('Turn-Off Energy Loss(\muJ)')
51 title('Energy-Off Loss - C3M0120090D')

53
   Tonp = [
55 0 0 0 0 0 0
   61.83 68.74 71.65 73.12 88 107.2
57 71.27 83.66 93.5 107 150.5 195
   79.33 98.32 113.3 140.5 213.5 290.6
59 88.47 114.2 131.8 175.7 282.8 391.5
   98.48 127.2 151.5 210.5 354.9 501.2
61 108.5 142.4 173.8 246.5 429.2 614.8
   118.4 155.3 195 284.3 509.9 735.2
63 130.1 172.1 218.6 323.3 603.6 857.5
   140.7 187.5 242 366.1 693.2 997.9];
65 x = [0 2 3.9 10 20 30 ]';
   y = [0 5.3 10.63 15.49 20.72 25.91 30.78 35.77 40.4 45.3]';
67 [xi,yi] = meshgrid(0:2.5:30, 0:2.5:1000);
   zi = griddata(x,y,Tonp,xi,yi);
69 figure
   surf(xi,yi,zi);
71 xlabel(' Gate-on Resistance ( ) ')
   ylabel('Drain-Source Current (A)')
73 zlabel('Turn-On Energy Loss(\muJ)')
   title ('Energy-On Loss - SCT3060AW7')
75 Toffp = [
   0 0 0 0 0 0
77 6.44 6.68 8.95 21.97 47.55 74.62
   10.35 17.4 25.63 58.16 114.3 167.5
79 17.57 32.36 45.45 96.81 180 257.1
   27.74 49.9 68.4 137.7 248.2 350.3
81 39.11 67.76 93.69 181.5 321.3 447
   53.88 88.86 120.2 226.7 395.6 546
83 69.3 112.1 148.3 276 473.7 647.7
   88.2 136 181.7 327.9 553.7 755.4

```

```

85 107.7 162.2 215.6 379.2 636.3 858.8];

87 x = [0 2 3.9 10 20 30]';
   y = [0 5.1 10.24 15.02 20.08 25.19 29.99 34.96 39.71 44.3]';
89 [xi,yi] = meshgrid(0:2.5:23.61, 0:2.5:600);
   zi = griddata(x,y,Toffp,xi,yi);
91 figure
   surf(xi,yi,zi);
93 xlabel(' Gate-Off Resistance ( ) ')
   ylabel('Drain-Source Current (A)')
95 zlabel('Turn-Off Energy Loss(\muJ)')
   title ('Energy-Off Loss - SCT3060AW7')
97 figure
   Toffp = [-2.038 -1.864 -1.686 -1.503 -1.315 -1.121 -0.9201 -0.7101 -0.4878
            -0.2515 0 0.272 0.5661 0.8772 1.204 1.545 1.899 2.269 2.651 3.048 3.459;
99 -2.121 -1.929 -1.733 -1.534 -1.332 -1.126 -0.9143 -0.6964 -0.473 -0.2387 0
            0.2558 0.528 0.8132 1.11 1.421 1.744 2.081 2.43 2.794 3.174;
            -2.378 -2.151 -1.922 -1.692 -1.461 -1.226 -0.9904 -0.7486 -0.5038 -0.2524 0
            0.2719 0.5552 0.848 1.151 1.464 1.79 2.129 2.48 2.846 3.226;
101 -2.81 -2.532 -2.255 -1.979 -1.701 -1.422 -1.143 -0.8602 -0.5755 -0.2886 0 0.3072
            0.6219 0.9461 1.278 1.619 1.97 2.335 2.714 3.105 3.515;
            -3.492 -3.144 -2.795 -2.446 -2.098 -1.751 -1.404 -1.054 -0.7048 -0.3525 0
            0.3674 0.744 1.127 1.519 1.922 2.334 2.763 3.209 3.672 4.157];
103 x = [-43 -38.7 -34.4 -30.1 -25.8 -21.5 -17.2 -12.9 -8.6 -4.3 0 4.3 8.6 12.9 17.2
            21.5 25.8 30.1 34.4 38.7 43];
   [xi,yi] = meshgrid(-43:2.5:43, 0:2.5:600);
105 y = [-25 25 75 125 175]
   zi = griddata(x,y,Toffp,xi,yi);
107 figure
   surf(xi,yi,zi);
109 xlabel(' Drain-Source Current (A) ')
   ylabel('Tj (C)')
111 zlabel('VDS (V)')
   title ('Conduction Losses - VG = 18 V - SCT3060AW7 ')
113
   figure
115 Toffp = [-5.389 -5.146 -4.895 -4.632 -4.357 -4.066 -3.754 -3.411 -3.038 -2.64
            0
            -5.184 -4.932 -4.672 -4.405 -4.127 -3.835 -3.523 -3.182 -2.834 -2.459 0
117 -5.264 -4.985 -4.701 -4.409 -4.107 -3.792 -3.456 -3.092 -2.724 -2.334 0
            -5.488 -5.174 -4.858 -4.534 -4.201 -3.857 -3.492 -3.094 -2.683 -2.25 0
119 -5.721 -5.379 -5.032 -4.681 -4.323 -3.954 -3.571 -3.152 -2.695 -2.191 0];
   x = [-44 -39.6 -35.2 -30.8 -26.4 -22 -17.6 -13.2 -8.8 -4.4 0 ]
121

123 y = [-25 25 75 125 175]
   zi = griddata(x,y,Toffp,xi,yi);
125 figure

```

```

surf(xi,yi,zi);
127 xlabel(' Drain-Source Current (A) ')
ylabel('T_j (C)')
129 zlabel('V_{DS} (V)')
title ('Conduction Losses - VG = 0V - SCT3060AW7 ')

```

```

    \% Federal University of Santa Catarina
2  \% Power Electronics Institute
    \% PPGEEL - UFSC
4  \% Student : Leonardo Bellincanta de Souza
    \% Diagramas - Soft-Switching - YDelta - Triangular Modulation
6  close all;
    clear all;
8  L = 82*10^-6
    fs = 10^5
10 clear all
    Vp = 400;
12 L = 82*10^-6;
    fs = 100*10^3;
14 Pb1 = NaN([1,10000]);
    Pb2 = NaN([1,10000]);
16 m = linspace(0.0005,5,10000)
    d = linspace(0.5,1.5,10000);
18 Pbase1 = Vp^2/(2*4*fs*L);
    Pbase2 = Vp^2/(2*fs*L*pi);
20
    Pby00inv = NaN([1,10000]);
22 Pby00sup = NaN([1,10000]);

24 for i=1:10000
    if(m(i)<=1)
26 Pby00inv(i) = (Vp^2*m(i).^2.*(1-m(i))/(4*fs*L*1.5));
        elseif (m(i)>1)
28 Pby00sup(i) = (Vp^2*(m(i)-1)/(m(i)*4*fs*L*1.5));
        end
30 end
    \% figure
32 plot(m,Pby00inv,'g',m,Pby00sup,'g','color','r');
    view(90,90);
34 set(gca, 'XDir','reverse')
    title('Soft-Swithcing Limits - Triangular Modulation - YY-00 - DAB Single-Phase
        Converter ')
36 xlabel('Voltage Gain - d ')
    ylabel('P_o ')
38
    Pby11inv = NaN([1,10000]);

```



```

40 Pby11sup = NaN([1,10000]);

42 for i=1:10000
    if(m(i)<=1)
44 Pby11inv(i) = (Vp^2*m(i).^2.*(1-m(i))/(4*fs*L*2));
        elseif (m(i)>1)
46 Pby11sup(i) = (Vp^2*(m(i)-1)/(m(i)*4*fs*L*2));
            end
48 end
    \% figure
50 \% plot(m,Pby11inv,'g',m,Pby11sup,'g','color','r');
    view(90,90);
52 set(gca, 'XDir','reverse')
    title('Soft-Swithcing Limits - Triangular Modulation - YY-11 - DAB Single-Phase
        Converter ')
54 xlabel('Voltage Gain - d ')
    ylabel('P_o ')
56
58
60
    for i=1:10000
62 if(m(i)<=1)
        Pb1(i) = (Vp^2*m(i).^2.*(1-m(i))/(4*fs*L));
64 elseif (m(i)>1)
        Pb2(i) = (Vp^2*(m(i)-1)/(m(i)*4*fs*L));
66 end
        end
68 \% figure
    \% plot(m,Pb1,'g',m,Pb2,'g','color','r');
70 view(90,90);
    set(gca, 'XDir','reverse')
72 title('Soft-Swithcing Limits - Triangular Modulation - DAB Single-Phase Converter ')
    xlabel('Voltage Gain - d ')
74 ylabel('P_o ')

76 hold on

78 \% SPS
    m = linspace(0.0005,5,10000);
80 Psup = zeros([1,10000]);
    Pinv = zeros([1,10000]);
82 deltasup = zeros([1,10000]);
    deltainv = zeros([1,10000]);
84
86 for i=1:10000

```

```

    if (m(i)> 1)
88
    Psup(i) = pi*(m(i)-1)/(2*(m(i)^2))*Vp^2*(m(i))/(2*pi*fs*L);
90 elseif m(i) < 1
92 Pinv(i) = (Vp^2*(m(i))/(2*pi*fs*L))*(m(i))*(1-(m(i)))*pi/4;
94 end
    end
96
98 figure
    plot(m,Psup,m,Pinv,'r')
100
    figure
102 plot(m,Pby00inv,'g',m,Pby00sup,'g','color','r');
    hold on
104 plot(m,Pby11inv,'g',m,Pby11sup,'g','color','r');
    hold on
106 plot(m,Pb1,'g',m,Pb2,'g','color','g');
    hold on
108 plot(m,Psup,'g',m,Pinv,'g','color','c');
    hold on
110 view(90,90);
    set(gca, 'XDir','reverse')
112 title('Soft-Swithcing Limits - SPS Modulation - DAB Single-Phase Converter ')
    xlabel('Voltage Gain - d ')
114 ylabel('P_o ')
    figure
116 plot(m,Pb1,m,Pb2,'color','r');
    hold on;
118 figure
    plot(m,Psup,m,Pinv,'color','b');
120
    view(90,90);
122 set(gca, 'XDir','reverse')
    legend('Triangular Modulation','','SPS Modulation')
124 title('Soft-Swithcing Limits - SPS and Triangular Modulations - DAB Single-Phase
        Converter ')
    xlabel('Voltage Gain - d ')
126 ylabel('P_o ')

```

```

    \% Federal University of Santa Catarina
2 \% Graduate Programme in Eletrical Engineering
    \% Diagramas de Modulações SPS - Triangular - YY
4 phi = linspace(0,pi/2,10000);

```

```

d = linspace(0.5,1.5,10000);
6 dinf = NaN([1,10000]);
  dsup = NaN([1,10000]);
8 Pinv = NaN([1,10000]);
  Psup = NaN([1,10000]);
10 figure
  Vp = 400;
12 fs = 100*10^3;
  L = 82*10^-6;
14 Pbase = Vp^2/(2*fs*L*pi);
  P = d*(pi/2)*((1-(pi/2)/pi)-(pi/(18*pi/2)));
16 plot(d,P,'r')
  hold on
18 for i=1:10000
  if phi(i) <= pi/3
20 dinf(i) = 1/(1- (3*phi(i)/(2*pi)));
  dsup(i) = 1- (3*phi(i)/(2*pi));
22 elseif (phi(i)<= pi/2) && (phi(i) > pi/3);
  dinf(i) = 1/((3/2)-(3*phi(i)/pi));
24 dsup(i) = (3/2)-(3*phi(i)/pi);
  end
26 end
  for i=1:10000
28 if phi(i)<=pi/3 && phi(i)>=0
  Pinv(i) = (Vp^2/(2*fs*L*pi))*phi(i)*dinf(i)*((2/3)-phi(i)/(2*pi));
30 Psup(i) = (Vp^2/(2*fs*L*pi))*phi(i)*dsup(i)*((2/3)-phi(i)/(2*pi)) ;
  elseif (phi(i)> pi/3) && (phi(i) <= pi/2);
32 Pinv(i) = (Vp^2/(2*fs*L*pi))*dinf(i)*phi(i)*(1-(phi(i)/pi)-(pi/(18*phi(i))));
  Psup(i) = (Vp^2/(2*fs*L*pi))*dsup(i)*phi(i)*(1-(phi(i)/pi)-(pi/(18*phi(i))));
34 end
  end
36
  plot(dinf,Pinv,'r');
38 hold on
  plot(dsup,Psup,'r')
40 hold on
  ylim([0 4000])
42 xlim([0.5 1.5])
  view(90,90);
44 set(gca, 'XDir','reverse')
  title('Diagramas de Comutação Suave para Modulação Triangular ')
46 xlabel('Ganho de Tensão - d ')
  ylabel('P_o (W)')
48
50
  Vp = 400;
52 L = 82*10^-6;

```

```

fs = 100*103;
54 Pb1 = NaN([1,10000]);
Pb2 = NaN([1,10000]);
56 m = linspace(0.0005,1.6,10000);
Pbase = 1
58 for i=1:10000
if(m(i)<=1)
60 Pb1(i) = (Vp2*m(i).2.*(1-m(i))/(4*fs*L*2))/Pbase;
elseif (m(i)>1)
62 Pb2(i) = (Vp2*(m(i)-1)/(m(i)*4*fs*L*2))/Pbase;
end
64 end

66 plot(m,Pb1,'y',m,Pb2,'y');
hold on
68 Vp = 400;
L = 82*10-6;
70 fs = 100*103;
Pb1 = NaN([1,10000]);
72 Pb2 = NaN([1,10000]);
m = linspace(0.0005,1.6,10000);
74 Pbase = 1
for i=1:10000
76 if(m(i)<=1)
Pb1(i) = (Vp2*m(i).2.*(1-m(i))/(4*fs*1.5*L))/Pbase;
78 elseif (m(i)>1)
Pb2(i) = (Vp2*(m(i)-1)/(m(i)*4*fs*L*1.5))/Pbase;
80 end
end
82 plot(m,Pb1,'b',m,Pb2,'b');
hold on
84
86

88 d = linspace(0.0005,1.6,10000);
phi1 = linspace(0,90,10000);
90 phi2 = zeros([1,10000])
kt = 0.0174533
92 Isingle = zeros([1,10000]);
Idual = zeros([1,10000]);
94 Idual1 = zeros([1,10000]);
Idual2 = zeros([1,10000]);
96 dphi = zeros([1,10000]);
Vp = 400
98 fs = 100*103
L = 82*10-6
100 Ls = 2*L;

```

```

Pbase = Vp^2/(2*fs*L*pi);
102
d = linspace(0.0005,1.6,10000);
104 phi1 = linspace(0,90,10000);
phi2 = zeros([1,10000])
106 kt = 0.0174533
Isingle = zeros([1,10000]);
108 Idual = zeros([1,10000]);
Idual1 = zeros([1,10000]);
110 Idual2 = zeros([1,10000]);
dphi = zeros([1,10000]);
112 Vp = 400
fs = 100*10^3
114 L = 82*10^-6
Ls = 1.5*L;
116 Pbase = Vp^2/(2*fs*L*pi);
for i=1:10000
118 if d(i) < 1

120
Idual(i) = pi/2*(d(i)-d(i)^2)*(Vp^2*d(i))/(2*pi*fs*Ls*Pbase);
122

124 elseif d(i) > 1

126 Idual(i) = (Vp^2*d(i)/(2*pi*fs*Ls*Pbase))*(pi/2)*(d(i)-1)/d(i)^2;

128

130

132
end
134 end

136 ylim([0 4000])
xlim([0.5 1.5])
138 view(90,90);
title(' Soft-Switching Capabilities - YY DAB Converter')
140 xlabel('Voltage Gain - d ')
ylabel('P_o ')
142 legend('','YY - Three-Phase SPS ','','YY Triangular - Mode 11','','YY Triangular -
Mode 00','','YY EPS - Mode 11', 'YY EPS - Mode 00','Location','northwest')

```

C

PLECS Data - Efficiency and Losses

The data are regarding $d = [0.5, 0.75, 1.25, 1.5]$ for PLECS software, with different modulations.

Table C.1 – $Y\Delta$ -10 - SPS - $d = 0.5$ - DAB- PLECS

<i>CL</i>	<i>SL</i>	<i>TL</i>	%	<i>P</i>
9,55	3,31	12,87	88,04	107,57
9,03	3,46	12,49	91,97	155,57
6,94	4,44	11,38	96,20	299,79
5,00	5,69	10,69	97,30	396,12
3,88	6,58	10,46	97,65	444,43
4,03	9,21	13,24	97,54	539,49

Source: From the author.

Table C.2 – $Y\Delta$ -10 - triangular modulation - DAB - $d = 0.5$ - DAB- PLECS

<i>SL</i>	<i>CL</i>	<i>TL</i>	%	<i>P</i>
1,00	0,57	1,56	98,39	96,70
1,23	1,04	2,27	98,44	145,23
1,69	2,93	4,62	98,41	291,52
2,93	4,49	7,41	98,00	370,76

Source: From the author.

Table C.3 – $Y\Delta$ -01 - SPS - $d = 0.5$ - DAB- PLECS

<i>SL</i>	<i>CL</i>	<i>TL</i>	%	<i>P</i>
10,96	4,31	15,28	85,73	107,04
10,67	4,41	15,08	90,29	155,26
9,67	5,04	14,71	95,10	300,11
8,35	5,80	14,15	96,44	396,85
7,45	6,31	13,76	96,91	445,34
5,46	7,64	13,10	97,58	542,45

Source: From the author.

Table C.4 – Y Δ -01 - triangular modulation - DAB - d = 0.5 - DAB- PLECS

<i>SL</i>	<i>CL</i>	<i>TL</i>	%	<i>P</i>
1,16	0,49	1,65	98,30	96,76
1,42	0,90	2,32	98,40	145,34
1,89	2,54	4,43	98,48	291,44
2,10	3,90	6,00	98,46	389,02
2,57	4,65	7,23	98,34	436,41

Source: From the author.

Table C.5 – Y Δ - SPS - three-phase - d = 0.5 - DAB- PLECS

<i>SL</i>	<i>CL</i>	<i>TL</i>	%	<i>P</i>
12,87	4,83	17,70	83,40	106,61
12,86	4,94	17,80	88,50	154,80
12,82	5,61	18,43	93,85	299,52
12,80	6,32	19,12	95,17	396,10
12,78	6,76	19,54	95,60	444,49
11,52	7,81	19,33	96,43	541,28
8,07	10,12	18,19	97,35	686,86
5,54	13,94	19,49	97,66	833,21

Source: From the author.

Table C.6 – YY-00 - SPS - d= 0.5 - DAB - PLECS

<i>SL</i>	<i>CL</i>	<i>TL</i>	%	<i>P</i>
12,94	4,44	17,38	83,59	105,90
12,49	4,53	17,02	88,95	154,09
11,03	5,19	16,22	94,57	298,85
9,83	5,98	15,81	96,00	395,51
8,99	6,50	15,50	96,51	443,96
7,10	7,88	14,98	97,23	540,98

Source: From the author.

Table C.7 – YY-00 - triangular modulation - DAB - d= 0.5 - DAB- PLECS

<i>SL</i>	<i>CL</i>	<i>TL</i>	%	<i>P</i>
1,16	0,49	1,65	98,30	96,77
1,42	0,90	2,32	98,40	145,36
1,89	2,54	4,43	98,48	291,47
2,10	3,90	6,00	98,46	389,05
2,57	4,65	7,23	98,34	436,44

Source: From the author.

Table C.8 – YY-11 - SPS - d=0.5 - DAB - PLECS

<i>SL</i>	<i>CL</i>	<i>TL</i>	%	<i>P</i>
9,52	3,38	12,90	87,51	103,26
9,20	3,52	12,72	91,60	151,47
7,22	4,48	11,70	96,05	296,36
5,28	5,72	11,00	97,20	393,23
4,16	6,59	10,75	97,57	441,86
4,01	9,20	13,20	97,55	539,53

Source: From the author.

Table C.9 – YY-11 - triangular modulation - DAB - d=0.5 - DAB - PLECS

<i>SL</i>	<i>CL</i>	<i>TL</i>	%	<i>P</i>
0,99	0,54	1,54	98,37	94,06
1,23	1,00	2,23	98,43	142,03
1,71	2,86	4,57	98,41	287,10
3,14	4,55	7,69	97,94	373,88

Source: From the author.

Table C.10 – YY - SPS - three-phase - d = 0.5 - DAB - PLECS

<i>SL</i>	<i>CL</i>	<i>TL</i>	%	<i>P</i>
13,63	4,82	18,45	82,93	108,07
13,42	4,93	18,35	88,26	156,28
12,41	5,59	18,00	94,02	301,08
11,40	6,35	17,75	95,54	397,76
10,79	6,84	17,63	96,05	446,20
9,48	8,07	17,55	96,77	543,16
7,29	10,64	17,92	97,40	689,02
5,84	14,43	20,27	97,57	835,48

Source: From the author.

Table C.11 – Y Δ -10 - SPS - d =0.75 - DAB - PLECS

<i>SL</i>	<i>CL</i>	<i>TL</i>	%	<i>P</i>
6,38	0,83	7,21	93,22	106,42
5,80	0,94	6,74	95,63	154,39
3,95	1,57	5,52	98,15	298,40
3,01	2,25	5,26	98,65	388,91
3,28	2,71	5,99	98,63	437,30
3,65	3,90	7,54	98,59	534,15

Source: From the author.

Table C.12 – $Y\Delta$ -10 - triangular modulation - $d = 0.75$ - DAB - PLECS

SL	CL	TL	%	P
0,71	0,27	0,97	98,96	96,61
0,87	0,49	1,36	99,06	145,14
1,24	1,39	2,63	99,10	290,89
2,49	2,14	4,62	98,79	382,17

Source: From the author.

Table C.13 – $Y\Delta$ -01 - SPS - $d = 0.75$ - DAB - PLECS

SL	CL	TL	%	P
8,99	1,11	10,10	90,04	101,45
8,39	1,18	9,57	93,61	149,64
6,47	1,60	8,07	97,26	294,31
5,03	2,08	7,10	98,18	390,84
4,26	2,38	6,63	98,49	439,19
2,99	3,12	6,10	98,86	535,90

Source: From the author.

Table C.14 – $Y\Delta$ -01 - triangular modulation - DAB - $d = 0.75$ - PLECS

CL	SL	TL	%	P
0,82	0,23	1,05	98,91	96,68
1,00	0,43	1,43	99,02	144,98
1,43	1,20	2,63	99,09	290,61
1,66	1,85	3,51	99,10	387,90
1,74	2,21	3,94	99,10	436,78
4,21	2,97	7,18	98,62	520,10

Source: From the author.

Table C.15 – $Y\Delta$ - three-phase - SPS - $d = 0.75$ - DAB - PLECS

SL	CL	TL	%	P
6,49	1,26	7,75	92,37	101,57
6,48	1,34	7,82	94,78	149,73
6,43	1,81	8,24	97,20	294,32
6,41	2,30	8,70	97,77	390,77
6,39	2,60	8,99	97,95	439,08
6,36	3,30	9,66	98,20	535,68
6,32	4,61	10,93	98,39	680,72
4,32	6,29	10,61	98,72	825,90

Source: From the author.

Table C.16 – YY-00 - SPS - d=0.75 - DAB - PLECS

<i>SL</i>	<i>CL</i>	<i>TL</i>	%	<i>P</i>
9,65	1,14	10,79	89,30	100,89
9,08	1,21	10,29	93,09	149,05
7,29	1,64	8,93	96,96	293,63
5,91	2,11	8,03	97,94	390,09
5,19	2,42	7,61	98,27	438,40
3,72	3,17	6,89	98,71	535,04

Source: From the author.

Table C.17 – YY-00 - triangular modulation - d =0.75 - DAB - PLECS

<i>SL</i>	<i>CL</i>	<i>TL</i>	%	<i>P</i>
0,82	0,23	1,05	98,91	96,69
1,00	0,43	1,43	99,02	144,98
1,43	1,20	2,63	99,09	290,61
1,66	1,85	3,51	99,10	387,90
1,74	2,21	3,94	99,10	436,79
4,21	2,97	7,18	98,62	520,16

Source: From the author.

Table C.18 – YY-11 - SPS - d = 0.75 - DAB - PLECS

<i>SL</i>	<i>CL</i>	<i>TL</i>	%	<i>P</i>
6,95	0,89	7,84	92,15	99,88
6,37	0,99	7,37	95,03	148,06
4,52	1,61	6,13	97,91	292,77
3,17	2,31	5,47	98,59	389,37
3,24	2,76	6,00	98,63	437,77
3,59	3,91	7,51	98,60	534,65

Source: From the author.

Table C.19 – YY-11 - triangular modulation - DAB - d=0.75 - DAB - PLECS

<i>SL</i>	<i>CL</i>	<i>TL</i>	%	<i>P</i>
0,69	0,26	0,95	98,93	93,85
0,85	0,47	1,32	99,07	141,24
1,21	1,34	2,55	99,10	284,18
2,69	2,18	4,87	98,74	387,69

Source: From the author.

Table C.20 – YY - SPS - three-phase - $d = 0.75$ - DAB - PLECS

SL	CL	TL	%	P
9,26	1,15	10,40	89,81	102,09
8,83	1,22	10,06	93,31	150,27
7,51	1,67	9,18	96,89	294,93
6,59	2,16	8,75	97,77	391,43
6,12	2,46	8,58	98,05	439,76
5,15	3,19	8,34	98,45	536,44
4,43	4,65	9,08	98,67	681,64
4,57	6,59	11,15	98,65	827,04

Source: From the author.

Table C.21 – $Y\Delta$ -10 - SPS - $d = 1.25$ - DAB - PLECS

SL	CL	TL	%	P
8,18	1,08	9,26	88,51	80,61
7,65	1,14	8,79	93,18	128,95
6,01	1,48	7,50	97,27	274,09
4,87	1,87	6,73	98,18	370,91
4,28	2,11	6,38	98,48	419,41
3,06	2,70	5,75	98,89	516,42

Source: From the author.

Table C.22 – $Y\Delta$ -10 - triangular modulation - DAB - $d = 1.25$ - PLECS

SL	CL	TL	%	P
0,33	0,18	0,51	98,96	96,12
0,41	0,33	0,74	99,31	144,06
0,63	0,94	1,56	99,46	287,61
0,77	1,44	2,21	99,42	383,77
0,84	1,72	2,56	99,41	431,69
2,39	2,33	4,72	99,10	522,49

Source: From the author.

Table C.23 – $Y\Delta$ -01 - SPS - $d = 1.25$ - DAB - PLECS

CL	CL	TL	%	P
8,57	1,12	9,69	89,25	90,12
8,20	1,16	9,36	93,24	138,36
7,15	1,39	8,53	96,99	283,15
6,43	1,64	8,07	97,87	379,71
6,06	1,80	7,86	98,16	428,06
5,31	2,19	7,50	98,57	524,73

Source: From the author.

Table C.24 – $Y\Delta$ -01 - triangular modulation - DAB - $d = 1.25$ - PLECS

SL	CL	TL	%	P
0,49	0,16	0,65	98,96	96,28
0,60	0,29	0,89	99,30	143,80
0,89	0,81	1,70	99,41	288,12
1,12	1,25	2,37	99,38	383,97
1,23	1,49	2,72	99,37	431,79
1,42	2,01	3,44	99,35	527,59

Source: From the author.

Table C.25 – $Y\Delta$ - three-phase - SPS - $d = 1.25$ - DAB- PLECS

SL	CL	TL	%	P
6,27	1,72	7,99	91,23	91,12
6,28	1,77	8,05	94,22	139,26
6,32	2,06	8,38	97,05	283,75
6,34	2,35	8,70	97,71	380,10
6,36	2,53	8,89	97,92	428,33
6,38	2,95	9,34	98,22	524,78
6,42	3,74	10,17	98,48	669,54
6,46	4,72	11,18	98,63	814,33
6,50	5,88	12,39	98,71	959,04

Source: From the author.

Table C.26 – YY -00 - SPS - $d=1.25$ - DAB - PLECS

SL	CL	TL	%	P
10,87	1,13	12,00	86,83	91,10
10,35	1,17	11,52	91,73	139,27
8,75	1,41	10,16	96,42	283,86
7,65	1,67	9,32	97,55	380,27
7,08	1,84	8,92	97,92	428,55
5,93	2,24	8,16	98,45	525,07

Source: From the author.

Table C.27 – YY-00 - triangular modulation - $d = 1.25$ - DAB - PLECS

SL	CL	TL	%	P
0,75	0,20	0,95	98,96	96,07
0,94	0,37	1,31	99,09	144,00
1,47	1,05	2,52	99,13	288,39
1,75	1,62	3,37	99,12	384,42
1,88	1,93	3,81	99,12	432,68
2,13	2,61	4,74	99,10	528,29

Source: From the author

Table C.28 – YY-11 - SPS - $d = 1.25$ - DAB - PLECS

SL	CL	TL	%	P
7,82	0,86	8,68	90,63	92,68
7,27	0,92	8,19	94,19	140,83
5,69	1,25	6,94	97,57	285,39
4,60	1,61	6,21	98,37	381,81
4,04	1,84	5,88	98,63	430,09
2,88	2,40	5,27	99,00	526,65

Source: From the author.

Table C.29 – YY-11 - triangular modulation - $d=1.25$ - DAB - PLECS

SL	CL	TL	%	P
0,66	0,24	0,89	98,88	89,52
0,81	0,43	1,24	99,09	136,08
1,31	1,20	2,51	99,09	276,39
1,62	1,85	3,47	99,07	371,20
1,76	2,20	3,96	99,05	418,27
2,02	2,97	4,99	99,03	512,97

Source: From the author

Table C.30 – YY - SPS - three-phase - $d = 1.25$ - DAB - PLECS

SL	CL	TL	%	P
11,25	1,51	12,77	85,96	90,90
10,85	1,56	12,41	91,08	139,05
9,63	1,81	11,44	95,96	283,54
8,84	2,08	10,93	97,12	379,88
8,46	2,25	10,71	97,50	428,12
7,67	2,66	10,32	98,03	524,57
6,45	3,43	9,89	98,52	669,34
5,19	4,43	9,63	98,82	814,15
4,07	5,67	9,74	98,98	958,92

Source: From the author

Table C.31 – $Y\Delta$ -10 - SPS - $d = 1.5$ - DAB - PLECS

SL	CL	TL	%	P
18,09	3,84	21,93	70,61	74,63
17,77	3,88	21,65	82,39	122,97
16,32	4,14	20,47	92,37	268,06
15,30	4,44	19,74	94,59	364,83
14,78	4,63	19,41	95,30	413,29
13,70	5,09	18,80	96,32	510,21

Source: From the author.

Table C.32 – $Y\Delta$ -10 - triangular modulation - DAB - $d = 1.5$ - PLECS

SL	CL	TL	%	P
0,50	0,23	0,73	98,96	96,24
0,63	0,43	1,06	99,27	144,31
1,00	1,21	2,21	99,23	288,03
1,21	1,87	3,08	99,20	384,65
1,30	2,23	3,54	99,18	432,53
1,49	3,02	4,51	99,15	528,75

Source: From the author.

Table C.33 – $Y\Delta$ -01 - SPS - $d = 1.5$ - DAB - PLECS

SL	CL	TL	%	P
18,39	4,30	22,69	73,45	85,49
18,23	4,33	22,55	83,13	133,67
17,73	4,50	22,23	92,01	278,27
17,44	4,70	22,14	94,09	374,68
17,26	4,82	22,09	94,78	422,95
16,81	5,13	21,94	95,78	519,45

Source: From the author.

Table C.34 – $Y\Delta$ -01 - triangular modulation - DAB - $d = 1.5$ - PLECS

SL	CL	TL	%	P
0,75	0,20	0,95	98,96	96,07
0,92	0,37	1,29	99,11	144,00
1,52	1,05	2,57	99,11	288,39
1,87	1,62	3,49	99,09	384,42
2,03	1,93	3,96	99,08	432,68
2,31	2,61	4,92	99,07	528,29

Source: From the author.

Table C.35 – $Y\Delta$ - SPS - three-phase - $d = 1.5$ - DAB - PLECS

SL	CL	TL	%	P
18,89	5,79	24,68	71,17	85,60
18,90	5,83	24,73	81,51	133,74
18,94	6,06	25,00	91,01	278,20
18,97	6,30	25,27	93,25	374,52
18,99	6,45	25,44	93,98	422,74
19,01	6,80	25,81	95,03	519,15
19,06	7,46	26,52	96,01	663,83
19,10	8,28	27,38	96,61	808,53
19,15	9,25	28,40	97,02	953,14

Source: From the author.

Table C.36 – YY-00 - SPS - d=1.5 - DAB - PLECS

<i>SL</i>	<i>CL</i>	<i>TL</i>	%	<i>P</i>
23,02	4,42	27,44	68,32	86,62
22,70	4,45	27,15	79,85	134,77
21,73	4,63	26,36	90,56	279,26
21,07	4,84	25,91	93,10	375,60
20,73	4,97	25,70	93,94	423,83
19,86	5,29	25,16	95,16	520,26

Source: From the author.

Table C.37 – YY-00 - triangular modulation - d= 1.5 - DAB - PLECS

<i>SL</i>	<i>CL</i>	<i>TL</i>	%	<i>P</i>
0,75	0,20	0,95	98,96	96,07
0,94	0,37	1,31	99,09	144,00
1,47	1,05	2,52	99,13	288,39
1,75	1,62	3,37	99,12	384,42
1,88	1,93	3,81	99,12	432,68
2,13	2,61	4,74	99,10	528,29

Source: From the author.

Table C.38 – YY-11 - SPS - d = 1.5 - DAB - PLECS

<i>SL</i>	<i>CL</i>	<i>TL</i>	%	<i>P</i>
18,01	3,33	21,34	76,10	89,27
17,51	3,37	20,88	84,81	137,41
15,96	3,63	19,59	93,05	281,91
14,89	3,92	18,81	95,03	378,27
14,37	4,10	18,46	95,67	426,52
13,36	4,54	17,89	96,58	523,00

Source: From the author.

Table C.39 – YY-11 - triangular modulation - d=1.5 - DAB - PLECS

<i>SL</i>	<i>CL</i>	<i>TL</i>	%	<i>P</i>
0,66	0,24	0,89	98,88	89,52
0,81	0,43	1,24	99,09	136,08
1,31	1,20	2,51	99,09	276,39
1,62	1,85	3,47	99,07	371,21
1,76	2,20	3,96	99,05	418,27
2,02	2,97	4,99	99,03	512,98

Source: From the author.

D

Losses Calculus Matlab Code

In this chapter are presented the MATLAB Codes developed to the theoretical calculation of switching and conduction losses of the YY-00 DAB Converter with voltage gains of $d = 0.5$ and $d = 0.75$, with the configurations described in previous sections. The values of drain-source resistance of the primary and secondary side switches are according to the described in Chapter 4. Primarily is presented the code regarding the voltage gain of $d = 0.5$ and secondarily is presented the MATLAB Code regarding the voltage gain of $d = 0.75$

```
Federal University of Santa Catarina
2 Graduate Programme in Electrical Engineering - PPGEEL
Power Electronics Institute - INEP
4 Advisor: Dr. André Luís Kirsten
MSc: Eng. Leonardo Bellincanta de Souza
6 Losses Calculation - Theoretical Analysis - YY00 SPS and Triangular - d =
0.5 - DAB Converter
8 clear all
L = 1.5*82*10^-6
10 Ronp = 120*10^-3
Rons = 60*10^-3
12 fs = 100000
Ts = 1/fs
14 d = 0.5
YY 00 SPS - SPS Losses
16 Losses Calculus Primary - Conduction Losses
ISp1 = [1.68987
18 1.71879
1.8667
20 2.01794
2.11026
22 2.33133]
ISp1max = [ 4.74908
24 4.89049
5.34893
26 5.6912
5.8772
28 6.2888 ];
```

```

    ISp2max = ISp1max/2;
30 ISp2 = ISp1/2;
    Pcondp1 = ISp1.^2*120*10^-3;
32 Pcondp2 = ISp2.^2*120*10^-3;
    Pcondtp = 2*Pcondp1+4*Pcondp2
34
36
38 Losses Calculus Secondary - Concution Losses
    ISs1 = [4.60707
40 4.70535
    5.16304
42 5.60663
    5.87218
44 6.49904];
    ISs2 = ISs1/2
46
    Pconds1 = 60*10^-3*ISs1.^2;
48 Pconds2 = 60*10^-3*ISs2.^2;
    Pcondst = 2*Pconds1 + 4*Pconds2;
50
52
54
56
    Switching Losses - Primary
58 tr = 0.6011*12+30.799;
    tf = 0.3687*12+6.745;
60 Pswp1 = zeros([6,1]);
    Pswp2 = zeros([6,1]);
62 Rg = 12
64 for i=1:6
    Pswp1(i) = (tf)*10^-9*ISp1max(i)*(400)*10^5*0.5
66 end
    for i=1:6
68 Pswp2(i) = (tf)*10^-9*ISp2max(i)*(400)*10^5*0.5
    end
70 Pswpt = zeros([6,1]);
    Pswpt = 2*Pswp1+4*Pswp2;
72 Primary
74 Secondary - Switching Losses
    SPS - YY
76 ISsmax1 = [9.49195

```

```

8.77255
78 6.44559
4.71364
80 3.077433
1.70052];
82 Pssw1 = zeros([6,1]);
Pssw2 = zeros([6,1]);
84
Switching Losses Secondary
86 Switch 1
for i=1:6
88     tr = 1.6838*10+12.68
tf = 1.6838*10+12.68
90
if i==6
92 Pssw1(i) = (tf)*10-9*ISsmax1(i)*(111)*105*0.5;
else
94
    Pssw1(i) = (tf+tr)*10-9*ISsmax1(i)*(111)*105*0.5;
96 end
98 end
Switch2
100 ISsmax2 = ISsmax1/2;
Switch 1
102 for i=1:6
    tf = 1.8496*10+10.049
104 tr= 1.8496*10+10.049
106 if i==6
    Pssw2(i) = (tf)*10-9*ISsmax2(i)*(111)*105*0.5;
108 else
110
    Pssw2(i) = (tf+tr)*10-9*ISsmax2(i)*(111)*105*0.5;
end
112
end
114
Pswst = 2*Pssw1+4*Pssw2;
116 Switch2
Total Losses
118 Psw05sps = Pswpt+ Pswst
Pcond05sps = Pcondst+Pcondtp;
120 Pcond =
Ptot = Pcondtp+ Pswpt+Pcondst+Pswst
122 Po = [99; 149; 293; 390; 439; 535];
NYY00sps = (Po./(Po+Ptot))*100;
124 Triangular Modulation

```

```
Conduction Losses - Primary - Triangular Modulation
126 ISp1 = [0.397414
0.539067
128 0.907787
1.12695
130 1.23631
0];
132 Ptcondp1 = 2*120*10-3*ISp1.^2;
ISp2 = ISp1/2
134 Ptcondp2 = 4*120*10-3*ISp2.^2;
Pcomnt = Ptcondp1+Ptcondp2 ;
136 Swiching Losses Primary - Triangular Modulation
ISs1max = [1.97782
138 2.42246
3.42544
140 3.95456
4.21729
142 0];
ISsecond = ISs1max
144 ISs2max = ISs1max/2;

146 Switching Losses - Triangular Modulation
tr = 0.6011*12+30.799;
148 tf = 0.3687*12+6.745;
Pswp1 = zeros([6,1]);
150 Pswp2 = zeros([6,1]);
Rg = 12
152
for i=1:6
154 Pswp1(i) = (tf)*10-9*ISs1max(i)*(400)*105*0.5
end
156 for i=1:6
Pswp2(i) = (tf)*10-9*ISs2max(i)*(400)*105*0.5
158 end

160 Pswpt = 2*Pswp1(i)+4*Pswp2;

162 Conduction Losses - Secondary - Triangular Modulation
Is1= [1.5143
164 2.05263
3.45305
166 4.28875
4.70724
168 0];
Is2 = Is1/2;
170 Is1max = [0.0268942
0.036634
172 0.0733926
```

```
0.0951802
174 0.802355
    0];
176 Is2max = Is1max/2
    Pcons1 = 2*60*10^-3*Is1.^2
178 Pcons2 = 4*60*10^-3*Is2.^2
    Pcons = Pcons1+Pcons2
180 Pswt1 = zeros([6,1])
    Pswt2 = zeros([6,1])
182 for i=1:6
        tr = 1.6838*10+12.68
184 tf = 1.6838*10+12.68

186 if i==6
    Pswt1(i) = (tr+tf)*10^-9*Is1max(i)*(111)*10^5*0.5;
188 else

190     Pswt1(i) = (tf)*10^-9*Is1max(i)*(111)*10^5*0.5;
    end
192 end
    for i=1:6
194         tr = 1.6838*10+12.68
        tf = 1.6838*10+12.68
196
        if i==6
198 Pswt2(i) = (tr+tf)*10^-9*Is2max(i)*(111)*10^5*0.5;
        else

200             Pswt2(i) = (tf)*10^-9*Is2max(i)*(111)*10^5*0.5;
202 end
        end
204
    Psws1 = 2*Pswt1
206 Psws2 = 4*Pswt2
    Psws = Psws1+Psws2
208 Pcondpf = Pcomnt
    Pcondsf = Pcons
210 Pcond05tri = Pcomnt +Pcons
    Pspf = Pswpt
212 Pssf = Psws
    Pstd05tri = Pswpt+Psws
214 Pdt = Pcomnt+Pswpt+Pcons+Psws
    Efficiency
216 Nt = (Po./(Po+Pdt))*100
```

```

Graduate Programme in Electrical Engineering - PPGEEL
3 Power Electronics Institute - INEP
  Advisor: Dr. André Luís Kirsten
5 MSc: Eng. Leonardo Bellincanta de Souza
  Losses Calculation - Theoretical Analysis - YY00 SPS and Triangular
7 Modulations - d = 0.75 - DAB Converter
  clear all
9 close all
  n = 0.37
11 Voltage Gain Value
  d = 0.75
13 L = 1.5*82*10^-6
  Ronp = 120*10^-3
15 Rons = 60*10^-3
  fs = 100000
17 Ts = 1/fs

19
  YY 00 SPS - SPS Losses
21 Losses Calculus Primary Part 1
  ISp1 = [0.866118;
23 0.901557;
  1.07003;
25 1.22447;
  1.31201;
27 1.5049]
  ISp1max = [2.5 2.65 3.07 3.38 3.54 3.88];
29 ISp2max = ISp1max/2;
  ISp2 = ISp1/2;
31 Conduction Losses - Primary
  Pcondp1 = ISp1.^2*120*10^-3;
33 Pcondp2 = ISp2.^2*120*10^-3;
  Pcondtp = 2*Pcondp1+4*Pcondp2
35

37
  Losses Calculus Primary Part 2
39 Conduction Losses Calculus Secondary Part 1
  ISs1 = [2.35 ;2.46 ;2.93; 3.36; 3.6; 4.13];
41 ISs2 = [1.13404;
  1.15914;
43 1.32221;
  1.49403;
45 1.59574;
  1.82629];
47
  Pconds1 = 60*10^-3*ISs1.^2;
49 Pconds2 = 60*10^-3*ISs2.^2;

```

```

Pcondst = 2*Pconds1 + 4*Pconds2;
51
53
55
57
Switching Losses - Primary
59 tr = 0.6011*12+30.799;
   tf = 0.3687*12+6.745;
61 Pswp1 = zeros([6,1]);
   Pswp2 = zeros([6,1]);
63 Rg = 12

65 for i=1:6
   Pswp1(i) = (tf)*10^-9*ISp1max(i)*(400)*10^5*0.5
67 end
   for i=1:6
69 Pswp2(i) = (tf)*10^-9*ISp2max(i)*(400)*10^5*0.5
   end
71 Pswpt = zeros([6,1]);
   Pswpt = 2*Pswp1+4*Pswp2;
73 Primary

75 Secondary
   SPS - YY
77 ISsmax1 = [4.52458;
   4.05684;
79 2.58811;
   1.54601;
81 1.00221;
   0];
83 Pssw1 = zeros([6,1]);
   Pssw2 = zeros([6,1]);
85

Switching Losses Secondary
87 Switch 1
   for i=1:6
89     tr = 1.6838*10+12.68
       tf = 1.6838*10+12.68
91
   if i==6
93 Pssw1(i) = (tf)*10^-9*ISsmax1(i)*(111)*10^5*0.5;
   else
95
       Pssw1(i) = (tf+tr)*10^-9*ISsmax1(i)*(111)*10^5*0.5;
97 end

```



```

99 end
Switch2
101 ISsmax2 = [2.6 2.4 1.7 1.24 1 0.48];
Switch 1
103 for i=1:6
    tf = 1.8496*10+10.049
105 tr= 1.8496*10+10.049

107 if i==6
    Pssw2(i) = (tf)*10-9*ISsmax2(i)*(111)*105*0.5;
109 else

111     Pssw2(i) = (tf+tr)*10-9*ISsmax2(i)*(111)*105*0.5;
end
113
end
115
Pswst = 2*Pssw1+4*Pssw2;
117 Switch2
Total Losses
119 Psw = Pswpt+ Pswst
Pcond075 = Pcondtp+Pcondst
121 Pcond =
Ptot = Pcondtp+ Pswpt+Pcondst+Pswst
123 Po = [99; 149; 293; 390; 439; 535];
NY00sps = (Po./(Po+Ptot))*100;
125 Triangular Modulation
Conduction Losses - Primary
127 ISp1 = [0.335635
0.454654
129 0.765318
0.94997
131 1.03821
1.22101];
133 Ptcondp1 = 2*120*10-3*ISp1.2;
ISp2 = ISp1/2
135 Ptcondp2 = 4*120*10-3*ISp2.2;
Pcomnt = Ptcondp1+Ptcondp2 ;
137 Switching Losses Primary - Triangular Modulation
ISs1max = [1.39633
139 1.70835
2.41388
141 2.78586
2.95478
143 3.31468];
ISsecond = ISs1max
145 ISs2max = ISs1max/2;

```

```

147 Switching Losses - Triangular Modulation
    tr = 0.6011*12+30.799;
149 tf = 0.3687*12+6.745;
    Pswp1 = zeros([6,1]);
151 Pswp2 = zeros([6,1]);
    Rg = 12
153
    for i=1:6
155 Pswp1(i) = (tf)*10-9*ISs1max(i)*(400)*105*0.5
        end
157 for i=1:6
    Pswp2(i) = (tf)*10-9*ISs2max(i)*(400)*105*0.5
159 end

161 Pswpt = 2*Pswp1(i)+4*Pswp2;

163 Conduction Losses - Secondary - Triangular Modulation
    Is1= [1.04026;
165 1.40869;
    2.37169;
167 2.95366;
    3.23271;
169 3.8325];
    Is2 = Is1/2;
171 Is1max = [0.018781700;
    0.023248900;
173 0.047857100;
    0.066529700;
175 0.075878300;
    2.391910000];
177 Is2max = Is1max/2
    Pcons1 = 2*60*10-3*Is1.^2
179 Pcons2 = 4*60*10-3*Is2.^2
    Pcons = Pcons1+Pcons2
181 Pswt1 = zeros([6,1])
    Pswt2 = zeros([6,1])
183 Switching Losses - Secondary - Triangular Modulation
    for i=1:6
185     tr = 1.6838*10+12.68
        tf = 1.6838*10+12.68
187
        if i==6
189 Pswt1(i) = (tf)*10-9*Is1max(i)*(111)*105*0.5;
            else
191
                Pswt1(i) = (tr)*10-9*Is1max(i)*(111)*105*0.5;
193 end

```

```

end
195 for i=1:6
    tr = 1.6838*10+12.68
197 tf = 1.6838*10+12.68

199 if i==6
    Pswt2(i) = (tf)*10-9*Is2max(i)*(111)*105*0.5;
201 else

203     Pswt2(i) = (tr)*10-9*Is2max(i)*(111)*105*0.5;
end
205 end

207 Psws1 = 2*Pswt1
    Psws2 = 4*Pswt2
209 Psws = Psws1+Psws2
    Pcondpf = Pcomnt
211 Pcondsf = Pcons
    Pcondtri = Pcons+Pcomnt
213 Pspf = Pswpt
    Pssf = Psws
215 Pst = Pswpt+Psws
    Pdt = Pcomnt+Pswpt+Pcons+Psws
217 Efficiency
    Nt = (Po./(Po+Pdt))*100
219

221 P = [Output Power Efficiency-SPS0.5   Output Power   Efficiency-Tri-0.5   Output Power
        Efficiency-SPS-0.75   Output Power Efficiency-Tri-0.75
    99  82.27565149   99  98.63418287  99  91.04663971   99  97.67897633;
223  149 87.78829718   149 98.69555674   149 94.06008614   149 98.2259903;
    293 93.86795411   293 98.64608879   293 97.19503707   293 98.71499209;
225  390 95.52142135   390 98.58512955   390 97.98130898   390 98.81813747;
    439 96.26593615   439 98.44182228   439 98.23812587   439 98.84718545 ];
227

figure
229 plot(P(:,1), P(:,2),P(:,3), P(:,4),P(:,5), P(:,6),P(:,7), P(:,8))
    legend('YY-00-SPS d=0.5', 'YY-00-Triangular d=0.5', 'YY-00-SPS d=0.75', 'YY-00-Triangular
        d = 0.75')
231 title('Efficiency - YY-00 DAB Converter - Triangular and SPS Modulations')
    xlabel('Po (W)')
233 ylabel('Efficiency ( )')

```